

APPENDIX: METHODS OF STUDY OF EARTH SURFACE PROCESSES, LANDFORMS AND SEDIMENTS

Appendix 1: Landforms, flow and sedimentary and processes

Measurement of land, water and ice surface topography

Land surface topography

Topography of the subaerial and shallow-subaqueous land surface has traditionally been measured using standard surveying techniques (e.g., digital tacheometry: total stations) and using stereo aerial photographs. Some older readers may even remember topographic surveying with compasses, chains, plane tables, and alidades. Relatively accurate surveying of land topography is now accomplished with GPS (global positioning system), with vertical and horizontal resolution of centimeters possible. Laser range finders are also now used for topographic mapping, and data from these can be tied into GPS data. LIDAR (light detection and ranging) is the acronym used for a variety of surveying techniques using light beams directed at a target. LIDAR can be done from the ground or from the air. Digital photogrammetry in combination with GIS-based digital elevation models has also been developed for measuring subaerial topography, although these methods are not yet as accurate as those mentioned above (e.g., Lane et al., 1998, 2001). Digital photogrammetry has also been used to determine the topography of subaqueous parts of shallow, clear water by making corrections for the effects of light refraction in water (Westaway et al., 2000; Lane et al, 2001). However, subaqueous land topography is normally obtained using depth soundings in combination with measurements of water-surface elevation, as discussed below.

The topography of the bed of deep rivers, lakes and the sea is usually determined by measuring water depth, after correcting for the topography of the water surface. Water depth in natural environments is usually measured either by lowering weighted graduated cables or graduated rods to the bed at points along a traverse, or by depth sounding along a grid of

surveyed lines. Most depth sounders are based on reflection of a vertically directed beam of sound. The spatial resolution of the bed topography increases as the width of the beam of sound that reaches the bed decreases. The depth resolution depends on frequency of the transmitted signal, and is commonly on the order of centimeters to decimeters. This means that most depth sounders are not capable of resolving ripples and small dunes on the bed. As it takes a finite amount of time for the transducer to transmit a pulse of sound and to change to receive mode, there is normally a minimum depth (commonly tens of centimeters) below which the received signal cannot be separated from the transmitted signal. Side-scan sonar and multi-beam sounders are used in some deep rivers and in the sea to measure the geometry of large areas of the bed in great detail (e.g., Parsons et al., 2005). Deep towed side-scan sonar (e.g., GLORIA, TOBI) has been used to image the ocean floor and shallow subsurface in great detail (Chapter 18). Ground-penetrating radar has also been used to measure flow depth in rivers (e.g., Spicer et al., 1997).

High frequency and ultrasonic sounders are used to measure depth in laboratory flumes (e.g., Best and Ashworth, 1994). The combination of very high frequency and narrow beam width yields high spatial resolution and accuracy, such that bed features on the order of millimeters in height and centimeters in width can be resolved. Such highly accurate depth sounders could only be used in shallow rivers if mounted on stable platforms.

The topography of the land beneath ice sheets and glaciers is measured by determining ice thickness using borings and geophysical profiling techniques such as seismic and ice-penetrating radar (Knight, 2006). Ice coring using hot water has been developed into an art. Ice surface elevation plus ice thickness gives the land surface topography beneath the ice.

Water and ice surface topography

Water surface topography of the sea, lakes and large rivers, and ice-surface topography of glaciers and ice sheets, can be measured using the same techniques as for the land surface (e.g., airborne or satellite-based LIDAR, digital photogrammetry with digital elevation models). However, waves on water surfaces make it difficult to determine the topography averaged over specified intervals of time and space. Nevertheless, modern LIDAR systems can measure some

water surface waves. Water surface waves on the ocean are also measured using buoys, hydrostatic-pressure or acoustic sensors attached to the bed (e.g., NOAA's DART system), and electronic staff gages on fixed platforms (normally at or near the coast).

In rivers, spatial variation of water-surface elevation is very difficult to measure with high accuracy and resolution, because the water surface fluctuates so much with turbulence and bed topography. It is rarely possible to get to parts of the water surface away from the banks in order to make accurate measurements directly. One way of measuring spatial variation in water surface elevation for relatively small rivers is to build stable measuring platforms. Indeed, such stable platforms are a necessity for very detailed measurement of the spatial and temporal variation of bed topography, depth, and flow velocity in small rivers. Building of measuring platforms is not possible for large rivers. In large rivers, water surface topography may be measured using LIDAR or digital photogrammetry, as discussed above.

Measurement of physical and chemical properties of water, air and ice

Physical properties of water, air and ice that are typically measured are density, sediment content, and relative amount of water (in air) or water and air (in ice). Molecular viscosity of water is normally calculated as a function of temperature. The rheological properties of ice have been studied extensively in the laboratory (reviews in Knight, 2006), although it is difficult to reproduce the small strain rates occurring over long time periods that are typical of glacier ice. The texture and fabric of ice are also studied in order to determine the nature of deformation that the ice has undergone.

Water samples are routinely analyzed in the field for Eh, pH, temperature, and electrical conductivity (a measure of salinity). Treatment and special handling are usually required to prevent contamination of the sample with atmospheric gasses. Chemical measurements (using a wide variety of analytical procedures) are routinely made of major inorganic dissolved components (Na^+ , K^+ , Mg^{2+} , Ca^{2+} , carbonate alkalinity, Cl^- , SO_4^{2-}), minor inorganic dissolved components such as nitrates, phosphates, and iron, various heavy metals such as mercury, lead, arsenic and cadmium, and a variety of organic compounds such as TCE and benzene. In

oceanographic studies, satellite measurements of the adsorption of various wavelengths of light by ocean water are used to determine water temperature and amount of chlorophyll (plankton productivity). Isotopic compositions of water and ice are also determined routinely by mass spectrometry. Variations in the isotopic compositions of water are used to identify water sources, evaluate mineral-water interactions, and assess water temperatures. Isotopic variations in glacial ice are extensively used in paleoclimate studies.

Differential absorption lidar (DIAL) is used to measure chemical concentrations (such as ozone, water vapor, pollutants) in the atmosphere. DIAL uses two different laser wavelengths, one of which is absorbed by the molecule of interest whereas the other is not. The difference in intensity of the two return signals can be used to deduce the concentration of the molecule being investigated.

Measurement of water flows

Flow velocity

In order to understand a natural water flow, it is ideally necessary to determine how the flow velocity vector, the water depth, and the elevations of the bed and water surface vary in space and time. Measurement of the spatial and temporal variation of water flow in natural environments is extremely difficult because of limitations of measuring equipment and of the ability to deploy it effectively, especially during highly energetic flow events (e.g., river floods, storms at sea).

When measuring flow velocity, the following issues need to be addressed. Can the flow meter measure velocity direction as well as magnitude? Can three orthogonal flow components be measured? Can the meter record turbulent fluctuations in the flow-velocity vector or just time-averaged velocity? What is the sensing volume of the meter? Is the flow meter small enough so that it can be placed very close to the bed? Does the meter interfere with and modify the flow that it is measuring? Does meter calibration account for flow interference? Will the meter be affected by moving solids such as sediment, vegetation, ice and human debris? Can enough

meters be deployed so that spatial variations in changing flows can be measured simultaneously? Is it possible to attain accurate results if the meter must be deployed from a boat? Can large amounts of flow data be recorded and stored quickly enough?

The ideal attributes of a flow meter are: non-intrusive or configured in a way to avoid flow disturbance; rugged, to resist moving sediment and other hard objects; small relative to the flow depth so that it can be placed close to bed and not disturb the flow too much; capable of measuring and recording magnitude of flow velocity in 3 orthogonal directions at time intervals on the same scale as turbulence; reliable calibration and little instrument drift or noise; inexpensive. These ideal characteristics are not generally obtainable except in the laboratory. Even then, if only one meter is available, there is still the problem of measuring time and space variation of flow over migrating bed forms.

Flow velocity meters commonly used in natural environments include the following types: propeller, electromagnetic, and acoustic-Doppler. In addition, hot-film anemometers and laser-Doppler anemometers are used in laboratory settings. Perhaps the most common type of flow meter used in rivers is the propeller type, where the number of revolutions of the propeller is proportional to the flow speed parallel to the propeller axis. Propeller-type meters have the advantage of being robust, relatively inexpensive, and easy to use. Although these meters undoubtedly modify the flow around them, calibration is fairly straightforward. The propeller should be as small as possible in order to minimize flow interference and to allow deployment close to the bed and banks, but a small meter is more susceptible to damage and fouling with vegetation and hair than a larger one. The propellers and housings are normally on the order of centimeters or decimeters in diameter, such that it is difficult to get sufficient readings in the lowest 10% of flow in shallow (<1m) flows.

Propeller meters are deployed on rods if the operator is wading, or from a stable platform such as a bridge or a pontoon. In this case, the orientation of the meter on the rod can be controlled fairly accurately, as can the position of the meter relative to the bed. Propeller meters are also suspended from boats or bridges on metal cables or ropes with bottom weights to minimize the effects of streaming in the flow, and with fins to orient the meter in the flow. It is

more difficult to control the position of these meters, and propeller orientation can only be obtained from an electronic compass in the meter body. Such compasses are generally not very accurate. Furthermore, propeller meters with built-in compasses are normally large, so that they cannot be deployed close to the bed. In some cases, two or three small meters are oriented orthogonal to each other on a frame in order to measure two or three components of velocity. Such arrays generally interfere excessively with the flow, and it is difficult to maintain and measure the orientation of the frame under high-flow conditions. Series of meters are also commonly located at different depths on mounting rods. Most propeller meters only yield time-averaged velocity magnitude and direction in the horizontal plane. Therefore, they are most commonly used to obtain time-averaged flow velocity at river gaging stations (at distances of $0.2d$, $0.4d$ and $0.8d$ from the bed). Small meters appropriately deployed can be used to measure vertical profiles of time-averaged velocity magnitude and direction in the horizontal plane.

Electromagnetic meters are commonly used in natural environments and in laboratory flumes. They are based on the principle that the voltage between two electrodes varies as a function of the velocity of water flow between the electrodes. Most electromagnetic flow meters measure two orthogonal components of velocity in the horizontal plane, so that the 3-D flow field at a point can be determined using two meters placed orthogonal to each other. These meters must usually be mounted on a rod or frame deployed from a stable platform, so that their orientation can be maintained and measured accurately. Some of the larger meters can be suspended on a cable: these have fins for orientation in the flow, and the orientation is measured using an electronic compass. The sensors of the smallest varieties are robust, and capable of being deployed close to the bed. Sensor diameters can vary from about 1 cm to several centimeters. However, the sensing volume has a diameter that is about double the diameter of the sensor. The biggest advantage of these meters over the propeller meters is that they can measure turbulent variations in flow velocity, but only the lowest frequencies (up to 10 Hz). Instrument drift may be a problem with these meters. The relatively high cost of electromagnetic meters is such that multiple meters are not commonly used for simultaneous flow measurement.

Acoustic Doppler Velocimeters (ADV) have been used recently to measure 3D turbulent variations in flow velocity in the sea, rivers and flumes (e.g., Kraus et al., 1994; Lemmin &

Rolland, 1997; Rolland & Lemmin, 1997; Lane et al., 1998; Nikora & Goring, 1998; Sukhudolov and Rhoads, 2001). SonTek ADVs transmit short acoustic pulses at frequencies of up to 16 MHz from a transmitter at the center of the probe head. As the pulse propagates through the fluid, acoustic energy is reflected by air bubbles and by suspended sediment. Three receivers around the probe head focus on a distant sampling volume that is on the order of 10^{-1} cm^3 . Therefore, measurements can be made at a point without the probe interfering with the flow. The acoustic signals have a Doppler shift that results from the velocity differential between the probe and the scattering objects. Three components of velocity in the sampling volume are calculated. Velocity of up to 2.5 m/s can be measured to an accuracy of $\pm 0.1 \text{ mm s}^{-1}$, and sampled at a frequency of up to 25 Hz (up to 100 Hz in flume versions). ADV signals are affected by Doppler noise, or white noise, associated with the measurement process. This noise at high frequencies may create an aliasing effect in frequencies greater than the Nyquist frequency, but can be filtered out. Deployment and correct orientation of ADVs are critical and difficult problems. To correct for misalignment of the velocity probe, it is also common to rotate velocity signals to maximize the mean streamwise velocity. Unfortunately, ADVs cannot measure velocity close to the bed and water surface. In some cases, the intensity of the back-scattered signal can be related to suspended sediment concentration, after careful calibration (see below).

Acoustic Doppler Current Profilers (ADCPs) use the same principles as ADVs, but provide a profile of time-averaged flow velocity and direction instead of turbulent variations in velocity at a single point (e.g., McLelland et al., 1999). ADCP's operate at an acoustic frequency of 0.25 to 3 MHz, and can measure flow velocity over a depth range up to about 100 m. There is a zone called the blanking range, up to about 1 m from the probe head, within which data cannot be collected. Data are collected from cells at specific depths, and the cell length is on the order of 10^{-1} m . One problem with these instruments is that the sensing region is a cone that increases in diameter with distance from the probe head. Therefore, flow velocity is averaged over a greater sensing volume as distance from the probe (i.e., depth) increases. These instruments can also yield data on suspended-sediment concentration (e.g., Thorne et al., 1996).

In rivers, it is commonly desirable to resolve mean flow velocity vectors into downstream (primary) and across-stream (secondary) flow components, in order to elucidate flow structures

such as secondary circulation (helical or spiral flow) cells and net across-stream flow patterns. In order to do this, it is necessary to define the mean downstream flow direction. This is easy to do for laboratory channels with parallel walls. However, it is commonly difficult to do in natural channels that have irregular, non-parallel banks and rapid spatial changes in plan-form curvature. Methods are discussed by Hey & Rainbird (1996) and Lane et al. (2000).

In laboratory flumes, the most common methods of measuring flow velocity are now laser-Doppler anemometry (LDA) and various kinds of flow visualization techniques, although ADVs are also being used. Flow measuring methods that are no longer used in laboratory flows include Pitot tubes and hot-film or hot-wire anemometers. Laser-Doppler anemometry (LDA) is used for measuring turbulence in flumes (e.g., Buchave et al., 1979; Nezu & Nakagawa, 1993). The principle of LDA is that a seed particle moving in a water flow relative to a fixed source of laser light scatters the light at a different frequency to that of the incident beam. The Doppler shift represents the difference between the two frequencies, and can be related to instantaneous particle velocity given the angle between the incident and scattered light. Thus, the velocity of the seed particle is measured rather than that of the actual fluid. In practice, two pairs of laser beams intersect to produce interference fringes of varying intensity that form the measurement volume. When a seed particle crosses through the fringe pattern, the scattered light intensity fluctuates with a frequency equal to particle velocity divided by fringe spacing. The frequencies of the beams are shifted relative to each other (using a Bragg cell) so that forward and backward velocities can be distinguished. Most of the laser light is scattered away from the laser. However, enough is scattered back towards the transmitter to allow measurement in the backscatter mode. This enables the transmission and receiving optics to be housed together. Particles must be neutrally buoyant and small enough to accurately track the flow, but large enough to scatter sufficient detectable light. Commonly, water has sufficient impurities that seed particles do not need to be added. If seed particles need to be added, water-based paint can be used. The advantages of LDA are that it is non-intrusive, and is capable of accurately measuring three components of velocity at high frequency in a small measurement volume. The disadvantages are that data collection rates depend on the amount of seed particles, their rate of arrival at the measurement volume, and whether or not they are detected properly. This means that data are unevenly spaced, and data collection rates are reduced in the presence of high

concentrations of suspended sediment. Also, use of backscatter mode may not be possible with high suspended-sediment concentrations. It is difficult to measure three component of velocity close to the bed, because of the configuration of the laser beams. Finally, LDA is expensive.

Phase Doppler anemometry (PDA) can be used in flumes to accurately measure the velocity of both fluid and suspended sediment, and grain size of suspended sediment (e.g., Buchhave, 1987; Bachalo, 1994; Best et al., 1997; Bennett et al., 1998). PDA relies upon detection of the phase shift of light scattered by seed particles as they pass through the intersection of two laser beams. The phase shift of light passing a spherical particle detected at two different locations is proportional to the local radius of curvature of the particle, which, for a perfect sphere, can be used to determine particle diameter. By using non-overlapping size distributions of fluid 'seed' particles and sediment grains, the fluid and sediment phases can be distinguished. Errors in particle sizing using PDA can be caused by dust contamination, by other foreign particulate matter in the flow, and by minor deviations from perfect sphericity of the particles. Errors associated with PDA arise from several different sources: variable data acquisition rates; cross-talk between the two phases, in which fluid and sediment particles are incorrectly classified due to particle asphericity and contamination in the flow; orientation of the measurement volume. These combined errors may be expected to yield errors in the mean and root-mean-square velocities of several percent. As with LDA, PDA equipment is expensive.

In laboratory flumes, the 2-D and 3-D structure of turbulent motion is commonly studied using various types of flow visualization medium (e.g., hydrogen bubbles, dye, smoke, illuminated tracers) coupled with high-speed photography. The most sophisticated techniques of particle-image velocimetry (PIV) use digital photography and pattern recognition software in order to reconstruct the turbulent flow field in two-dimensional sections (e.g., Tait et al., 1996; Fujita et al, 1998; Nezu & Onitsuka, 2001). Small, reflective and neutrally buoyant seed particles are illuminated at short time intervals and photographed. Automated analysis of successive images gives the 2-D and 3-D velocity field. The advantage of PIV is that the whole flow field is measured simultaneously rather than successively as a flow meter is moved from point to point. Finally, flow velocity and direction at the water surface can be measured using aerial video photography of floating tracers such vegetation, dead animals, or human flotsam.

Fluid shear stress

Fluid shear stress is an important characteristic of boundary-layer flows, and bed shear stress is particularly important because of its control on sediment transport. Fluid shear stress is rarely measured directly, and is usually calculated from distributions of fluid velocity, as explained in Chapters 5 to 8.

Measurement of air flows

Flow velocity measurements in air pose the same problems as with turbulent water flows. The equivalent of the propeller-type flow meter used in water is the 3 or 5 cup anemometer, used for measuring mean wind speed. Turbulence is commonly measured with hot-wire anemometers, but these are expensive and easily damaged by sand in suspension. Laser-Doppler and Radar-Doppler anemometry are also used for atmospheric velocity measurements. Flow visualization techniques include use of streamers and smoke candles.

3D measurement of air flow and composition in atmospheric boundary layers is extremely difficult because of the enormous volumes and heights above the ground. Measuring equipment must be deployed in aircraft, or unmanned drones and balloons. Measurements of air flow in the atmosphere can be made remotely from satellites.

Measurement of ice flows

Flow velocities within ice flows are determined by measurement of fixed objects within tunnels, and by the rate of deformation of boreholes through the ice (using tilt meters). Ice surface velocities are obtained by analysis of tracers in sequential aerial photographs or satellite images. Thickness of ice is measured using boreholes and geophysical profiling techniques such as seismic and ice-penetrating radar. Water pressure in and under the ice is also measured in boreholes using pressure sensors. The water pressure within subglacial sediment is an important

control on movement of the overlying ice. The shear strength of such sediment is measured using ploughmeters and dragometers (described in Knight, 2006).

Measurement of sediment transport rate

Bedload transport samplers

A typical bedload transport sampler for use under water is essentially a heavy metal box with a rectangular opening through which bedload sediment enters. The cross sectional area of the box increases from front to back in order to cause deceleration of the flow. A mesh bag is attached to the back of the sampler for collecting the sediment. The mesh size is 0.125 mm, to allow fine-grained suspended sediment to pass through (theoretically). The sampler may be lowered to the bed on a cable or using a wading rod, and a fin may be added to help orient the sampler in the flow. The Helley-Smith sampler (Figure A-1), a variant of the well-known Arnhem sampler, has been very widely used (e.g., Emmett, 1980; Bridge & Jarvis, 1982;



Figure A-1. Helley-Smith bedload sampler deployed from a measuring bridge.

Dietrich & Smith, 1984; Hubbell et al., 1985, 1987; Bridge & Gabel, 1992; Kleinhans & Ten Brinke, 2001). One of the problems with this sampler is that the height of the front opening (76 mm) does not allow entry of larger gravel grains, but catches a large amount of suspended sand on sand beds. Also, scouring around the front of sampler causes it to sink into the bed and under-sample.

Incorrect orientation in the flow reduces the measured load (Gaudet et al., 1994). On a dune-covered bed, the sampler may be put in the trough region (yielding no sample) or in the avalanche face (in which case it sinks into the bed and acts as a dredge). The solution to this problem with dune-covered beds is to take many samples in time and space.

Perhaps the best (and most expensive) method of direct measurement of bed-load transport rate in rivers is to use sediment traps inserted into the bed across its width. Ideally, it should be possible to open and close individual traps across the width of the river, to be able to empty the traps before they fill, and to sample the sediment collected. It is also desirable to have a way of continuously measuring the weight or volume of sediment in the traps. This would require some kind of conveyor belt system for moving the sediment from the traps, and possibly insertion of balances in the bed. Sediment traps of various types have also been used to measure aeolian bedload transport. They suffer from the same shortcomings as those used underwater.

Observation of the motion of individual tagged grains from and/or past fixed points in the bed give an indication of when and how far the grain moved during a transport event (e.g., a flood). The grains may be tagged by painting them or by inserting devices to allow their detection (e.g., metal or radioactive source). However, such methods cannot yield comprehensive information on sediment transport rate. Other methods of measuring bedload sediment transport include subaqueous video photography (see below), and acoustic methods that relate bedload transport rate to the noise created by grain-bed collisions. The least inexpensive (but indirect) method for determining bed-load transport is using bed-form geometry and migration rate (see Chapter 5 and below).

Suspended sediment sampling

A recent review of techniques of suspended-sediment measurement in water is by Wren et al. (2001). The commonly used techniques mentioned here can be used in any water depth and any type of water flow. The most common method of measuring suspended-sediment transport rate in rivers is with a bottle in a housing that has an orifice facing into the flow and an opening to allow air to escape from the bottle (e.g., USGS model DH-48). The sampler can be attached to a wading rod or suspended on a cable. This type of sampler can be used in depth-integrating mode, when the sampler is lowered and raised at constant speed through the water depth. It can also be used in point-integrating mode, when it is deployed at a single point with a switch to open and close the orifice. A problem with the design of this sampler is that it is not possible to place the orifice within 10 cm of the river bed where suspended-sediment concentration is

highest. Although very widely used, these samplers are flow intrusive, and are not capable of resolving short-term variations in suspended-sediment concentration.

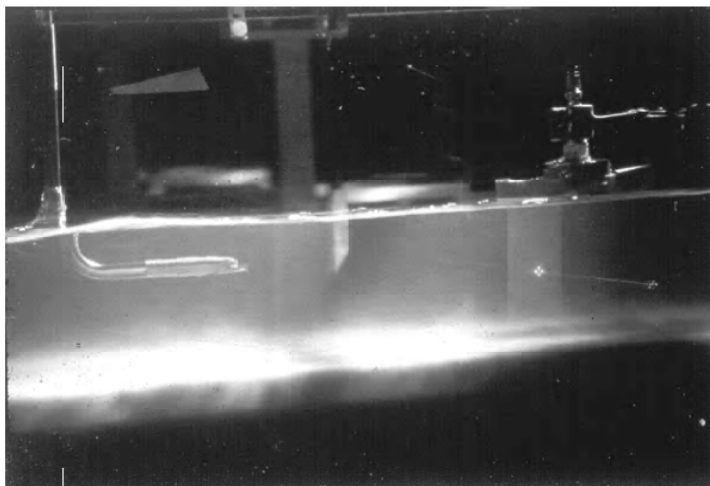


Figure A-2. Measurement of flow and sediment transport in a flume. Siphon-type suspended sediment sampler to left, transducer of an ultrasonic depth profiler to right, and four laser beams associated with a phase-Doppler anemometer.

Another method, especially suitable for flumes, is to orient the open end of a plastic tube into the flow and start siphoning the water and suspended sediment into a bottle (Figure A-2). The level of the collecting bottle is adjusted so that the discharge from the tube is the same as the discharge of the water entering the tube. This method can be very accurate. As with the bottle method, this method is flow intrusive, and has poor temporal

resolution. A commonly used variant of this method is pumping sediment-laden water into collecting bottles.

Optical backscatter (OBS) probes measure water turbidity, hence sediment concentration. These probes operate by transmitting an infrared signal and measuring the strength of the signal scattered back by particles in the flow. Hence, the probes need to be at least 0.2 m from any solid object. For sediment of uniform size, their response is linear over a wide range of concentrations (Wren et al, 2001). OBS sensors have good spatial and temporal resolution. However, the concentrations determined by OBS probes are greatly dependent on the size of the particles. Calibration is accomplished by comparing turbidity with directly measured suspended-sediment concentrations.

Acoustic backscatter probes have also been widely used for measuring suspended-sediment concentration and grain size (e.g., Thorne et al, 1993, 1996; Kostaschuk & Villard, 1999; Shen & Lemmin, 1999; McLelland et al., 1999; Wren et al., 2001). This method has the

advantage of being non-intrusive, is capable of measuring sediment parameters over a range of several meters, and has spatial and temporal resolution of about 10 mm and 0.1 sec, respectively. It has the disadvantage of difficulty in calibration, and signal attenuation at high sediment concentrations.

Photographic methods

Sediment transport in laboratory channels and natural environments is commonly observed and recorded using video photography (e.g., Hammond et al., 1984; Drake et al., 1988). Quantitative studies of individual particle motions are now possible using PIV (discussed above) and digital particle tracking (Middleton et al., 2000).

Topographic methods

By analogy with calculation of sediment transport rate from the geometry and migration rate of bed forms like ripples and dunes, it is possible to estimate large-scale patterns of sediment transport by repeated topographic surveys of river beds. This has been attempted, for example, using digital photogrammetry in combination with GIS-based digital elevation models (e.g., Lane et al., 1995; Ashmore & Church, 1998; Stojic et al., 1998).

Measurement of flow and sediment transport over bed forms

Flow velocity and sediment transport rate vary markedly in space over bed forms such as ripples, dunes, antidunes, and bars. Furthermore, as bed forms migrate, the flow and sediment transport at a fixed measuring station will change in time. For example, measurement of a vertical profile of flow velocity with one flow meter typically takes about 600 s (10 measurement points throughout the depth, and a 60 s record at each point in order to allow averaging over turbulence). If flow depth is 1 m, mean dune length is 6 m, and mean dune speed is 0.1 mm/s, an average dune will have migrated 10% of its length in the time taken to measure the velocity profile. This problem becomes more critical as dune size decreases and migration rate increases (Gabel, 1993; Leclair, 2002). This problem of flow velocity and sediment transport rate over bed

forms varying in space and time is the reason why most laboratory flume studies of flow over bed forms have been conducted with fixed beds and no sediment transport. These studies are of limited value in view of the interaction between the flow, sediment transport and bed forms. However, simultaneous measurement of the flow in many different positions is becoming possible using PIV (in flumes) and ADCPs. Strategies for taking representative sediment transport samples in rivers are discussed by, for example, Gaweesh & Van Rijn (1994), Gomez & Troutman (1977), and Kleinhans & Ten Brinke (2001).

Measurement of bed form geometry and kinematics



Figure A-3. Operation of a high-resolution depth profiler from moveable railways attached to bridges over a small river

In order to adequately define and understand the geometry and migration characteristics of bed forms, it is necessary to make repeated measurements of bed topography over a representative bed area over a period of time that allows recognition of the changes expected over at least major flow events (single floods, storms at sea). Equipment needed includes: a depth profiler with adequate resolution; a stable platform for the depth profiler;

a positioning system to allow accurate relocation of survey lines. Many depth profilers suitable for field use have resolution of only decimeters and must be operated from boats, the movement of which reduces accuracy. Therefore, it is only possible to recognize large dunes and bars (but not ripples or low dunes). However, modern multibeam sonar has resolution of centimeters. The location of survey lines for boats has not been very accurate unless the boats were attached to fixed lines, but now differential global positioning systems (DGPS) allow positioning to within decimeters or centimeters (Ten Brinke et al., 1999; McLelland et al., 1999; Ashworth et al., 2000). There have been a few examples of construction of stable measuring platforms across small rivers (e.g., Bridge and Jarvis, 1982; Bridge and Gabel, 1992; Gabel, 1993: Figure A-3).

These allow accurate positioning and the stability needed for using high-resolution (order of a centimeter) profilers that can resolve ripples and low dunes on the bed. In flumes, it is possible to use laser range finders or high-resolution depth profilers (accurate to less than 1 mm) fixed to moveable carriages (e.g., Dingler, Boylls & Lowe, 1977; Best & Ashworth, 1994).

The bed area surveyed should allow observation of a representative number of bed forms (100 say). The survey area should be wider than an isolated 3-D bed form, and the along-stream length of the survey area should be at least several bed forms and preferably longer than a typical bed form excursion. It is very difficult to define the 3-D geometry of bedforms using only a grid of orthogonal survey lines (e.g., Gabel, 1993). However, 3D geometry of bedforms such as dunes and bars can be measured with modern sidescan and multibeam sonar (Ten Brinke et al., 1999; McLelland et al., 1999; Ashworth et al., 2000; Parsons et al., 2005). Laboratory flumes are also commonly not long enough to define dune excursions, nor wide enough to allow description of the 3-D geometry of large bedforms such as dunes.

If temporal changes in bedform geometry and migration rate are to be measured, sonar surveys over a chosen bed area must be repeated with sufficient frequency to allow recognition of individual bedforms from one survey to the next. Furthermore, it is desirable to observe individual bedforms up to 10 times during a bedform period, which is the time taken to move one bedform length (Gabel, 1993; Leclair, 2002). In the case of dunes that are 6 m long migrating at 0.1 mm/s, the bedform period is 60,000 s. Surveys should therefore ideally be made at 6000 s (100 minute) intervals. Furthermore, in order to understand bedform lag effects, the chosen bed area should be surveyed every day for weeks or months throughout periods of changing flows (e.g., river floods, tidal periods, storms at sea).

Analysis of sequential depth-profiler measurements is easiest if the data are digital. The accuracy of the positioning of sequential surveys and of the depth readings must be appreciated at the outset. The first analytical step is removal of spurious readings. 3-D bed forms will move laterally as well as downstream, such that an apparent change in length or height in an alongstream profile may be associated with lateral movement. The edges of 3-D bed forms or spurs in bed form troughs may move in and out of the plane of the profile, suggesting small,

short-lived bed forms. Thus, the variability of heights, lengths and migration rates of bed forms defined from 2-D profiles will reflect the 3-D nature of individuals as well as the variability between individuals. Furthermore, it is difficult to define the nature of change of individual bed forms and the timing of creation and destruction of individual bed forms when they move in and out of a sounding line.

Methods of sampling bed-surface sediment

The texture of bed-surface material has a direct bearing on the nature of bed load and suspended load transport, and great care must be taken in sampling. Sampling of gravels presents unique problems that do not exist with sand sampling. Gravels contain a large range of particle sizes that are commonly bimodal and span 10 or more phi intervals (defined below). This makes it difficult to obtain a sample size that is statistically representative, because the largest grains dominate the sample weight. In order to obtain an unbiased grain size distribution, a much larger weight of small grains must be sampled than large grains. Mosley & Tindale (1985) suggest that the largest particle should not make up more than 5% of the total sample weight, whereas Church et al. (1987) preferred a limit of 1%. Gale & Hoare (1992) suggest that both of these (arbitrary) estimates are too generous and show that larger sample sizes are required, especially for poorly sorted sediments. For beds of pebbles and cobbles, individual sample weights may need to be hundreds of kilograms.

There are commonly large spatial variations in texture within natural environments (e.g. over bars and channels), requiring a large number of samples to adequately represent the distribution (De Vries, 1971; Gale & Hoare, 1992; Mosley & Tindale, 1985; Crowder & Diplas, 1997). Commonly, many tens or hundreds of samples will be required, and at each sample site it may be necessary (in the case of gravels) to sample the surface (armor) layer as well as the subsurface sediment.

Subaqueous sampling of gravels is difficult because: (1) it is difficult to collect large samples using underwater samplers, especially if the water is so deep that the sample must be

retrieved from a boat, and; (2) fine-grained sediment can easily be washed out of the sample during collection. Different methods of bed sediment sampling are discussed below.

Bulk sampling

Bulk sampling can be accomplished by shoveling sediment into a sample container. Internal structures and fabric are destroyed using this technique. This method is satisfactory for subaerial samples, but subaqueous samples can suffer from extreme washing out of fine-grained particles. This can be mitigated somewhat by collecting samples with an open ended bucket pointing upstream, so that fine-grained sediment cannot escape. Gravel armor layers (surface layers about one grain diameter thick that lack interstitial fines) should be sampled separately from subsurface layers (Ettema, 1984; Church et al., 1987; Gomez, 1983; Diplas & Fripp, 1992). Bulk samples of sand can be obtained fairly easily using grabs (e.g., Van Veen Grab) and dredges.

Freeze sampling

River gravels have been sampled using liquid CO₂ or N₂ to freeze the sediment surrounding a feeder pipe driven into the ground (Carling, 1981; Carling & Reader, 1981; Thoms, 1992, 1994). The sediment surrounding the pipe freezes to the pipe and, when the pipe is pulled out of the ground, all the frozen sediment comes out with it. This technique provides a representative bulk sample of all grain sizes smaller than -6ϕ (64 mm). Heterogeneous sediments can be sampled both above and below the water table. In addition, the sample can be oriented, and original sediment fabric and porosity can be preserved (Stocker & Williams, 1972). Expansion of interstitial water as it freezes causes minor distortion, especially in muds (Simola et al., 1986). However, the equipment is bulky and expensive, and it takes up to 15 minutes to obtain one sample.

Grid sampling

Grid sampling arose from a need to sample surface gravel particles without the inconvenience of dealing with large sediment volumes. With Wolman's (1954) method, the bed area of interest is divided up into a grid of 100 squares with dimensions greater than D_{95} , the diameter of the grain that is larger than 95% of all of the grains. One particle is chosen from each square. To ensure objectivity, the grain is selected by bending over and touching a stone under the toe of the sampler's boot with a straight, vertical finger with eyes averted or closed. The first stone touched will be chosen. The intermediate (B) axis length of the stone is measured as the stone is picked up. The stone is then replaced in its original position. An alternative grid-sampling method is to select samples at fixed intervals in transects. Samples may also be taken at random over an area.

Grid sampling is cheap and simple, and very large particle sizes can be sampled. It can be done under shallow water as well as subaerially. Although grid sampling does not allow specific surface sedimentary facies to be sampled, most facies on a sediment surface will be represented if the grid is set up properly (Walcott & Church, 1991). However, grid sampling seriously under-represents the proportion of particles with grain size less than 15 mm (Fripp & Diplas, 1993; Crowder & Diplas, 1997). Random sampling from a chosen area also leads to under-representation of the sediment size (Wohl et al., 1996). Significant sampling error can also be introduced by having different people doing the sampling, even if they are given standard training (Hey & Thorne, 1983; Wohl et al., 1996). This is primarily due to subjectivity in sample selection, although errors in measurement and analysis may also occur. As the grid sampling is only from the surface layer, it cannot be compared with results from a bulk sample without mathematical conversions. Fines and sub-surface sediments cannot be sampled using this method.

Areal sampling

Areal sampling involves measurement of all the surface material within a given area, either by pushing a clay-covered flat plate on to the bed surface or by pouring hot wax on to the surface. Areal sampling (especially clay sampling) does not give a true representation of the surface material, and Diplas & Sutherland (1988) suggest that the maximum grain size that can

be sampled is 4 mm. This type of sampling cannot be done under water, and subsurface samples cannot be taken. As areal sampling only takes material from a 2-D surface, conversion to a volumetric equivalent is necessary, as discussed below.

Controversy exists as to whether the wax sampling technique is a truly areal sampling method because wax seeps down below the surface layer. Wax seepage varies depending on whether the sediment is matrix supported or framework supported. In matrix-supported gravels, coarse and fine fractions are sampled in the same way, whereas in framework-supported gravels the coarse fraction is sampled areally but the fine fraction is sampled volumetrically (Diplas & Fripp, 1992). The minimum surface area to be sampled areally should be $100D_n^2$ (where D_n is the mean grain size of the coarsest fraction).

A hybrid technique for sampling a wider range of grain sizes using a combination of grid and areal sampling has been proposed by Fripp & Diplas (1993). Sampling of the 4 mm to 15 mm range is still a problem however, and, as this size range is common in gravel-bed rivers, this hybrid technique may not be of much benefit.

Photographic techniques

Bed-surface sediment-size distributions can also be determined from photographs of the bed. Grain sizes can be measured by hand or using a computerized pattern-recognition technique. Grains could be measured on a grid or all grains could be measured in a given area. It is necessary to determine which length will be measured on an irregular-shaped grain, and to realize that the sizes are only those in the plane parallel to the bed surface. This may be a problem with imbricated gravel grains. The resulting grain-size distribution would be expressed in number percentages.

Conversion of surface samples to volumetric equivalents

If surface sediment is sampled in terms of number or weight of grains of a given size in a given area, it may be necessary to convert these distributions to volumetric samples. Diplas and

Fripp (1992) show that sediments with different proportions of fine and coarse grains are not sampled the same way by areal methods. Thus conversion to volumetric equivalents is essential. Methods for converting areal weight percentage to volumetric weight percentage are given by Kellerhals & Bray (1971), Diplas & Sutherland (1988), Fraccarollo & Marion (1995), and Marion & Fraccarollo (1997). Size fractions in terms of number percentage can also be converted to weight percentages (De Vries, 1971).

Measurement of erosion and deposition

Rates of erosion and deposition can be determined by sequential surveying of bed surfaces or by aerial photography. Such surveys are snapshots in time, giving only the net erosion or deposition that occurred over the time separating the successive surveys. They cannot give details of the history of erosion and deposition unless the time interval between surveys is very small. Furthermore, the accuracy of determination of rates of net erosion and deposition depends on the spatial resolution of the surveying method. Erosion rates are commonly determined by hammering metal pins into river banks or sea cliffs, and periodically measuring the amount of recession relative to the end of each stationary pin. Erosion pins will of course disturb the host material and interfere with the water flow past them. Erosion of sediment beds has been measured using metal chains fixed deep into the bed and extending onto the sediment bed. As erosion proceeds, more of the chain is exposed and streams down flow. It may then be buried with sediment. If the chain can be rediscovered, the extra length of chain streaming down flow indicates the maximum amount of erosion since it was first buried. Such scour will be a time average, and will probably record the maximum depth of scour of the troughs of bedforms that passed the site. Deposition rates can be determined by dating of buried material. Deposition rates on floodplains have also been measured by placing mats or trays on the land surface to collect sediment deposited during overbank floods.

Appendix 2: Sediment deposits

Sampling and description of sediment deposits

If sediment deposits are to be understood, they should be described in as much detail as possible, preferably in three dimensions (see Stow, 2005). Sediment deposits can be sampled directly from natural surface exposures (e.g., rocky hillsides, sea cliffs and stream banks), artificial surface exposures (quarries, road and railway cuttings, trenches), mines, and various types of cores. Field measurement of sediments and sedimentary rocks typically involves direct logging of spatial variation of sedimentary properties such as color, composition, mean grain size, stratification (geometry, type and orientation), and paleocurrent directions. Permeability might also be measured directly in the field. It is common to take overlapping photographs of large exposures to enable construction of photomosaics, which help in describing large-scale bedding geometry. Samples are taken from exposures or cores for laboratory analysis of sediment texture, bulk sediment properties, composition, and small-scale sedimentary structures. It is common for rock samples to be slabbed, etched or X-rayed in order to allow sedimentary structures to be seen. Sediment deposits can also be sampled remotely using geophysical techniques, as discussed below.

Natural and artificial exposures

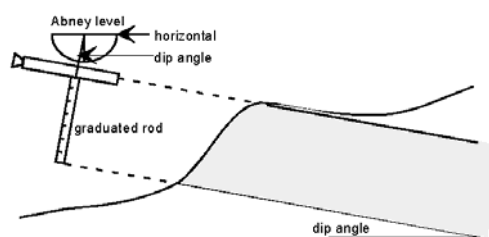


Figure A-4. *Measuring thickness of dipping strata on a walkable slope using an Abney level sliding up and down a graduated rod.*

Exposures of unconsolidated sediment can only be seen above the water table, unless water is pumped out of an excavation. Sedimentary features in fresh exposures of unconsolidated sediment become visible once the sediment dries out but before it starts to avalanche down. In the case of consolidated rocks, weathering at the Earth's surface commonly elucidates stratification and sedimentary structures. Exposures vary in quality from scattered hillside outcrops, to

continuous stream sections, to large two- and three-dimensional exposures in quarries, rail and road cuts, coastal cliffs, and dissected arid terrains.

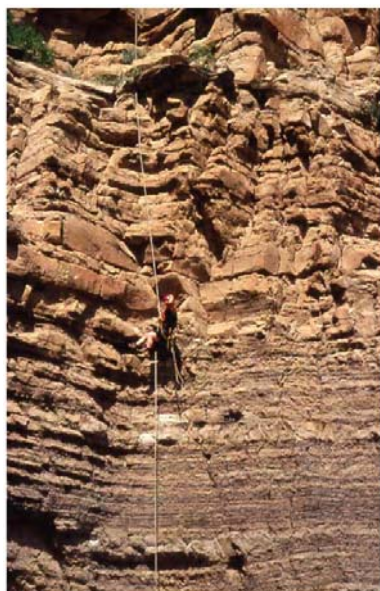


Figure A-5.
Measuring sedimentological logs on outcrops (cliffs) that cannot be walked

With large, continuous exposures of unconsolidated sediments and sedimentary rocks, a series of two-dimensional sections can be produced using photomosaics in combination with

detailed logs of the sedimentary features. Sedimentological logs normally include measurement of the upward variation through the sedimentary sequence of stratal thickness, texture, color, composition, fossils, sedimentary structures and paleocurrent directions. Measurement of true stratal thickness in dipping strata is accomplished using an Abney level on a ranging pole (e.g., Figure A-4). This, of course, cannot be done if the section

is being measured while hanging from ropes (Figure A-5). Location of positions in sedimentological logs can now be measured using differential GPS. Figure A-6 illustrates how logged sedimentary features can be represented graphically. Figure A-7 is a typical legend for sedimentological logs (used in this book), and there are many other legend designs to suit specific needs. Computer software is available for recording and displaying sedimentological logs, but, as with most software, it is not always flexible or easy to use.

When constructing photomosaics, it is necessary to minimize the distortion in the photos related to varying distance of the exposure from the camera. As a rule, the line of sight of the camera should be normal to the

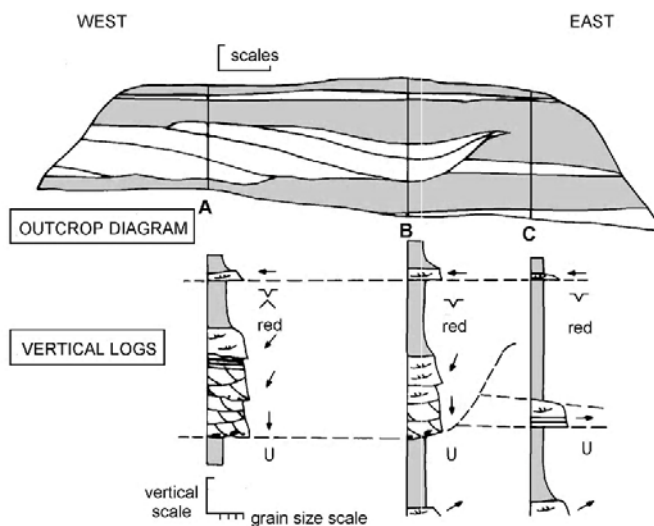


Figure A-6. *Sedimentological data obtainable from large 2-D exposures.*

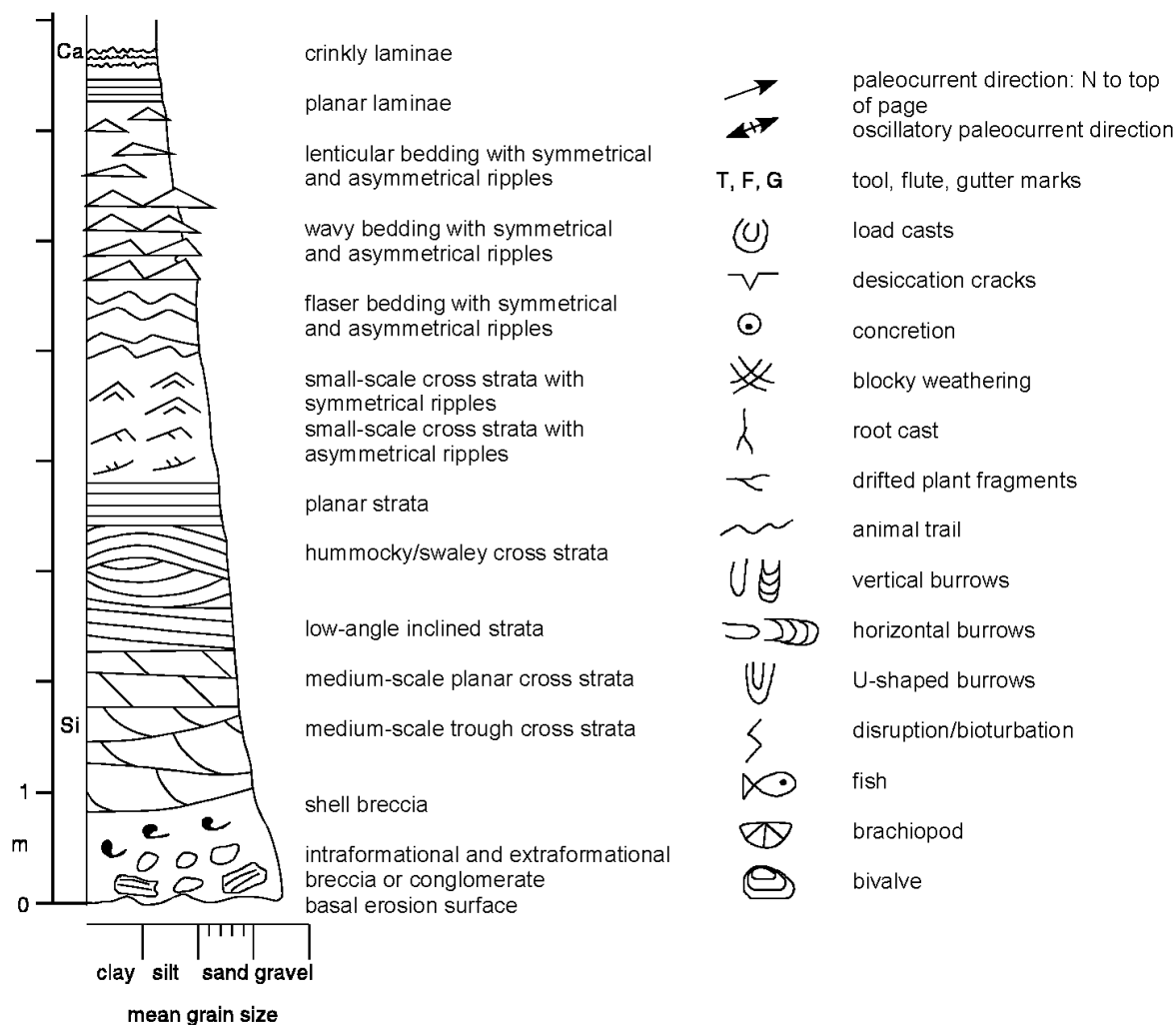


Figure A-7. Typical (recommended) legend used for sedimentological logs. The left-most column can be used for describing sediment composition (e.g. siliciclastic, calcareous). The grain-size scale is normally subdivided (e.g. very-fine, fine, medium, coarse, very-coarse sand). Additional symbols can be used as necessary. Symbols used should ideally look something like the feature it represents.

outcrop face, there should be 50% overlap of adjacent photos, and two ranging poles should be included in each frame for scale and to facilitate aligning the photos (e.g., Figure A-8). In some cases, the appropriate camera position can only be obtained from a helicopter. In order to assemble photomosaics, it is necessary to establish a datum that should be surveyed during photography, possibly using a level. A better alternative is to use GPS and a laser range-finder for proper positioning of outcrop images (e.g., Xu et al., 2002). Digital photographs or scanned photos can be assembled into photomosaics using computer software. Photomosaics are analyzed

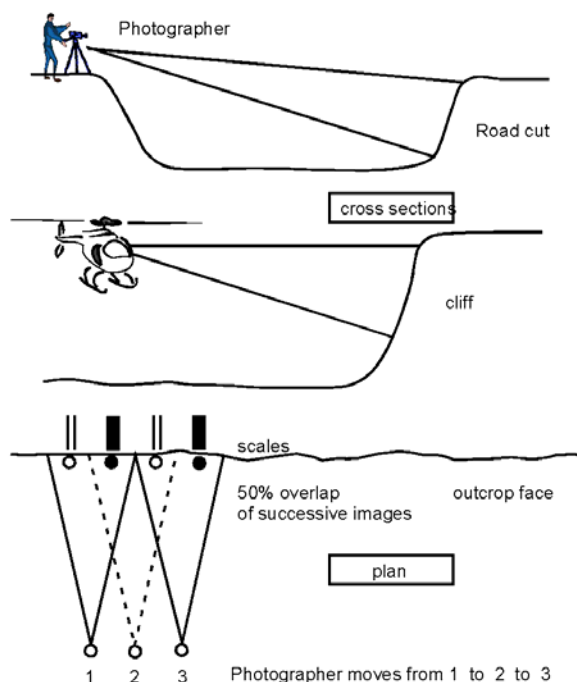


Figure A-8. *Methods of reducing optical*

Meene et al., 1979; Mendez et al., 2003) is suitable for sands, suction coring and push coring are suitable for muds, and percussion coring (hammering a tube into the ground) can be used for all sediment types. Coring can induce soft-sediment deformation, especially in high porosity, low permeability sediments (mud to fine sand). Drilling or augering of unconsolidated sediments usually results in disturbed samples. However, undisturbed samples of frozen sands and gravels in permafrost regions can be obtained either using hollow-stem augers or rotary drills. Refrigerated air or fluid can be used as a drilling fluid in order to keep the sediment frozen during coring.

in the laboratory and in the field, and it is common to construct overlays for marking surfaces and sedimentary facies.

Cores of unconsolidated sediment

Unconsolidated sediment can be sampled easily using various types of coring or drilling methods, many of which yield undisturbed samples (Figure A-9). Box corers can be used on land and under water, but most are only suitable for sands and muds (Bouma, 1969). Vibracoring (e.g., Lanesky et al., 1979; Smith, 1984, 1998) or suction coring (Van de

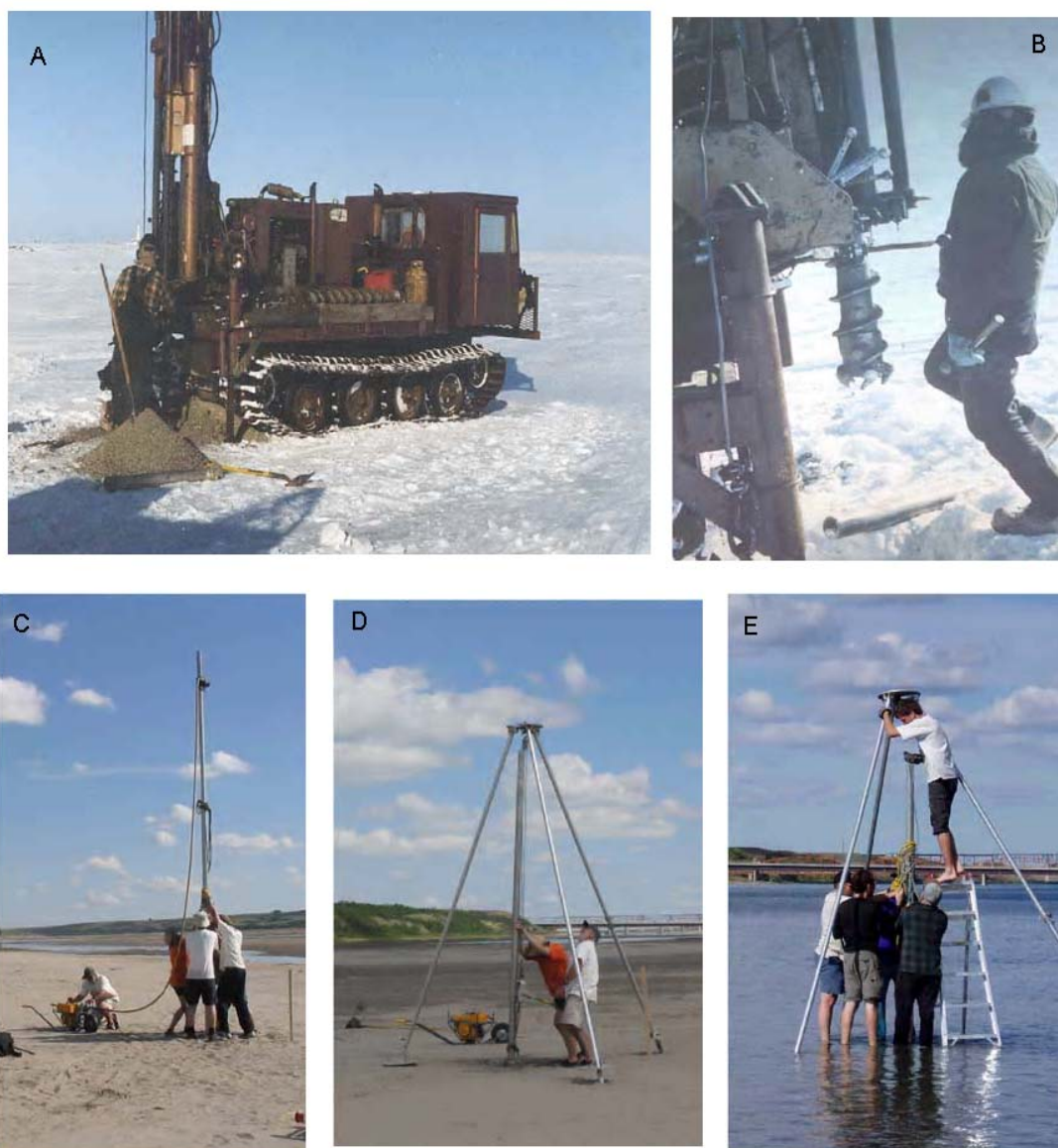


Figure A-9. Various types of soft-sediment coring operations. (A,B) Hollow stem auger drilling through frozen gravel in Alaska. (C) Vibracoring through sand. (D) Retrieving the vibracore. (E) Suction coring in sand. C to E from Saskatchewan, Canada

Peels (surface impregnations) of unconsolidated sediment surfaces can be made using various kinds of glue such as epoxy resin or polyester resin (Bouma, 1969). With peels, glue spread over the sediment surface sinks into the sediment a distance determined by the permeability of the sediment. Differences in permeability are related to texture. Thus

sedimentary structures are effectively highlighted in peels (e.g., Chapters 5 and 7). The method used to make peels is determined by the nature of the sediment surface. For vertical or near-vertical sediment faces of sand such as in trenches or cut banks, it is common to pin cheesecloth to the face and then spray or pour the glue onto the cheesecloth and sediment. The cheesecloth holds the glue and stops the sediment from falling away. Another method useable for small trenches is to pour glue between the trench face and a board that is gradually pressed up against the trench face. The glue must be stopped from escaping from the sides of the board. With cores, the glue can be poured directly on cleaned, horizontal surfaces. The choice of glue is critical for obtaining high-quality peels. The viscosity of the glue controls the method of application and the depth of penetration. The glue must ideally set quickly (few hours) in either wet or dry sediment. The resulting peel should be durable and not too brittle. The glue must also be affordable and easily available. Epoxy resin can be obtained in a variety of types to fit all applications, although it is quite expensive. Peels in sands and gravels have been made successfully using Ciba-Geigy Araldite resin GY 6010 and hardener HY 955. Shell Oil Company developed a method to vacuum-embed cores of carbonate sediment in epoxy resin (Ginsburg et al., 1966). This technique, which is still commonly used for unconsolidated or poorly consolidated carbonate sediments, allows thin sections of the epoxy-embedded sediment to be made.

Rock cores and cuttings

Rock cores are continuous, one-dimensional records of sediment accumulation, and are used to calibrate geophysical data. Mudstone strata are normally sampled much more completely in cores than in surface exposures, where they are commonly covered or excessively weathered. However, due to the large cost and difficulty of coring through solid rock, the number of high quality cores is commonly limited, as is the length of core in any given hole. Cores are typically 5 to 15 cm in diameter. Therefore, a drawback of cores is difficulty in recognition and documentation of the relatively large-scale sedimentary structures. For example, it is difficult to distinguish the various types of medium-scale cross strata, hummocky cross strata and swaley cross strata in cores. Such stratasegments are typically on the order of decimeters thick and decimeters to meters in lateral extent. Strata that are meters thick and tens to hundreds of meters in lateral extent clearly cannot be described adequately from cores. As documentation of these relatively

large-scale sedimentary structures is essential for comprehensive interpretation of the depositional environments, the level of interpretation possible from core data is limited.

Cuttings are rock chips a few millimeters in size that are produced by rock drilling, and that are circulated with the drilling mud. Examination of these chips as drilling proceeds is called mud logging. The chips can indicate rock types and yield microfossils: however, exactly where in the borehole they came from is uncertain.

Petrophysical logs

Petrophysical logs can give one-dimensional, continuous records of stratal attitude, sediment composition and texture, density, porosity, and hydrocarbon content, when the various types of log are used in combination (e.g., Asquith, 1982; Rider, 1990; Hurst et al., 1993; Doveton, 1994; Kearey et al, 2002: Figure A-10). However, the relationship between sediment type and log response may not always be clear, especially when using single log types.

Gamma-ray tools measure natural radioactivity in rocks (API units), and radioactive minerals are concentrated in clay minerals and volcanic ash. Thus, sandstone and limestone normally have a low gamma-ray value, and mudstone and shale have a high value, because of the relatively high radioactivity of clay sediments. Furthermore, gamma-ray logs are commonly used as a measure of mean grain size in sandstones, because radioactivity may increase as clay content increases with decreasing sand size.

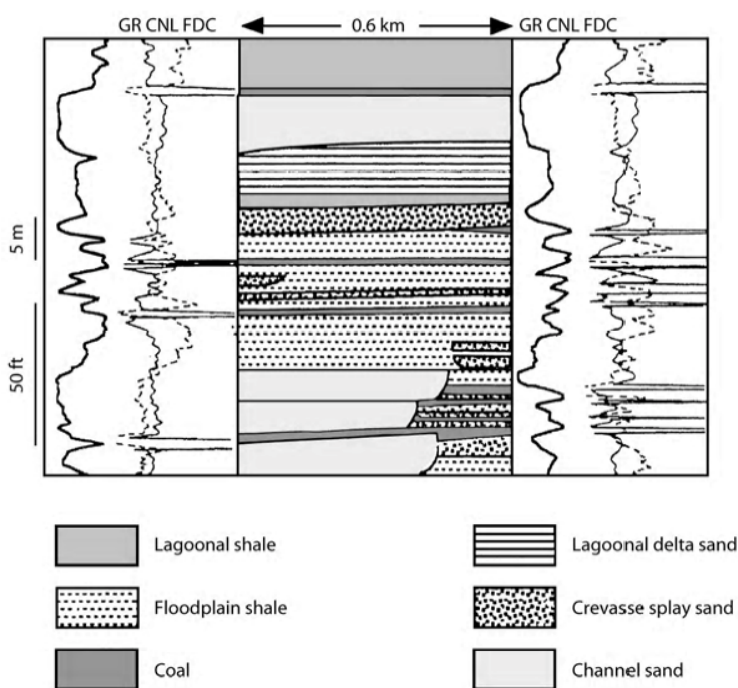


Figure A-10. Wireline logs and cores through fluvial deposits. GR = gamma ray; FDC = density log; CNL = compensated neutron log. Correlation between logs is speculative. (from Bridge, 2003).

However, radioactivity may also be high in sandstones if there are abundant claystone clasts (e.g., above some erosion surfaces) or radioactive sand grains (as with volcanoclastic sands). Coal seams may also have low radioactivity, like sandstones, but their density will be much less (as seen in density and sonic logs: Figure A-10).

Spontaneous potential (SP) logs are a record of the potential difference (in millivolts) between a moveable electrode in a borehole and the fixed potential of a surface electrode. In muddy formations, abundant cations in the saline formation water diffuse towards the drilling mud, giving a positive electrical current (a deflection to the right). In porous and permeable units such as sandstone and limestone, cations and anions diffuse from the formation water to the drilling mud, giving a net negative current (a deflection to the left). Thus, the shape of SP logs is similar to gamma-ray logs.

Resistivity, sonic and density logs are essentially measures of porosity. Most rock types have high electrical resistance in the dry state (except those with abundant clay minerals). However, formation waters are normally saline and act as electrolytes. Resistivity depends on the salinity, amount, and continuity of pore water (hence porosity and permeability). Thus resistivity is low for sandstones, limestones and dolomites, intermediate for muddy or cemented sandstones, and is high for evaporites, coal and oil. Sonic logs measure the velocity of sound through rocks, which is dependent upon formation density, hence rock type and porosity. Sonic logs are commonly run with gamma-ray logs, and are used to calibrate seismic data. Coal seams are very obvious on sonic logs because of their very low density. With formation-density logs, a radioactive source emits gamma rays that are scattered by the rock formation. The rate of scattering depends on the density of electrons in the formation, which depends on rock density, porosity, and the composition of the formation fluids. A neutron-density log uses a radioactive source that emits neutrons that collide with nuclei of the formation material, resulting in an energy loss. The greatest energy loss occurs when neutrons collide with hydrogen nuclei, as in water and hydrocarbons.

Sandstones have relatively low density, due to relatively high porosity. If gas is present in the pore spaces, the density will be even lower. The neutron-density log measures the hydrogen

ion concentration (in water, oil, or gas), and is expected to increase with increasing porosity (low density). The log gives a deflection to the left as density increases or porosity increases.

However, if gas is present in the pores of sandstones, the hydrogen-ion concentration will be relatively low, giving the impression of low porosity and high density. A difference between the density and neutron-density logs in sandstones indicates the presence of gas, the so-called gas effect (Figure A-10).

Relatively new tools such as the Formation Micro Scanner (FMS, based on high-resolution resistivity measurement) or acoustic borehole imagers can yield 3-D images of sedimentary structures and paleocurrent data. However, these tools are expensive to deploy, and data analysis requires much care and effort. Furthermore, the spatial resolution of any of these geophysical tools is controlled by the physical size of the tool, and by the volume of rock surrounding the borehole that is being sampled by the tool.

Seismic profiles

Geophysical profiling (e.g., seismic, ground-penetrating radar) gives two- and three-dimensional information on the nature of reflectors (and refractors) associated with changes in the physical properties of rocks (Kearey et al., 2002; Chapter 18). In the case of reflection seismic profiling, reflections are generated at relatively abrupt changes in acoustic impedance, and such changes are related to rock density, porosity and fluid type. Mudstones and sandstones have sufficiently large contrasts in acoustic impedance to generate reflections at mudstone-sandstone boundaries. The depth of penetration and spatial resolution of reflected seismic waves depend on the magnitude of the energy source and the degree of attenuation of the different wave frequencies. High frequencies are attenuated more rapidly than low frequencies, such that the frequency of the reflected waves decreases as depth increases. The minimum thickness of strata resolvable using this method is generally taken as a quarter of the wavelength of a reflected wave (Sheriff, 1984). For depths of penetration of 2 to 4 km, frequencies of reflected sound waves would probably be less than 50Hz. Therefore, wavelength (equal to wave velocity/frequency) would typically be $5400\text{ms}^{-1}/50\text{Hz} = 108\text{ m}$. Thus, the best vertical resolution of stratal thickness is on the order of 10^1 m (i.e., the scale of formations or members). High-frequency seismic is

restricted to the upper km of the crust, and has a best vertical resolution on the order of 10^0 to 10^1 m. Seismic records are normally processed prior to analysis, and such processing includes filtering out instrument noise, gain control, deconvolution, and migration.

Major stratal boundaries, unconformities (e.g., erosional valley margins), sets of inclined strata that are at least tens of meters thick (e.g., due to shoreline progradation), and other large disconformities such as associated with faults and intrusions can be recognized on seismic records. In addition, the lateral extent (continuity), orientation, amplitude and frequency of reflectors can be related to stratal geometry, rock type and hydrocarbon content (e.g., amplitude-versus-offset analysis). Porosity can also be derived from seismic data. Such data are most useful when cores are available for calibration. However, there are commonly problems associated with poor-quality data, multiples, and insufficient resolution of strata. It is certainly not possible to identify individual, meters-thick sandstone bodies using seismic data. However, the proportion of sandstones in a sequence of sandstone and mudstone can be related to acoustic impedance. Recent development of high-resolution, 3-D seismic methods has greatly improved the ability to describe subsurface deposits. For example, amplitude analysis of 3-D seismic time slices (Weber, 1993; Brown, 1996; Weimer and Davis, 1996; Posamentier and Kolla, 2003: Chapter 13 and 18) can yield information on the location, orientation, width, planform and thickness of ancient sandstone bodies. The advantage of 3-D seismic over 2-D seismic is related to the much denser survey grid for 3-D seismic (e.g., 25 m spacing). This results in improved recognition of reflections, but cannot increase the vertical resolution. Thus, sandstone bodies less than about 10 m thick still cannot be resolved using seismic methods.

Ground penetrating radar profiles

Ground-penetrating radar (GPR) profiling is a high-resolution, shallow-subsurface geophysical technique analogous to seismic reflection, but using electromagnetic radiation with frequencies typically 10 to 1000 MHz (reviews in Bristow and Jol, 2003; Neal, 2004). The velocity of radar waves is dependent mainly upon the dielectric permittivity, which in turn is controlled mainly by water content (Table A-1; Davis & Annan, 1989). As water content varies significantly between adjacent strata, GPR is particularly useful for imaging sedimentary strata.

Table A-1. Electrical properties of different materials

| Material | Dielectric permittivity (K) | Radar velocity (m/ns) | Conductivity (mS/m) | Attenuation (dB/m) |
|-----------------|--|----------------------------------|--------------------------------|-------------------------------|
| Air | 1 | 0.3 | 0 | 0 |
| Freshwater | 80 | 0.033 | 0.01 | 0.1 |
| Seawater | 80 | 0.01 | 30,000 | 1000 |
| Ice | 3-4 | 0.16 | 0.01 | 0.01 |
| Dry sand | 3-5 | 0.15 | 0.01 | 0.01 |
| Wet sand | 20-30 | 0.06 | 0.1-1.0 | 0.03-0.3 |
| Clay | 5-40 | 0.06-0.9 | 1-1000 | 1-300 |

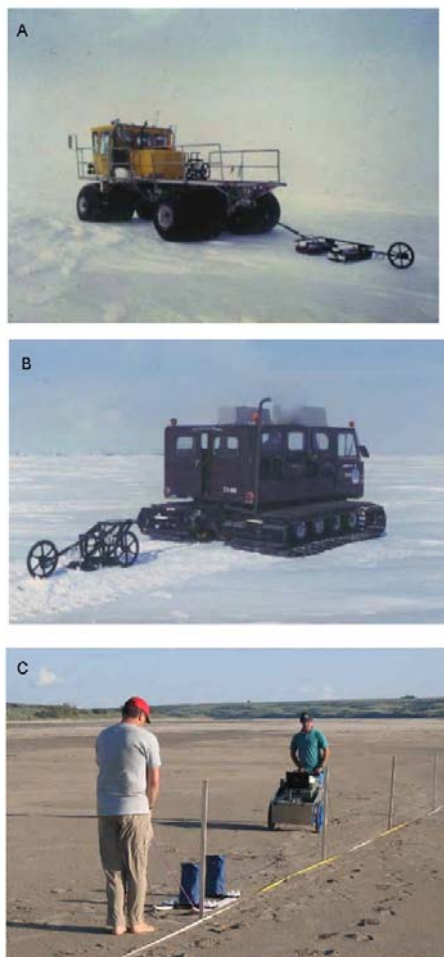


Figure A-11. GPR surveying. (A,B) Towing GPR antennae over a frozen river in Alaska. (C) GPR surveying in Saskatchewan, Canada

GPR reflection profiling involves pulling transmitting and receiving antennae mounted on a sled along a profile line (Figure A-11). Processing of radar records is accomplished using methods similar to seismic processing (see above). The records must also be corrected for land-surface topography. Use of 2-D and 3-D GPR in stratigraphic studies of dry, saturated and frozen sand and gravel (and equivalent rock) has resulted in depth of penetration up to 30 meters, and resolution of reflectors with a vertical spacing of decimeters. Radar facies based on the amplitude, shape, orientation and continuity of reflections can be recognized and linked directly to sedimentological characteristics seen in cores and trenches (e.g. Chapter 13). Thus, when combined with coring or trenching, GPR is a powerful technique for documenting large-scale stratal geometry and lithofacies variation in 3-D. If permeability and porosity can also be determined from the strata, GPR data can be used to help build subsurface fluid-flow models.

The ability of GPR to image sedimentary strata is dependent upon the depth of signal penetration and the resolution required. Both of these properties are primarily dependent upon the center frequency of the radar antennae. As the center frequency increases, the depth of penetration decreases but the reflections are more finely resolved. Vertical resolution of features larger than $1/4$ wavelength is theoretically possible (Reynolds, 1997): therefore, greater resolution is achieved at higher frequencies as the pulse wavelength decreases. Signal loss due to wave scattering and absorption is greater at higher frequencies, leading to a decrease in signal penetration depths. Thus, there is a trade-off between

signal penetration depth and vertical resolution that is dependent upon the choice of antenna frequency. Signal penetration depth depends on the GPR unit's performance, signal attenuation and energy loss factors such as signal scattering, geometrical spreading, and energy absorption at reflection interfaces (Reynolds, 1997).

The vertical variation of radar velocity at a location is normally measured using common-mid-point (CMP) analysis. Here, the transmitting and receiving antennae are moved away from a point on the surface in opposite directions at equal distances until no more signals are recorded. Cross-hole tomography makes use of borehole radar instruments that are moved up and down in adjacent boreholes. This method produces the radar velocity field in the 2-D plane between the boreholes.

Resistivity profiles

Electrical-resistivity ground imaging (ERGI) is a relatively new technique for geophysical profiling of the shallow (depth < 200m) subsurface (Reynolds, 1997; Baines et al., 2002). Using four electrodes connected to steel stakes stuck into the ground, ERGI makes measurements of the resistance to electrical current flow through the ground. Measurements of resistivity along a profile line are made using a large array of electrodes in which the computer-controlled positions of the four active electrodes are repeatedly switched around in order to collect data points at different depths and distances along the profile. These data are then used to reconstruct the 2D resistivity distribution beneath the profile line using inversion and forward modeling software. This is a significant advance over DC-Resistivity, the precursor to ERGI, which required manually moving the four electrodes for each measurement. The depth of measurement is about 20% of the length of the survey line, and the resolution is approximately half of the electrode spacing. For example, an array of 28 electrodes with 1 m spacing will allow a measurement depth of about 5 m with a resolution of about 0.5 m.

Resistivity depends on properties of Earth materials such as rock and sediment composition, grain size, water content, and chemical composition of that water. For unconsolidated sediments, resistivity generally decreases with grain size. However, resistivity is

also influenced by the proportion and chemistry of the groundwater. For example, gravel with pores that are completely filled with water will have lower resistivity than a similar gravel with air-filled pores. ERGI is particularly useful for delineating relatively large bodies of gravel and sand (such as channel belts) within silt and clay, and vice versa. ERGI is a useful complement to GPR, in that highly conductive materials such as clays attenuate GPR signals.

Sampling volume of cores, geophysical logs and profiles

Subsurface data from cores, well logs and geophysical profiling represent an extremely small sample of the volume of rock of interest (North, 1996). Therefore, analysis of subsurface data must be considered as dominantly interpretive rather than descriptive. This is also true of deductions about shallow subsurface geology from surface outcrops.

Direct measurement of sediment properties

Modern methods of direct measurement of sediment properties are reviewed in books by Bouma (1969), Carver (1971), Lewis (1984), Tucker (1988), and Stow (2005).

Composition

Direct observations of the chemical and physical properties of sedimentary minerals are commonly made in the field with the help of a hand lens, knife, magnet, geiger counter, and bottle of dilute hydrochloric acid. Optical properties of sedimentary minerals in thin sections examined under the petrographic microscope were traditionally used to determine their approximate composition (useful reference books are Adams and MacKenzie, 1998; Adams et al., 1984; Scholle, 1978, 1979; Tucker, 2001). Optical examination of thin sections now focuses primarily on the texture and fabric of the sediments, with X-ray diffraction analysis used to determine mineral composition, particularly for feldspars, clays and calcium carbonate grains. The scanning electron microscope (SEM) is also routinely used to provide information on the texture and fabric of fine-grained sediments, particularly clays and mudstones (e.g. Bennett et al., 1991). SEMs equipped with X-ray dispersive capabilities can provide major and minor element

Table A-2. Heavy mineral associations linked to source rocks

| Source Rocks | Heavy minerals |
|------------------------|---|
| Reworked sediments | Rutile, tourmaline, zircon (well rounded) |
| Low-grade metamorphic | Biotite, chlorite, muscovite, spessartite garnet, tourmaline |
| High-grade metamorphic | Actinolite, andalusite, apatite, almandine garnet, biotite, diopside, epidote, clinozoisite, glaucophane, hornblende, ilmenite, kyanite, magnetite, muscovite, sillimanite, sphene, staurolite, tourmaline, tremolite, zircon |
| Felsic igneous | Apatite, biotite, hornblende, ilmenite, monazite, muscovite, rutile, sphene, tourmaline, zircon |
| Mafic igneous | Augite, diopside, epidote, hornblende, hypersthene, ilmenite, magnetite, olivine, oxyhornblende, pyrope garnet, serpentine |
| Pegmatites | Apatite, biotite, cassiterite, garnet, monazite, muscovite, rutile, tourmaline |
| Volcanic ash | Apatite, augite, biotite, hornblende, zircon (euhedral crystals) |

compositions. Other, more sophisticated methods of chemical analysis are used to get major, minor, and trace elemental compositions of minerals. These instruments include electron microprobes, ion microprobes, and Raman spectroscopy. Elemental mass spectrometers provide information on the isotopic composition of various elements. Sedimentologists have focused on the isotopic distributions of carbon, oxygen, sulfur, and strontium.

Heavy minerals are accessory terrigenous minerals with density greater than 2800 kg m^{-3} . They are used to indicate source rocks of terrigenous sediments, and the degree of chemical alteration and physical abrasion that sediment grains have undergone. As heavy minerals are accessory minerals (commonly less than 1% by volume), they are usually concentrated prior to analysis. This involves disintegration of the sedimentary rock, and separation of heavy minerals from the light minerals using a heavy fluid such as bromoform or tetrabromoethane. Certain groups of heavy minerals can be distinguished using magnetic methods. However, heavy minerals are normally identified from their optical properties observed in whole-grain mounts. It is very difficult to identify minerals in grain mounts, and this seems to be a dying art. If there are enough heavy minerals in a sample, it may be possible to make a thin section for examination under a petrographic microscope, and to use X-ray analysis or electron probes. Normally, heavy minerals in different size ranges are identified, because heavy-mineral composition is dependent on grain size. Analysis of heavy minerals involves identification of characteristic associations of minerals, and linking them to source rock types (e.g., Table A-2). In some cases, a specific species of a mineral can be matched with a specific rock type. This type of analysis requires extensive background knowledge of mineralogy and petrology of all rock types.

Calcium-carbonate grains in limestones are recognized by their softness and effervescence in dilute hydrochloric acid (for aragonite and calcite). Stains are commonly used to distinguish calcium-carbonate grains with varying amounts of Fe and Mg in addition to Ca. Alizarin Red S indicates the presence of Mg, and Potassium Ferricyanide indicates the presence of Fe. These two stains are commonly used together as follows:

| | Alizarin Red S | Potassium Ferricyanide | Both stains |
|----------------|-----------------------|-------------------------------|--------------------|
| Calcite | red | no color | red |

| | | | |
|--------------------|----------|-----------|-----------|
| Fe calcite | red | blue | mauve |
| Dolomite | no color | no color | no color |
| Fe dolomite | no color | pale blue | pale blue |

The relative amounts of Mg and Ca can be determined using X-ray diffraction. Different generations of calcium-carbonate cement are distinguished using luminescence.

Density

Density of minerals can be deduced from knowledge of composition. Density can be determined directly by measuring the weight of a grain in air and then in a fluid such as water. The density of the grain is equal to the density of water (1000 kg m^{-3}) divided by $1 - (\text{weight in water}/\text{weight in air})$. Another way is to immerse a grain in fluids of progressively increasing density, and determine in which density fluid the grain just floats. Bulk density of subsurface rocks is routinely calculated from petrophysical logs.

Color

Color of sediments and sedimentary rocks should be defined based on a defined scale, such as the GSA color chart based on the Munsell system. This system recognizes three main aspects of color: hue, value (lightness), and chroma (degree of saturation). Each of these properties is given a numerical value. For example, grayish-red sediment is designated as 10 R 4/2. The 10 R is the designation of the hue (red). Number 4 is lightness, on a scale from 9 (lightest) to 1 (darkest). Number 2 is the chroma, on a scale of 2 to 6 with the most vivid color having the highest value. Wet sediments are darker than dry sediments, but wetness does not influence hue or chroma.

Size

Sediments contain a range of different grain sizes. Grain size is difficult to define for non-spherical grains, and the definition used depends on the method of measurement. The grain-

size scale used is normally a geometric scale, whereby the size intervals are obtained by multiplying or dividing by a constant factor (remember that the scale divisions of arithmetic scales are obtained by adding or subtracting a constant factor). Geometric scales have larger class intervals for larger grains, and smaller class intervals for smaller grains. They are used because a change in grain size from 100 mm to 101 mm is not considered as important as a change in grain size from 1 mm to 2 mm. One type of geometric scale used by sedimentologists is the phi scale, where phi is defined as

$$\phi = -\log_2 D \quad (\text{A-1})$$

$$D = 2^{-\phi} \quad (\text{A-2})$$

in which D is grain diameter in millimeters. Here, the multiplying or dividing factor is 2, and the negative sign means that the largest grains have the smallest phi values (which is peculiar). The phi scale is divided into Wentworth size classes: gravel, sand, and mud, and these terms are further subdivided as shown in Table A-3. Therefore, if the mean size of sand is between 3 and 4 phi, it would be called very fine sand. Classification of sediment based on size characteristics is discussed more fully below.

Methods of measuring the size of sediment grains include: comparison of sediment samples with sediment of known mean size (and sorting in some cases); direct measurement of individual grains (loose gravel); sieving (loose sand and gravel); settling tubes (loose sand and mud); laser diffraction (loose sand and mud), and; measurement of grains in cut sections (consolidated sand and gravel) (Carver, 1971; Tucker 1988; Syvitski, 1991; Table A-3). The mean size of loose or consolidated sediment is commonly estimated by comparing samples with sediment samples of predetermined size (grain-size comparators). This method is essential for field description of sediments, but does not give a grain-size distribution. The shape of a non-spherical grain is normally approximated by a regular triaxial ellipsoid, allowing the definition of three orthogonal axis lengths (Figure A-12A). These three lengths can be used in various combinations to define measures of grain size and shape (Figure A-12B). This type of size analysis is normally only performed on gravel grains where the three axis lengths can be measured easily.

The most common grain-size measuring technique for unconsolidated sand and fine gravel is sieving. Stacks of sieves, with the mesh size decreasing downwards in each stack, are shaken in a mechanical sieve shaker for a fixed time interval, normally 10 to 15 minutes. The total number of sieves used is commonly between about 10 and 20, with more sieves used for higher grain-size resolution and for samples with a large range of sediment sizes. Careful preparation for sieving is necessary. The sieves must be clean, such that old sediment stuck in the mesh is not added to the sample. The bane of the siever is if the previous user (normally a student) did not clean the sieves properly. The amount of sediment on each sieve must be small enough to allow free passage of sediment through the mesh. Guidelines for the maximum amount of sediment allowed to be retained on a sieve are given by Carver (1971) and Tucker (1988). In general, the maximum weight of sediment allowed on each sieve is a few tens of grams, such that the maximum total weight of the sample will be on the order of hundreds of grams. Therefore, sediment samples may need to be split (see Carver, 1971, for details). As mentioned above, some sandy-gravel samples must be kilograms in weight, in order that the largest gravel grains do not bias the sample. The gravel fraction in these samples may need to be measured by hand, and the sand fraction will always need to be split prior to sieving. The sediment retained on each sieve is carefully and systematically removed from the sieve and weighed. The weight retained on each sieve is the weight in the size range from the mesh size of the retaining sieve to the (larger) mesh size of the sieve above. The mesh sizes of standard sieves follow the phi scale, with the sizes being whole numbers, or halves, or quarters on the phi scale. The grain size measured by sieving is actually some measure of the least cross-sectional area of a

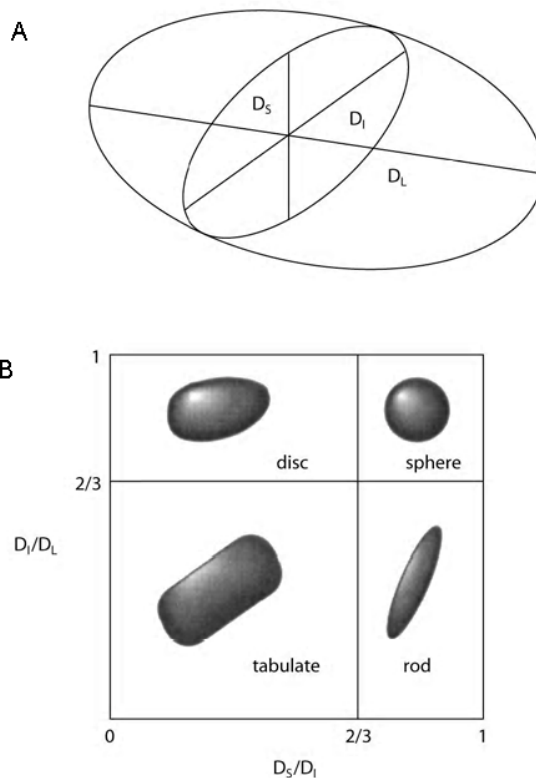


Figure A-12. Definitions of grain shape. (A) Triaxial ellipsoid with three orthogonal axis lengths indicated. (B) Classification of grain shapes using ratios of axis lengths.

grain, but is commonly assumed to be equivalent to the intermediate grain diameter (D_I in Figure A-12A).

The velocity of fall of a grain in a still fluid of lesser density than the grain is an important property that is related to the nature of sediment transport. When a grain falls in a viscous fluid, it experiences fluid drag that increases as the fall velocity increases (see Chapter 5). The terminal fall velocity (or settling velocity) is the constant velocity attained when the fluid drag on a falling grain is exactly balanced by the immersed weight of the grain. The terminal fall velocity depends on the density and viscosity of the fluid, and the size, shape and density of the grain. Therefore, the terminal fall velocity can be related to grain size if the other parameters can be determined. Terminal settling velocity is routinely measured in order to determine the grain size of muds and the finer sand sizes.

Terminal settling velocity is measured in a settling-tube full of water. The water is kept at constant temperature so that its viscosity and density can be determined. The density of the sediment can either be measured or assumed to be quartz density (2650 kg m^{-3}). A sample of unconsolidated sediment is introduced at the top of the settling tube, and the length of time taken for the various grains to settle a fixed distance is recorded. Either the volume or the weight of grains that have reached the fixed point is measured at fixed time intervals. This gives the cumulative volume or weight of grains that exceed a given settling velocity (or grain size). As time progresses, the settling velocity (grain size) of the grains reaching the point decreases. The measured settling velocity is related to grain diameter using either theoretical equations (Stokes Law, applicable to grains less than 0.1 mm in water: Chapter 5) or empirical equations. These equations normally require knowledge of grain shape and density, which can be difficult to measure accurately for all grains. Therefore, it is commonly assumed that the grains can be approximated as quartz-density spheres, resulting in an *equivalent diameter* that is actually a combined measure of size, shape and density.

There are some significant caveats associated with measurement of terminal settling velocity and in determining grain size from it. First, it is common practice to disperse cohering mud particles prior to insertion in a settling tube. However, as the original muds may actually

have been transported and deposited as pellets or flocs, the grain size of individual clay minerals is not relevant. Second, the equations that relate grain properties to terminal settling velocity are strictly applicable only to the settling of single grains in fluids of “infinite” extent: that is, there should be no interference from the walls or other settling grains (resulting in hindered settling – see Chapter 5). Therefore, introduction of a relatively large concentration of grains at the top of a settling tube is a potential problem, and special techniques must be used for introducing the grains. It must also be assumed that settling grains reach their terminal settling velocity very quickly after being introduced. Third, the assumption that silt and clay grains can be approximated as quartz-density spheres is commonly not a good one. Fourth, it is difficult to measure the settling velocity of the largest grains (that settle very quickly, in seconds) and the smallest grains (that settle very slowly, possibly days).

Laser diffraction techniques have been used recently for grain size analysis, and there are at least three manufacturers of these instruments. This method is based on the principle that particles scatter (diffract) light at certain angles based on their size, shape, and optical properties. Commercial measuring equipment has complicated optical processors and sensors, and the nature of particle dispersion and the concentration of particles in the dispersion are critical. Grain size is calculated from the diffraction pattern using the Fraunhofer and Mie theories, and the calculations assume the diffraction pattern is due to single scattering events by spherical particles. The size calculated is that of the sphere with the same diffraction pattern as the particle measured. The advantages of this technique include ease of operation, large range of detectable particle sizes (0.04 to 2000 microns), accuracy, and reproducibility. However, the non-spherical nature of many natural grains, particularly the plate-like clay minerals, means that there will be differences in the grain size analyses done by different techniques (Syvitski, 1991). The laser diffraction technique apparently underestimates the proportion of clay minerals.

Measurement of the grain size of sedimentary rocks, from which the grains cannot be disaggregated, is normally undertaken by cutting sections through the rocks. Thin sections can be examined under a petrographic microscope and can be projected onto a screen. However, a recent variant of this technique is to examine either thin sections or cut sections using image-analysis software on a computer (Seelos and Sirocko, 2005). These methods of determining grain

size suffer from the fact that the sections give random slices through grains that may have a preferred orientation in the rock. Therefore, sections through the edges of grains will make grains appear small, and the apparent sizes of non-spherical grains may well vary among sections cut parallel and normal to stratification. There is no unique solution to this problem, and, as with all measuring techniques, the method of measurement should be standardized and the results should not be compared with results using other techniques. A common method is to measure the apparent long axes of 200 to 500 grains at intersection points on a grid, resulting in numbers of grains in particular size ranges. However, it may be possible to measure all of the grains in a section, especially with computerized methods. It is desirable to find empirical relationships between grain-size distributions measured in different ways by measuring a given set of sediments using the different methods. Grain-size comparators are also available for sections through sedimentary rocks, in order to estimate mean grain size and sorting.

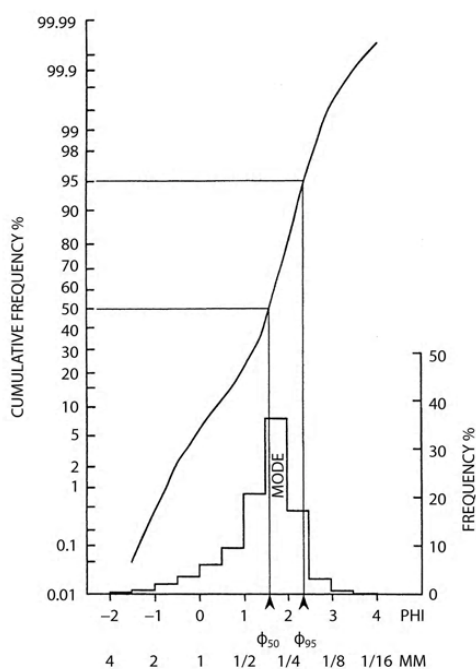


Figure A-13. Histogram and cumulative frequency curve of grain size distribution. The 50 and 95 phi percentiles are shown. The cumulative frequency is drawn using a Gaussian probability scale.

The end point of grain-size measurement is frequency distributions of weights, volumes or numbers of grains in a particular range of sizes. These are appropriately presented as histograms and cumulative frequency curves (Figure A-13). The logarithm of grain size is normally used, and sedimentary geologists use the phi scale discussed above, such that the largest grain sizes occur on the left-hand side of the graph. The frequency scales may be arithmetic, but the cumulative frequency scale is commonly a Gaussian probability scale. If the grain-size distribution is log-Gaussian, the cumulative frequency curve will be a straight line. However, natural grain size distributions are rarely log-Gaussian (Bridge, 1981). The probability scale expands the tails of cumulative distributions, which is considered to be advantageous by some

workers. Other types of scales can be used to plot cumulative frequency curves in order to test whether the distribution follows a specific distribution equation (e.g., log-Gaussian, Rosin, double-exponential).

The shapes of grain-size histograms and cumulative frequency curves should be described qualitatively, because they suggest the relative values of parameters of the distributions such as standard deviation (size range or sorting), skewness (asymmetry), and kurtosis (peakedness). The number and location of peaks (modes) should be described, as should the nature and position of marked changes in slope of cumulative frequency curves (Middleton, 1976; Bridge, 1981). It has been suggested that cumulative grain-size distributions can be subdivided into several straight-line segments, each one representing a log-Gaussian sub-distribution, and that these sub-distributions are related to mechanics of sediment transport and deposition, and to depositional environments. These concepts have now been substantially discredited.

The median, mean, standard deviation, skewness, and kurtosis of the grain-size distribution are represented by D_{50} , D_m , D_{sd} , D_{sk} , D_{ku} , respectively. These parameters of the distribution can be calculated from combinations of percentiles (e.g., ϕ_{50} , ϕ_{95} ; Figure A-13) determined from the cumulative curve, or using raw data by the method of moments (Tucker, 1988). Expressions for the distribution parameters using percentiles are:

$$\text{Mean, } \phi_m = (\phi_{16} + \phi_{50} + \phi_{84}) / 3$$

$$\text{Standard deviation, } \phi_{sd} = [(\phi_{84} - \phi_{16}) / 4] + [(\phi_{95} - \phi_5) / 6.6]$$

$$\text{Skewness, } \phi_{sk} = [(\phi_{16} + \phi_{84} - 2\phi_{50}) / 2(\phi_{84} - \phi_{16})] + [(\phi_5 + \phi_{95} - 2\phi_{50}) / 2(\phi_{95} - \phi_5)]$$

Other equations use different percentiles. Why use these particular percentiles in the equations? This is a long story involving a need for a wide range of percentile values, and (unjustified) assumptions about the log-Gaussian nature of grain-size distributions.

The best way of determining distribution parameters is non-graphical, and is the method of moments. This method uses all of the measurements used to define the distribution. Equations for the distribution parameters are:

$$\text{Mean, } \phi_m = \sum (f m) / 100$$

$$\text{Standard deviation, } \phi_{sd} = \sqrt{[\sum (f m^2) / 100 - \phi_m^2]}$$

$$\text{Skewness, } \phi_{sk} = [\sum (f m^3) / 100 - 3\phi_m \sum (f m^2) / 100 + 2\phi_m^3] / \phi_{sd}^3$$

in which f is weight percent in each phi interval and m is the mid point of each phi interval. Normally, the method of moments and the graphical percentile method give similar values for the mean and standard deviation, but the moment method gives more accurate skewness and kurtosis. Calculations of grain-size distribution parameters are usually done on a computer.

Shape

Grain shape encompasses the surface texture, roundness, sphericity, and “form” of grains. Surface texture refers to the various indentations on the surface of sediment grains, ranging from the straight striations on pebbles from glacial environments, to the “frosting” of sand grains in desert environments. Such textures arise from physical contacts with other grains and by chemical etching. Microscopic marks are well shown using scanning electron microscopy, and specific types (e.g., upturned plates, v-shaped notches) have been ascribed to specific physical impact mechanisms.

Roundness is concerned with the curvature of the corners of grains, and is defined as either average radius of corners / radius of maximum inscribed circle or minimum radius of corners / radius of maximum inscribed circle. Thus, roundness ranges from near zero (very angular grains with many small corners) to unity (well rounded grains with no corners). Roundness might be measured by comparing a projected grain image with a template containing circles of varying radius. Such a time-consuming activity requires superhuman dedication and perseverance. Some workers even digitize the perimeter of sediment grains and perform Fourier

and fractal analysis on these wavy lines. In the interests of sanity, roundness is commonly estimated by comparison with grain images of known roundness (Figure A-14).

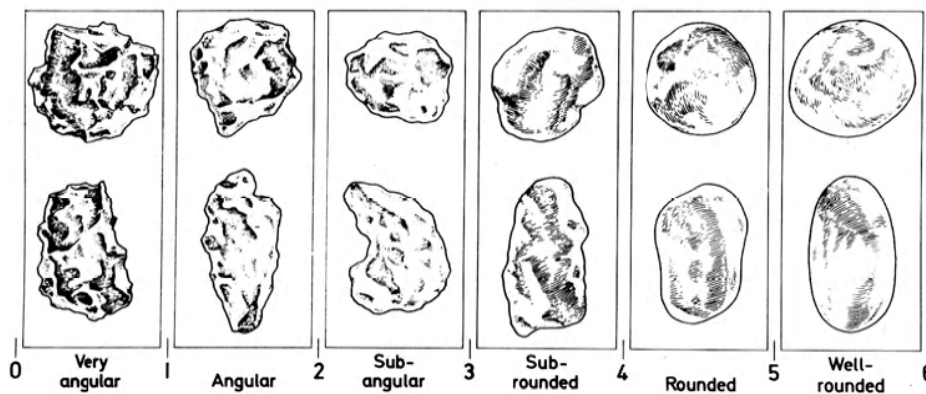


Figure A-14. Template for grain roundness (based on Powers, 1953).

Sphericity is the degree to which a grain approaches the shape of a sphere. Sphericity is defined in two main ways, both of which assume that a non-spherical grain can be approximated by a triaxial ellipsoid with short axis a , intermediate axis b , long axis c , and volume $\pi abc/6$:

$$\text{Sphericity} = \sqrt[3]{(abc) / c}$$

which represents the diameter of a sphere with the same volume as the grain divided by the diameter of the circumscribing sphere;

$$\text{Maximum projection sphericity} = a / \sqrt[3]{(abc)}$$

which represents the diameter of the sphere with the same projection area as the particle (the inscribed sphere) divided by the diameter of the sphere with the same volume as the particle. The Corey shape factor, commonly used by engineers, is also a sphericity measure, and is given by $a / \sqrt{(bc)}$. All of these sphericity measures range from zero (far from spherical) to unity (spherical). Many natural grains have a sphericity around 0.7.

Sphericity does not adequately account for the effect of grain shape on the behavior of a grain during transport. The “form” of a grain, defined by ratios of the axis lengths of a triaxial ellipsoid (Figure A-12B), is possibly a better shape measure. Grains that are disc-shaped, tabular, or rod-shaped behave differently during transport, but Figure A-12A shows that these different

forms may have the same sphericity. However, both sphericity and form are difficult to measure for grain sizes smaller than gravel. Other shape measures that are supposedly related to their behavior during transport include rollability and pivotability. It is probable that no single shape measure sufficiently determines the transport behavior of sediment grains.

Packing

Packing, a bulk property of sediment, is the relative spacing of grains of different size and shape. Packing is controlled by depositional mechanics and subsequent diagenetic changes. Packing influences porosity and permeability, along with grain size, shape and orientation. For example, the closest possible (rhombohedral) packing of equal-sized smooth spheres has a porosity of 26%, whereas the loosest possible (cubic) packing has a porosity of 47.6%. In

sediments with a large amount of fine-grained sediment relative to coarse-grained sediment, the coarse grains may be separated from each other by the “matrix” of fine-grained sediment, and do not form a “framework”. This is typical of debris-flow deposits, most bioturbated sediments, and glacial lodgement till composed of mixtures of mud, sand and gravel, and such sediments have low permeability. In other sediments, the larger grains are in contact with each other and form a framework within which smaller grains can occur. Sediments with minor amounts of fine-

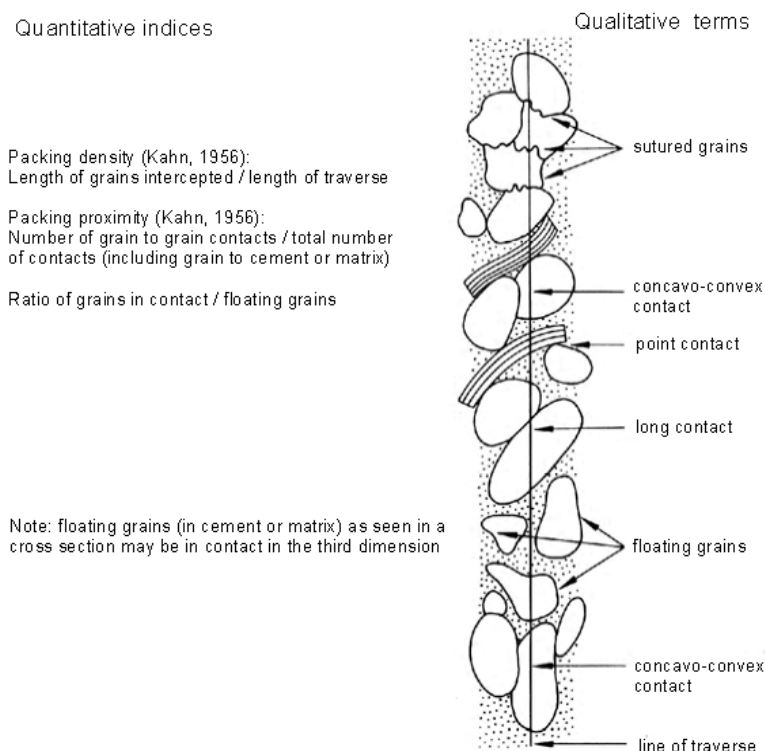


Figure A-15. Grain packing terminology (from Pettijohn et al., 1972).

grained sediment within the pore spaces between the framework grains are referred to as “open-framework”, as opposed to “closed framework”. Open-framework gravels have extremely large permeability.

Packing is difficult to measure. Kahn (1956) devised two measures of packing, as determined along linear traverses (Figure A-15). Packing density is the total length of grains (i.e., excluding pore space or cement) / total traverse length, and is a measure of the porosity of a sediment free of cement or fine-grained material in pore spaces. Packing proximity is the number of grain-grain contacts/total number of grains. Types of grain-to-grain contacts can also be described as tangential, long, sutured, concavo-convex (Figure A-15).

Grain orientation

Non-spherical grains can be oriented on the sediment bed by a depositing current, or after burial by tectonic forces. For example, elongate grains may be oriented parallel or normal to depositing currents, and discoidal and tabular grains can be oriented with their largest side dipping either upstream (imbrication) or downstream (pseudo-imbrication). Depositional grain orientation can indicate paleocurrent direction. Also, the long axes of non-spherical grains can be oriented normal to maximum compressive stress within the crust. Permeability is normally greatest in the direction of grain orientation.

It is difficult to measure the 3-D orientation of grains, but easier to measure the orientation of two orthogonal planes. It is common to measure only the orientation of long axes of grains, or the orientation plus the inclination. Such data can be plotted on circular histograms or stereographic projections in order to detect preferred directions (see section below on paleocurrent analysis).

Porosity

Porosity is a fundamentally important bulk property of sediments that determines the amount of fluid that can be stored. Porosity is defined as the volume of void space divided by the total volume of grains plus void space. Primary porosity is due to the void spaces between grain, whereas secondary porosity includes void spaces produced during diagenesis (dissolution, recrystallization) and tectonism (fracturing). Effective porosity (as opposed to total porosity) is that due to connected void spaces from which fluid can be removed under vacuum. Effective porosity can be measured easily in the laboratory by removing fluid from a saturated sediment (under vacuum), or adding fluid to a sediment that is completely dry. Subsurface porosity is routinely calculated from a range of petrophysical logs (see above). Porosity can be visualized by scanning a sediment using image-analysis software, or by filling the pore space with a solidifying agent and then dissolving the grains.

Permeability and hydraulic conductivity

Permeability and hydraulic conductivity are measures of the ability of fluids to flow through unconsolidated sediments or rocks, dependent on the size and connection of void spaces, and the physical properties of the fluid. Permeability, k (darcys or m^2), is defined by Darcy's law as:

$$k = Q\mu / (\partial p / \partial x)$$

where Q is the fluid discharge through unit cross section of sediment or rock, μ is fluid viscosity, and $\partial p / \partial x$ is the fluid pressure gradient in the flow direction. Hydraulic conductivity is defined as

$$K = k\rho g / \mu$$

in which g is gravitational acceleration (9.81 ms^{-2}), ρ is fluid density, and K has units of ms^{-1} .

Permeability can be measured in the laboratory by directly measuring the discharge of water through a sample. The simple measuring apparatus is a cylinder with an internal cross sectional area A that contains a sample with length L . The sample rests on a mesh disc that fits tightly in the tube that in turn rests on large glass beads or small pebbles in the bottom of the

tube. A flexible tube extends from the base of the sample cylinder and is clamped at a measured distance h below the top of the sample cylinder. The end of this bottom tube is pinched off until the measurement starts. The sample cylinder is filled with water until it starts to overflow, and the water supply is maintained. The end of the bottom tube is unpinched so that water can flow through the sample and into the measuring cylinder while the water level at the top of the sample cylinder is maintained. The discharge Q is calculated by timing the rate of change of volume in the measuring cylinder. Permeability can then be calculated directly using Darcy's law re-written as

$$k = Q\mu L / \rho g A h$$

This method only works if the flow through the sample is laminar. This can be tested by varying the head h and repeating the experiment. If Darcy's law holds, the permeability should not vary with flow conditions. Flow through highly permeable sediment like open-framework gravel may be turbulent unless the discharge (and head) is very small. This type of equipment is called a constant-head permeameter. Permeability can also be measured with a falling-head permeameter in which the head decreases with time. Calculations for this method are a little more complicated.

Another method of measuring permeability, in the field and laboratory, is the portable minipermeameter (e.g. Hartkamp-Bakker and Donselaar, 1993). Gas is injected into permeable sediment using a hand-held probe with a small (say 2 mm diameter) tip-seal opening. The injection pressure and the flow-induced pressure differential are recorded by a micro-manometer, and used to calculate gas flow rate using Darcy's law. Permeability values are then calculated from a series of calibration curves. This method cannot be used if gas flow is turbulent. The permeability measured is that of a hemispherical volume of rock with a radius about twice that of the tip-seal diameter (say 4 mm). When using this apparatus in the field, weathered material should be removed first.

Cohesion

Most sediment grains are cohesionless, but clays and grains with organic coatings are cohesive. Cohesiveness gives grains cohesive strength, which influences the ability of

gravitational forces or fluid forces to move the grains relative to each other. Cohesiveness is defined in Chapter 8 within the Navier-Coulomb equation: i.e. shear strength is the sum of frictional resistance (product of normal load and a friction coefficient) and shear resistance due to cohesion. Shear resistance due to cohesion is commonly measured by placing a sample in a shear box under a given normal load, and then applying an increasing shearing force until the sample fails.

Stratification and sedimentary structures

Sediment is normally deposited in layers, which can be recognized because of an ordered arrangement of grains of a given size, shape or composition. The boundaries of strata are clearly seen when they are sharply defined, due to a sharp change in depositional conditions, erosion, or diagenesis. The term gradational boundary is widely used, but is of course an oxymoron. If sediment properties vary gradually within a stratum, a boundary cannot be defined objectively. Relief features may occur on stratal boundaries (called external structures). Sole structures occur on the bases of strata, and may be formed when an erosional mark in the top of one stratum is filled by sediment from the stratum above. The top of a stratum may preserve bedforms such as ripples. Systematic arrangement of grains within a stratum may give rise to internal structures, which may take the form of internal strata.

The word stratum (plural strata) is the general term referring to all thicknesses of sediment layers. Strata have been subdivided into beds and laminae. According to McKee and Weir (1953), a bed is a sedimentary stratum greater than 10 mm thick, whereas a lamina is less than 10 mm thick. The divide at 10 mm is completely arbitrary, and not based on objective statistical analysis of stratal thickness, nor on any genetic implication. Beds and laminae generally occur in sets (bedsets, laminasets) that are distinctive in terms of the orientation, texture and composition of beds or laminae within the set (Figure A-16). If the beds or laminae within a set are inclined at more than a few degrees relative to the set boundaries, the beds or laminae are given the prefix cross or inclined (e.g., set of cross laminae, or cross-lamina set). Bedsets or laminasets also occur in sets. For example, a set of similar cross-lamina sets or cross-

bed sets is referred to as a simple set or coset (Figure A-16), according to McKee and Weir (1953). A set or different types of bedsets or laminasets is called a composite set (Figure A-16).

This terminology for defining beds, laminae, bedsets, and laminasets is widely used but is not without its problems and detractors. Modifications to the terminology shown in Figure A-16 suggest that there was a desire to use the term bed for a larger scale of stratum than that defined by McKee and Weir (1953). The term bed may therefore refer to a set of strata rather than a single stratum with no internal subdivision. Another problem with McKee and Weir's terminology is that both laminae and beds may occur in the same set of strata. This problem arises because of the arbitrary division of strata into beds and laminae. A single strataset containing beds and laminae could logically be called a composite set, but this term has already been used for a set of different sets rather than a set of different strata. Perhaps the greatest difficulty with all of the different methods for defining strata and sets of strata is that there is no consistent use of terms for referring to the many different superimposed scales of strata and sets of strata in sedimentary basins. The terms used for the smaller stratasesets (bedset, laminaset) have not been applied to the larger-scale stratasesets. Instead, poorly defined, inexplicit terms such as storey, architectural element, and parasequence have been used.

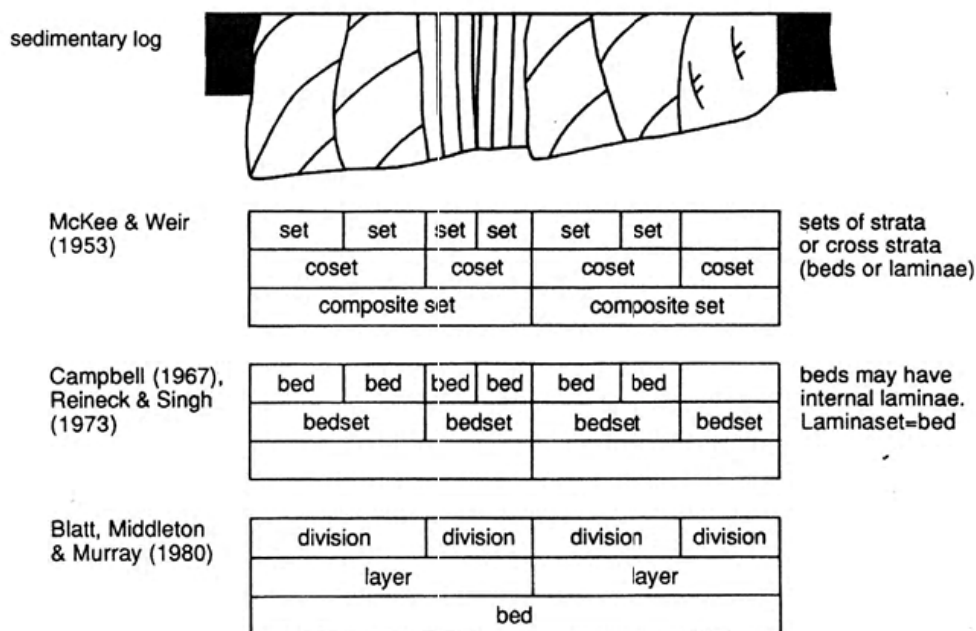


Figure A-16. Comparison of terminology for describing stratification (from Bridge, 1993).

Bridge (1993) argued that, in order to describe hierarchies of different-scale strata, it is desirable to use a reasonably small number of explicit terms consistently irrespective of scale, and to use qualifying terms to describe relative scale of strata. Figure A-17 shows an example of this approach applied to river deposits, and includes interpretation as well as descriptive terminology. An alternative method of describing hierarchies of strata of different scale is by numerically ordering their bounding surfaces (e.g., Brookfield, 1977; Allen, 1983; Miall, 1996). As discussed by Bridge (1993), this approach is difficult to use in practice.

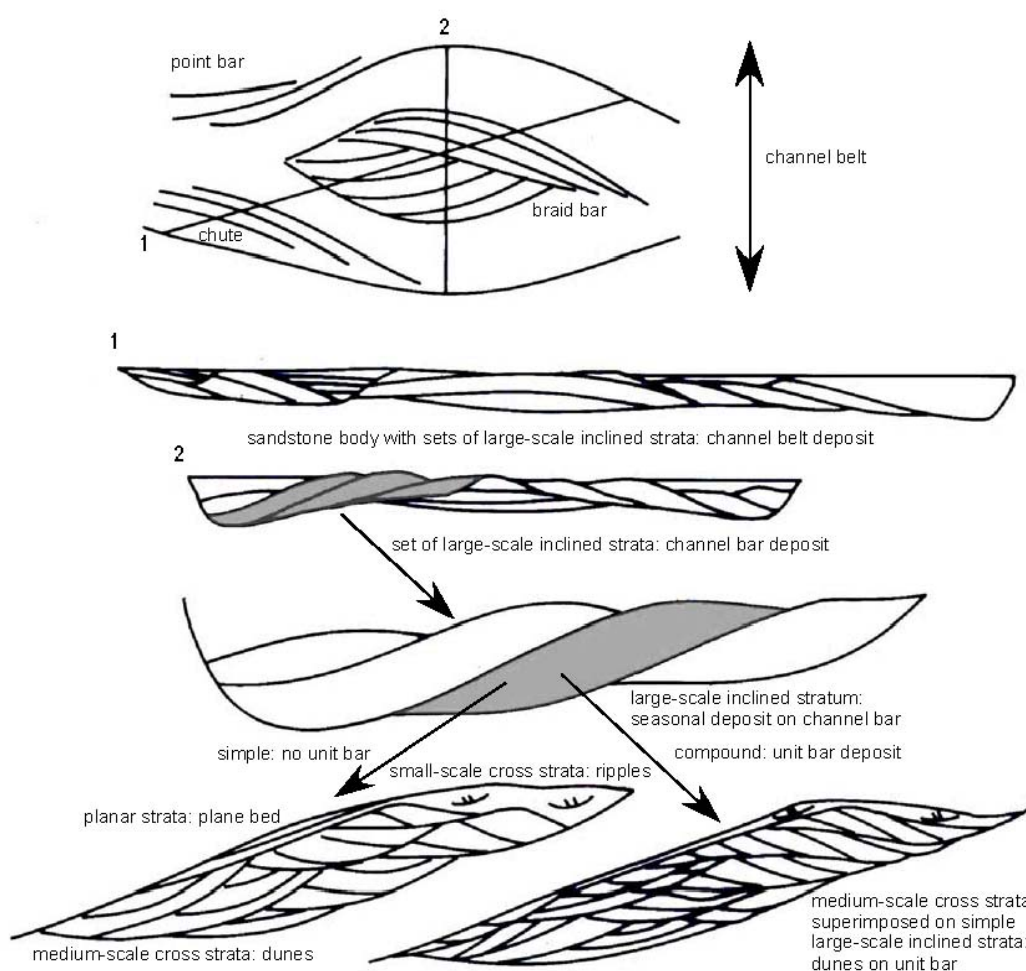


Figure A-17. Proposed terminology for the case of superimposed scales of strata, using river channel deposits as an example (modified from Bridge, 1993).

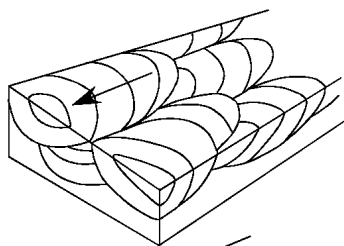
Beds have also been sub-classified based on their thickness, and terms such as thin-bedded and thick-bedded have been defined based on arbitrary boundaries of thickness class (e.g. Tucker, 2001; Stow, 2005). Such subdivision of bed thickness is not usually based on consistent scale divisions or on natural groupings of bed thickness defined by statistical analysis. Furthermore, these thickness terms have different meanings in different classifications. Therefore, it is recommended that descriptions of bed thickness should be given in measured units rather than using ambiguous terms.

Paleocurrent analysis

Paleocurrents are analyzed in order to help indicate local depositional environment (e.g., fluvial, tidal) and regional sediment-dispersal directions (e.g., relative position of the land and

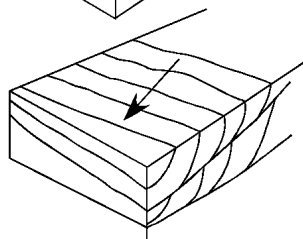
Trough cross strata

Orientation of axis and sides of troughs.
(forget dip of cross strata)



Planar cross strata

Direction of dip of cross strata



Asymmetrical ripples and dunes with lunate, sinuous, and linguoid crest lines

Mean direction of steepest dipping side



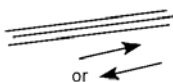
Flute mark, scour mark

Steep end points upstream



Tool marks, parting lamination

Parallel to flow, but cannot normally discern direction



Symmetrical ripple marks

Wave currents parallel to dips of sides

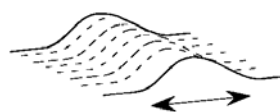


Figure A-18. *Paleocurrent indicators.*

sea, orientations of deltas or deep-sea fans). Paleocurrent orientations can also suggest directions of change in mean grain size of deposits (e.g., decrease downcurrent), and directional variations in porosity and permeability (e.g., permeability may be larger in the paleocurrent direction than transverse to it).

Paleocurrent directions are normally indicated by sedimentary structures such as cross strata, ripple marks, flute and tool casts, and channel fills, and the orientation of certain types of sediment grains (Figure A-18). As a general rule, it is desirable to measure as many paleocurrent indicators from as many different

structures as possible in an outcrop. The readings from each type of structure should be kept separate, and it is desirable also to measure the dimensions of each structure. The spatial relationships among all of the measured structures should also be recorded carefully on photomosaics and sedimentary logs. Measurement of paleocurrent indicators from large 3-D structures (e.g., trough cross strata, channel fills) that are not well exposed is a challenge. Measurement of paleocurrent orientations from oriented cores, image logs, or dipmeter logs is even more of a challenge, because the sample of the sedimentary structure may be much smaller than the structure itself.

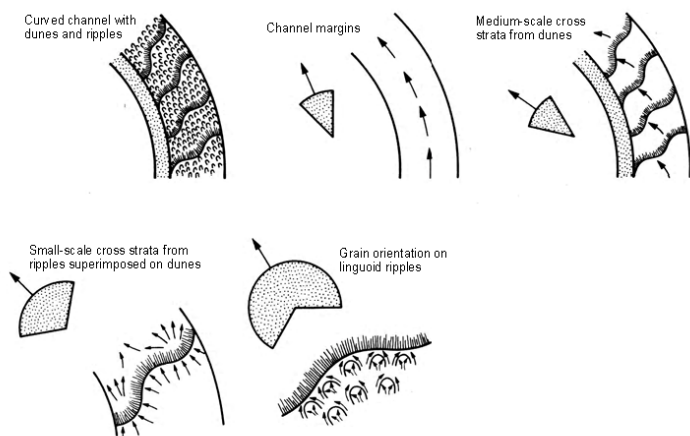


Figure A-19. Hierarchies of bedforms, sedimentary structures, and paleocurrents (modified from Allen, 1966).

for the different types and scales of structures. The mean and variance of paleocurrent directions also depends on the nature of preservation of strata (e.g. Figure A-20). In general, the variance of paleocurrent directions is less in preserved deposits than in modern environments, and the mean directions may also differ (Figure A-20).

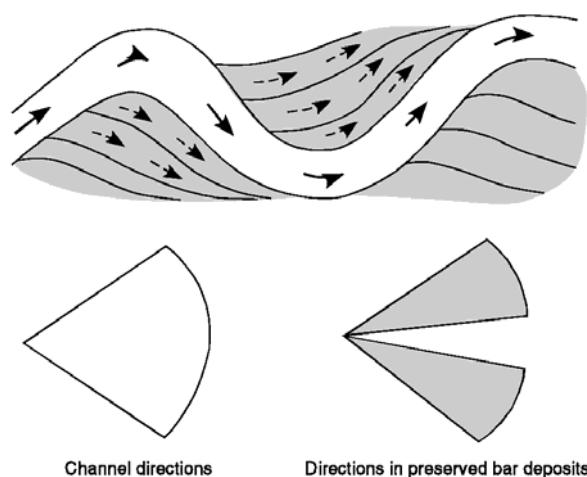


Figure A-20. Preservation bias in paleocurrents. Paleocurrents derived from preserved point bar deposits are different from channel directions.

It is usual to recognize hierarchies of bedforms, sedimentary structures, and hence paleocurrent indicators (Figure A-19; Allen, 1966). Within any modern environment, the variability of paleocurrent directions normally increases as the scales of the bedform and associated sedimentary structure decrease (Figure A-19). The mean paleocurrent direction may also differ

Different types and scales of paleocurrent indicators carry different implications about current strength and importance in a depositional environment. For example, medium-scale trough cross strata formed by river dunes indicate relatively strong water currents and the main current directions over channel bars. In contrast, small-scale cross strata formed by current ripples indicate relatively weak currents with directions determined by local orientations of flow over the larger bedforms. Paleocurrent information from all of these scales of structure is useful for interpreting details of depositional environments. Regional dispersal directions are indicated by the mean orientation of the largest structures. Thus, the method of data collection and interpretation to be used depends on the objective of the study.

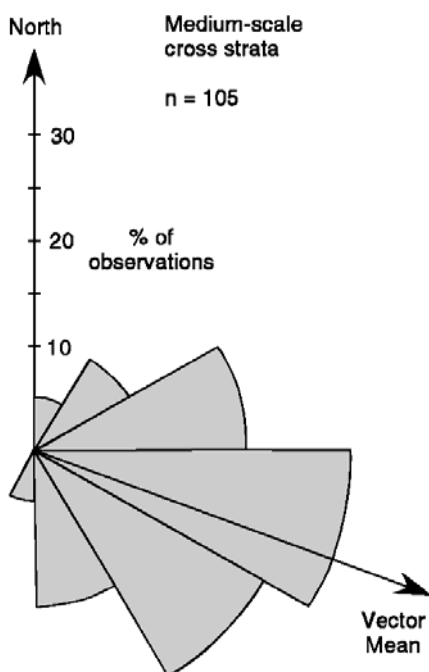


Figure A-21. Paleocurrent circular histogram.

Assume that a large number of paleocurrent readings have been obtained from medium-scale trough cross strata from a series of outcrops of a specific formation, and that it is desirable to estimate the mean and variance of the readings. The first step in the analysis would be to correct the paleocurrent readings for tectonic dip, if this is greater than 20° . This correction can be done slowly using a stereonet (Figure A-21), or quickly using a computer program (Curry, 1956; Potter and Pettijohn, 1977). The corrected readings are then plotted on a circular histogram (also known as a current rose: Figure A-21). The class interval is commonly between 20° and 30° , but depends on the variability of directions and the number of

observations. The length of a segment in a circular histogram is proportional to the percentage of the readings in a class interval. A circular histogram should contain a North arrow, the scale for the segment lengths, and a statement of the number of readings used and the type of structure measured (Figure A-21).

The mean and variance of the paleocurrent readings are calculated using vector algebra. Most commonly, each directional reading is assigned a magnitude of unity (i.e., it is a unit vector). In some cases, a reading may be given a magnitude related to the volume or thickness of the structure from which the reading is taken. Doing this opens up a can of worms, related to assumptions about the relative importance of structures of a given type but of varying preserved size. The vector mean is the azimuth of the resultant vector, θ_m , given by

$$\theta_m = \tan^{-1} (\Sigma \sin \theta / \Sigma \cos \theta)$$

A measure of the variance of the readings about the vector mean (the dispersion measure, θ_d) is the length (magnitude) of the resultant vector, divided by the number of readings, n :

$$\theta_d = \sqrt{[(\Sigma \sin \theta)^2 + (\Sigma \cos \theta)^2] / n}$$

If all of the paleocurrent readings are in the same direction (no variance), the dispersion measure equals unity. If the directions are perfectly random, the dispersion measure tends to zero. The dispersion measure would also equal zero if the measurements were perfectly bimodal in opposite directions. Clearly, the vector mean and dispersion measure only have any real meaning if there is a single mode. Polymodal histograms indicate either multiple paleocurrent directions or inappropriate choice of class interval for the data collected. The construction of circular histograms and calculation of statistics can be done easily with a computer.

Fossils

Fossils occur in Phanerozoic rocks, and some are composed primarily of skeletal fragments. In weathered mudstones, fossils may be simply pried out of the outcrop (or from large samples) and cleaned with dental tools. Fossiliferous limestones interstratified with mudstones also provide good prospects for fossil collection. Separating fossils from well-cemented sandstones and limestones may be difficult, so large blocks must be taken and possibly slabbed in order to describe the fossil content. Calcium carbonate shells that have been silicified, and fossils composed of silica or other non-carbonate materials, can be freed from limestones by dissolution of limestone blocks in acid. Conodonts are routinely collected in this way. The skeletons of large vertebrates require special collection techniques.

Systematic collections of fossils from measured sections can be laborious, as large volumes of rock must be collected. Obviously, the more fossils collected the more representative a sample will be obtained, and statistical techniques must be used to interpret the results. For example, the Linnaean hierarchical system for defining taxonomy recognizes species organized into higher level taxa: genera, families, orders, classes and phyla. Recovery of higher-level taxa requires large samples. For example, within 1 phylum, upwards of 1000-2000 specimens might need to be collected to account for all classes present (Raup and Stanley, 1978). Bedding surfaces strewn with fossils are commonly spectacular, but may not be representative of the fossils in the rocks. Commonly such surfaces are so-called 'condensation' surfaces and interpreted to represent substantial breaks in sedimentation, especially if there is evidence of hardground formation (Chapter 19). Statistical sampling of such bedding surfaces includes various grid counting methods.

Two important problems must be addressed in interpreting fossils. The first is whether the collected fossils were in place or transported. Most fossils have been transported, abraded, and sorted by currents. Such fossil assemblages may not be representative of the communities they lived in. The fossils of pelagic organisms are not found in the place they lived. All fossil bats and birds are known from lagoon or lake sediments, yet these organisms clearly did not live there. It is especially difficult to interpret whether or not fossils in shale are in place because muds typically undergo 70 to 80% compaction upon burial and conversion to shales or mudrocks.

The second hurdle in interpreting fossils of extinct organisms is how and where they lived. If the organism is extant, or has close relatives, this is not an issue. However, the environmental significance of extinct groups is more difficult to interpret. For example, although most modern brachiopods live in fairly deep shelf settings, it is clear from sedimentological evidence that Paleozoic brachiopods were spread throughout shelf settings. For many extinct organisms, *functional morphological* arguments are necessary in order to interpret their significance. Some groups of organisms have strict salinity tolerances, and such *stenohaline* groups such as green algae, corals, cephalopods, and echinoderms are generally taken as signaling "normal" marine settings. Groups such as gastropods, bivalves and ostracods

have broad salinity tolerances, with bryozoans, brachiopods and benthic foraminiferans intermediate in their salinity tolerances. Analysis of the paleoecology and taphonomy of fossils is commonly attempted (reviews in Raup and Stanley, 1978; Gastaldo et al., 2004; Prothero, 2004).

Classification of sediments based on texture and composition

Rationale

Classification and naming of sediments and sedimentary rocks is desirable because we want to refer to a type of sediment without having to describe all of its properties. Any classification scheme should have the following properties: (1) descriptive rather than interpretive; (2) sediment properties measurable easily and unambiguously; (3) precisely defined, mutually exclusive categories; (4) explicit terms for different categories. Sediment properties that carry some sort of genetic implication are commonly chosen. However, properties such as texture and composition cannot shed light on all aspects of the origin of sediment. Furthermore, it is impossible to select a single group of properties that allows manageable classification of all sediment types. For example, properties of terrigenous sediments that allow classification and shed light on origin may be meaningless for biogenic and chemogenic sediments.

A general (but unsatisfactory) classification based on sediment composition is illustrated in Figure A-22 (terrigenous, biogenic, chemogenic end members). Terrigenous sediments are produced by weathering of pre-existing rocks, and are composed mainly of siliciclastic gravels, sands and muds. Biogenic sediments are produced by organic precipitation of minerals such as calcium carbonate, silica, and carbon, forming the hard parts of organisms.

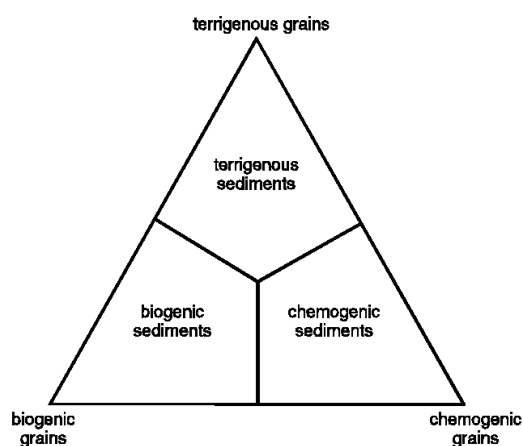


Figure A-22. Classification of sediments based on origin

Chemogenic sediments are inorganic precipitates. It will be noticed that several rules of

classification have been broken in this classification. First, the terms are interpretive rather than descriptive. Second, it may be difficult to determine whether a chemically precipitated grain (such as calcium carbonate mud) was precipitated with or without the involvement of organisms. Third, some biogenic or chemogenic sediments may be released by terrestrial weathering of pre-existing rocks, making them terrigenous sediments. Fourth, volcanogenic grains are ignored in this classification. Thus, although the genetic terms terrigenous, biogenic, chemogenic, and volcanogenic were useful for describing the origin of grains in Chapters 3,4 and 9, they should not really be used in a classification of sediment types. Better, purely-descriptive compositional terms would be silicate rocks, lime rocks, salt rocks, carbonaceous rocks, and iron-rich rocks.

Figure A-22 illustrates use of the end-member concept, where each component in the classification is the corner of a triangle or tetrahedron. Most Earth scientists don't feel comfortable dealing with more than three or four end members simultaneously. Statistical methods such as cluster, discriminant and factor analysis can be used to objectively classify sediments with any number of components. Triangular diagrams are most commonly used, because these facilitate insertion of boundaries to separate different types of sediment (Figure A-22). The boundaries are normally placed arbitrarily, without paying heed to natural groupings of sediment type. Many different sediment classifications have been published that vary in the end members chosen, the placing of boundaries to separate categories, and the names chosen for the categories (Pettijohn et al, 1972; Folk, 1974; Pettijohn, 1975; Blatt et al, 1980; Tucker, 2001). Fortunately, there is a degree of consensus on which types of classification are most useful, and these are briefly mentioned here.

Gravel-sand-silt-clay diagrams

Classification of sediment by mean grain size follows the Wentworth scale (Table A-3). However, in some cases it is necessary to use terms that convey more information about the range of sizes in sediment. Any three

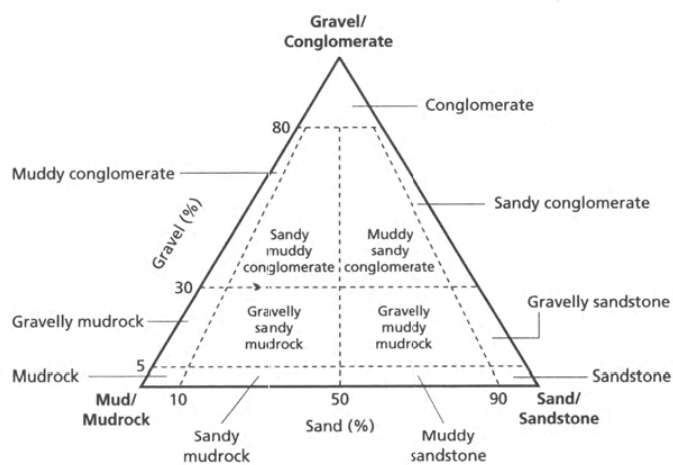


Figure A-23. Textural classifications using gravel, sand and mud as end members. From Tucker (2001).

of gravel, sand, silt, and clay can be used as end members of triangular diagrams to represent the proportions of these components in a mixture of sizes (e.g. Figure A-23). The space within the triangle is typically split arbitrarily into sections that are assigned terms such as sandy gravel, silty sand, and so on. Such subdivisions are not normally based on natural groupings, and there are many different classification schemes available. Clay means grain size, not composition.

Figure A-23 shows that consolidated sands are called sandstones, and consolidated muds are called mudstones. Strangely, consolidated gravels are called conglomerates: they should be called gravelstones for consistency. Other textural terms are: arenite (sandstone); rudite (conglomerate); argillite, lutite, and pelite (mudstone)

Other texture classifications

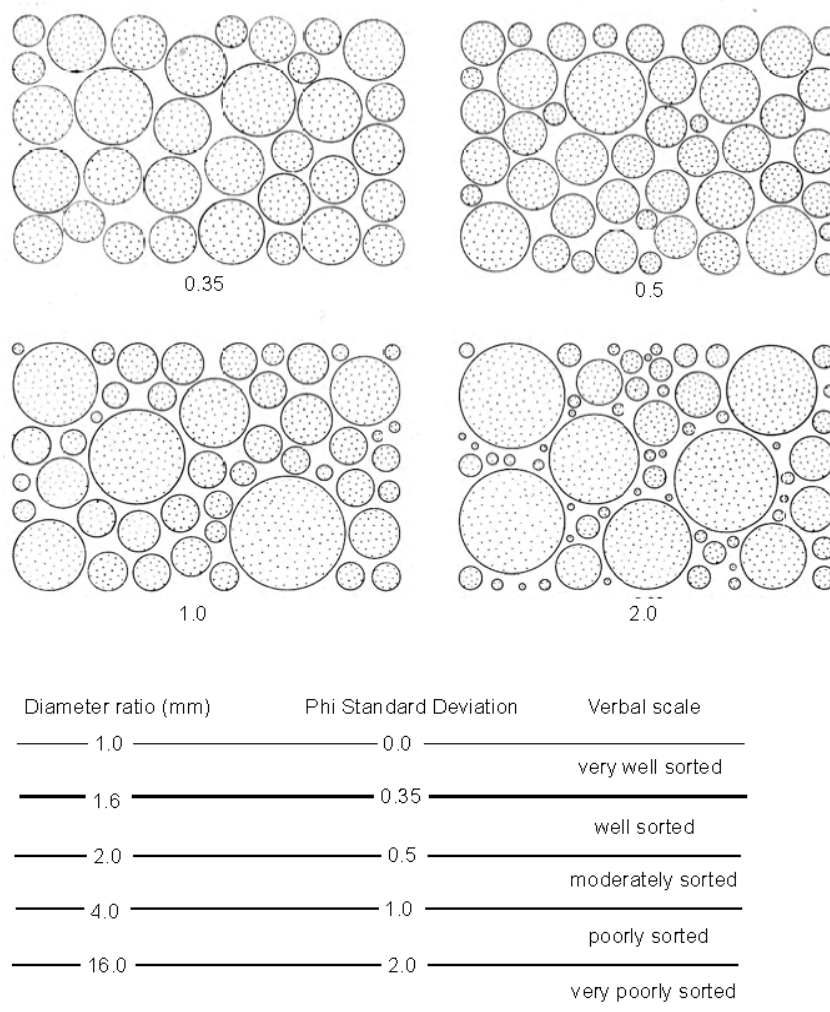


Figure A-24. *Sorting classification and visual template (from Pettijohn et al., 1972).*

Sorting classifications are based on phi standard deviations derived from grain size analysis (e.g. Figure A-24). Such classifications should really be in combination with mean grain size, as mean size and sorting are normally related. If a grain-size analysis is not available, visual templates can be used, similar to grain-size comparators (Figure A-24). Conglomerates that have gravel grains supported by a sandy or muddy matrix are called paraconglomerates.

Conglomerates in which gravel grains form a framework are called orthoconglomerates. The frameworks in orthoconglomerates can be open or closed, depending on whether or not the pore spaces between the framework gravels are filled with finer-grained sediment. The term breccia is used for gravels with angular grains, whereas conglomerates are normally assumed to have rounded grains. However, the distinction between breccia and conglomerate is not based on an objective measurement of grain angularity.

Compositional classification of gravels and conglomerates

Various names are given to conglomerates, dependent on their composition. Calcirudites are calcareous conglomerates. Oligomictic conglomerates have gravel grains of one dominant rock type. Polymictic conglomerates have gravel grains of several different rock types. Conglomerates with a large range of gravel, sand and mud grains are called diamictons in the literature on glacial environments: in many cases, diamictons are polymictic paraconglomerates. Conglomerates made of volcanic rock types are commonly called agglomerates. Conglomerates made of sediment fragments derived from re-erosion of contemporaneous, local deposits (e.g. lumps of desiccated floodplain mud or channel bank material) are called intraformational conglomerates, as distinct from extraformational conglomerates.

Compositional classification of sandstones

There are many different compositional classifications of terrigenous sandstones, but there is some tendency to agreement on one type (e.g. Figure A-25). The most common end members are quartz (perhaps with chert and quartzitic rock fragments), feldspar, and rock fragments (commonly excluding quartzitic ones). The main terms used are quartz arenite (or

orthoquartzite), feldspathic arenite (or arkose), and lithic arenite (or litharenite). The amount of quartz relative to feldspar and rock fragments is an indicator of chemical and mineralogical maturity, which is largely dependent on the number of cycles of weathering, erosion, transport, deposition, burial and re-exposure that sediment has undergone (see Chapter 3).

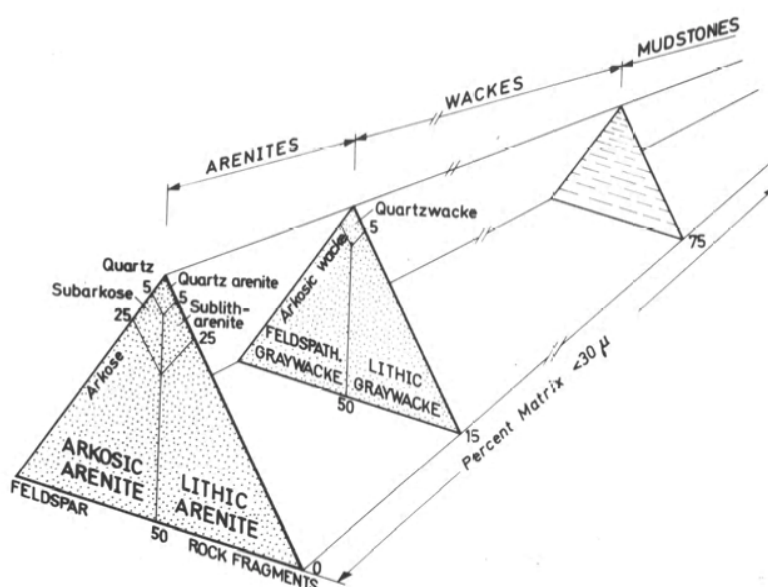


Figure A-25. One of many compositional classifications of sandstones (from Pettijohn et al., 1972).

Some classifications also include detrital clay as a fourth end member, but the explicit use of detrital clay in a classification is controversial. Abundant clay in sandstones is interpreted to indicate lack of grain-size sorting by turbulent currents, implying deposition by laminar flows (e.g., sediment gravity flows) or accumulation without being carried by water or air currents (e.g., deposited from melting ice). However, the clay may not be a primary deposit. Clay can occur by crushing of mudstone fragments, post-depositional infiltration (elluviation), or by authigenic crystallization after burial. Also, it is extremely difficult to distinguish individual detrital clays from crushed mudstones or micaceous rock fragments. If the proportion of detrital clay is used in a classification, terms such as wacke, graywacke, and muddy are used. The term graywacke was originally a field term for gray muddy sandstone. However, the term has subsequently been used for sandstones of almost any composition. We recommend not using clay minerals in a compositional classification of sandstones.

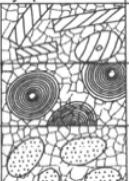
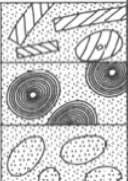
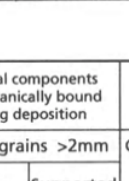
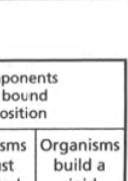
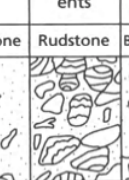
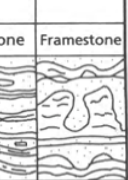
Compositional classification of mudstones

The composition of mudstone (shale if fissile) is indicated by its color. Red mudstone contains hematite, green mudstone contains chlorite, and black mudstone is rich in organic matter (mainly kerogen) and commonly iron sulphide. Sapropelite is very rich in kerogen, and oil shale contains oil, gas, and bitumen. Marl is calcareous mudstone and loam is a mixture of clay, silt and sand in roughly equal proportions.

Limestone classifications

The most common classifications of limestones are by Folk (1962) and Dunham (1962) (Figure A-26). Both classifications are essentially based on texture and fabric. Folk (1962) recognized three main components of carbonate sediments: (1) allochemical grains (bioclasts,

Folk

| Principal grains in limestone | Limestone types | | | |
|-------------------------------|-----------------|--|--------------------------------|---|
| | | Cemented by sparite | | With a micrite matrix |
| Skeletal grains (bioclasts) | Biosparite |  | Biomicrite |  |
| Ooids | Oosparite |  | Oomicrite |  |
| Peloids | Pelsparite |  | Pelmicrite |  |
| Intraclasts | Intrasparite |  | Intramicroite |  |
| Limestone formed in situ | Biolithite |  | Fenestral limestone-dismicrite |  |

Dunham, modified by Embry and Klovan

| Original components not bound together during deposition | | | | Original components bound together | Depositional texture not recognizable | Original components not organically bound during deposition | | Original components organically bound during deposition | | | |
|---|---|---|---|---|---|---|--|---|---|---|-----------------------------------|
| Contains lime mud | | | | | | Crystalline carbonate | >10% grains >2mm | | Organisms act as baffles | Organisms encrust and bind | Organisms build a rigid framework |
| Mud-supported | | Grain-supported | Lacks mud and is grain supported | | | | Matrix supported | Supported by > 2mm components | | | |
| Less than 10% grains | More than 10% grains | | | | | | | | | | |
| Mudstone | Wackestone | Packstone | Grainstone | Boundstone | Crystalline | Floatstone | Rudstone | Baffle stone | Bindstone | Framestone | |
|  |  |  |  |  |  |  |  |  |  |  | |

Figure A-26. Limestone classifications of Folk (1962), Dunham (1962), and Embry and Klovan (1971). From Tucker (2001).

ooliths, pellets and intraclasts); (2) carbonate mud (micrite), and; (3) sparry cement. The terms used depend on the relative proportions of these three end members. Folk (1962) also recommended use of the Wentworth grain size scale for the allochemical grains. Framework reef rocks were called biolithite. Dunham's (1962) classification also recognizes the distinction between mud (smaller than 20 microns), "grains" (larger than 20 microns), and cement, but emphasizes the fabric (whether mud supported or grain supported, and the relative proportions of mud and grains). Framework reef rocks were called boundstone. Embry and Klovan (1971) modified this classification to include other types of fabric (Figure A-26). The terms used in this classification are not explicit and some are interpretive.

It is commonly assumed that a mud-supported limestone was deposited in the absence of turbulent water currents, and *vice versa* for a mud-free limestone. However, the texture and fabric of biogenic and chemogenic grains are difficult to relate to transport mechanisms, because of the possibility of *in-situ* accumulation with little transport, and because of original rounded shapes. Furthermore, carbonate mud may be produced diagenetically by micritization or infiltration. Classification is commonly made difficult by diagenetic modification of original textures and fabrics. Figure A-27 shows the classification of limestone porosity by Choquette and Pray (1970).

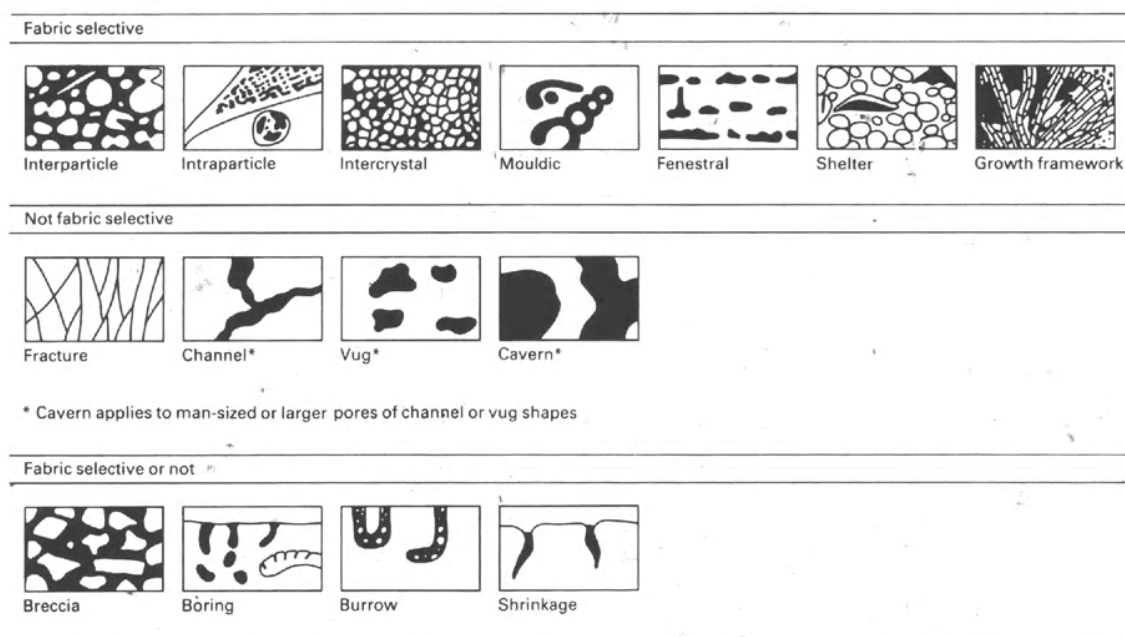


Figure A-27. Classification of limestone porosity according to Choquette and Pray (1970).

Classification of siliceous sediments

Chert is a general term for fine-grained siliceous sediment irrespective of origin. The silica in chert is fine-grained quartz of varying crystal size, and chalcedonic quartz has characteristic radiating fibrous crystals (Chapters 4, 19). Flint is a synonym for chert, but is most frequently used for chert nodules in Cretaceous chalk rocks. Jasper is red chert, due to the presence of hematite dust. Porcelanite is chert with a texture similar to unglazed porcelain. Ancient cherts are commonly either bedded or nodular (occurring particularly in limestones). The modern equivalents of ancient bedded cherts are siliceous (amorphous opaline silica) oozes composed of radiolarians, diatoms, or sponge spicules. Most nodular cherts are diagenetic, and formed by replacement of a host sediment. Although most of these host sediments are marine limestones, silcretes are nodular cherts formed in soils.

Classification of iron-rich sediments

Iron-rich sedimentary rocks are normally separated into two distinct types: Precambrian banded iron formations (BIFs), and Phanerozoic ironstones. Precambrian ironstones are typically composed of chert interbedded with hematite and magnetite, but also siderite, pyrite and greenalite. Phanerozoic ironstones (e.g., Clinton and Minette types) are composed of hematite and/or chamosite and/or siderite minerals, and tend to have an oolitic texture. Phanerozoic ironstones also include: blackband and clayband ironstones, which are fine-grained siderite nodules in shales, commonly associated with coals, and; bog iron ores that form in peat swamps and poorly drained lakes, and are composed of minerals such as goethite and siderite which may be pisolitic or oolitic. Ferromanganese nodules and crusts also occur on the deep sea floor (Chapter 18).

Classification of coal

Most coal is humic coal, formed from *in situ* accumulation of woody plant material. Humic coals form a continuous series from peat to lignite (brown coal: woody, lusterless and poorly jointed) to bituminous coal and anthracite (that are well bedded with a bright to dull

luster). These changes in coal rank are related to increasing temperature of burial, and are manifested in increasing carbon content, calorific value, and vitrinite reflectance. Sapropelic coal is formed of transported organic matter such as algae, spores and plant debris. The two common types of sapropelic coals are cannel coal and boghead coal. These coals are unlaminated, fine grained, and have conchoidal fracture, and differ in their component plant material.

Coal petrology is studied using a polished surface and a reflected-light microscope. Microscopic constituents of coals are called macerals which are different types of macerated plant material analogous to minerals. The main types are: *vitrinite* - composed of cellular or structureless material, formerly wood; *exinite* (or *liptinite*) - spores and leaf cuticles, and; *inertinite* - broken cell walls from rotted or burnt wood.

Humic coals are subdivided into 4 main lithotypes on the basis of luster and other physical properties: *vitrain* is bright and vitreous, and composed mainly of vitrinite; *clarain* is less bright, silky, and laminated, and composed of all three macerals; *durain* is dull and matt, and composed of exinite and inertinite; *fusain* is sooty, black and friable, and made of inertinite (specifically fusinite).

Classification of volcanogenic sediments

Volcaniclastic (pyroclastic) sediment is classified based on grain size: dust < 0.063 mm; ash 0.063-2 mm; lapilli 2-64 mm; blocks and bombs > 64 mm. Accretionary lapilli are concentric layers of (originally wet) ash around a nucleus such as a crystal. Scoria are clinker-like lapilli or bombs. The sediment grains are actually rock fragments of lava or country rocks, crystals, and broken bits of volcanic glass called shards.

Volcaniclastic sediments or sedimentary rocks are called tuff if composed mainly of ash, lapillistone if composed mainly of lapilli, and breccia or agglomerate if composed mainly of bombs and blocks. Tuffs are named based on relative amounts of rock fragments, crystals and glass: i.e., lithic, crystal, and vitric tuffs. Pyroclasts may be hot enough to be welded together, and welded particles are typically flattened. Welded tuffs are sometimes called ignimbrites.

Bentonites are montmorillonite clays formed by devitrification and chemical alteration of volcanic ash: they contain relict crystals and glass shards.

Definition of distinctive sediment types (facies)

In order to describe and interpret sedimentary strata, it is necessary to recognize distinctive sediment types, and these are commonly referred to as *facies*. The word *facies* is derived from the Latin noun *facia*, meaning the “appearance”. A lithofacies is thus a type of rock that is distinctive in its observable sedimentary properties (i.e., geometry, color, composition, texture, sedimentary structures). Biofacies are rocks that have distinctive fossil types, and seismic facies and radar facies are defined based on distinctive geophysical properties.

Lithofacies should be defined based on objectively observable features, not interpreted origin,

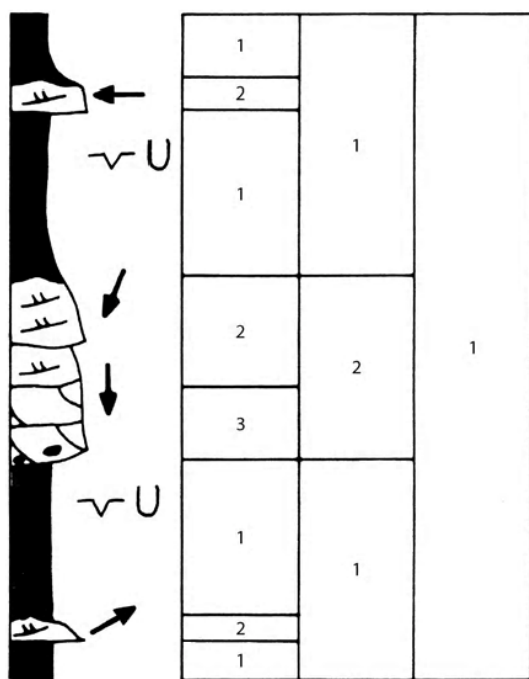


Figure A-28. Different ways of defining lithofacies of sedimentary strata.

and the terms used to refer to such facies should clearly reflect the most important features. A typical example is a “cross-stratified sandstone facies”, the name conveying information on grain size, sedimentary structure and composition. There are many examples of genetic definitions of facies in the literature (e.g., fluvial, turbidite, or post-orogenic facies). Such definitions give no information on the appearance of the rocks, and the interpreted origin must be taken on faith. Such usage is more acceptable for modern deposits because the environment of deposition can be observed rather than interpreted. Practical definition of lithofacies depends on the variety of sedimentary features present, and on the detail required (e.g. Figure A-28).

Lithofacies normally occur together repeatedly in sets (or sequences or cycles) of various superimposed scales. It is important to recognize and describe all the different types and scales of stratasesets. In the case of GPR profiling, it may be necessary to use different antenna frequencies in order to recognize all of the different scales of radar facies. Different terms have been used for each scale of set, and examples of these terms in approximate order of increasing scale are: strataset (also bedset and laminaset), subfacies, facies, facies association (more-or-less equivalent to facies succession, lithosome, architectural element, parasequence), parasequence set (also magnafacies), systems tract, unconformity-bounded sequence. There is clearly a confusion of terminology, and there are no hard and fast rules for basic definition of a facies. Also, somewhere in this confusion of terminology, formations and members (distinctive mappable units, normally greater than 10 m thick) must be fitted in.

Any scheme for definition (and classification) of different types and scales of strata should be based on easily measurable parameters that are used to define mutually exclusive classes. Terms used to refer to these classes should be explicit. For example, the terms small-scale inclined strata, medium-scale inclined strata, and large-scale inclined strata, clearly convey the relative scale and orientation of strata. The prefixes, microscale, mesoscale and macroscale could also be used. Traditionally, geologists have used the term cross-strata to define strata inclined relative to some bounding surface: the term "cross" is clearly not explicit and is quite misleading. A diagram is essential to clearly define terms used to classify sedimentary strata.

Bridge (1993, 1995) critically discusses these problems of facies definition and terminology, specifically the tendency to erect a prescribed set of facies types for a given depositional environment, where each facies type has its own acronym for reference and a unique interpretation (e.g., Miall, 1996; Clark and Pickering, 1996; Stow et al., 1996). The use of standardized codes (acronyms) to refer to a prescribed set of lithofacies tends to discourage close observation and recognition of varieties and superpositions of lithofacies. It has also led to such a proliferation of acronyms in the literature that it appears we now have to read two languages simultaneously. It has been suggested that each lithofacies can be assigned a unique interpretation. This is much too simplistic a view, and many stated interpretations are misleading or wrong. In classifications of architectural elements (e.g., Miall, 1996; Clark and Pickering,

1996), the different classes are not mutually exclusive, and they are referred to using a mixture of descriptive and interpretive terms. Numerical ordering of stratal bounding surfaces (rather than the strata themselves) as a way of classifying hierarchical scales of strata (e.g., Miall, 1996; Clark and Pickering, 1996) is very difficult to use in practice.

Some sedimentary geologists have attempted to quantify the nature of cyclicity in sedimentary properties or facies using a variety of statistical techniques, some of which are described in appendix 3 (summaries in Davis, 1973; Schwarzacher, 1975, 1985). These techniques were especially popular in the 1960s and 1970s, and seem to be coming back in vogue. They are normally applied to successions of strata measured in the direction normal to bedding, as lateral variations are very difficult to define. When applying such techniques, it is necessary to be aware of the following potential problems: (1) simplification or modification of the observed data to facilitate statistical analysis; (2) computation of idealized facies sequences that may have no real-world significance, and; (3) use of stratal thickness as a surrogate for time in time-series analyses.

Definition of lithostratigraphic units

Lithostratigraphic units are lithofacies units that are sufficiently distinctive, thick and laterally extensive to be put on a geological map (typical scales are 1:24000, 1: 50,000 and 1:100,000), and to be recognizable in seismic sections. It is normally stated that the fundamental lithostratigraphic unit is the Formation (North American Commission on Stratigraphic Nomenclature, 1983; Whittaker et al., 1991). However, Formations are routinely subdivided into Members, and lumped together into Groups. Formations are typically meters to hundreds of meters thick, and Groups may be kilometers thick. The thickness of a formal lithostratigraphic unit, and the degree of subdivision, actually depends as much on the attention it has received as the lithofacies variability of the strata. Some well-studied Formations may be only meters thick, whereas Formations that are not known well may be hundreds of meters thick. At some time in the future, lesser-known thick Formations may be renamed as Groups and subdivided into several Formations. Formations and Groups are named according to locations where there is good, complete exposure (i.e. *type sections* where the *stratotype* is defined). A descriptive term

may also be added to the name (e.g., Ithaca Shale Formation). Any formal lithostratigraphic unit must be fully described, including specific information on the location of its base and its lithofacies units in accordance with strict guidelines set up by international stratigraphic committees. In view of the fact that lithofacies associations are related to depositional environment, and that depositional environments vary in space (e.g. floodplain to coast to sea) and time (e.g. during a marine transgression), it is most likely that lithostratigraphic units will have limited lateral extent and have diachronous boundaries.

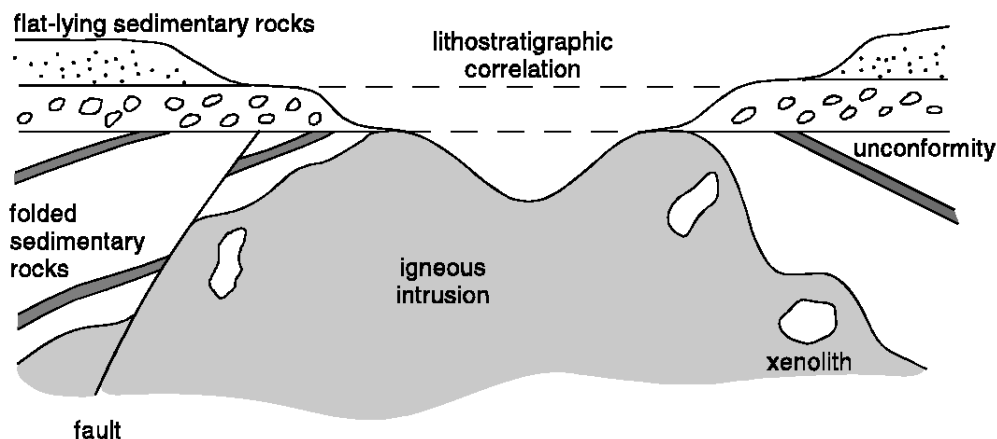
An allostratigraphic unit is the term invented by sequence stratigraphers (Chapter 20) used to refer to a specific type of lithostratigraphic unit (called a sequence or parasequence) that is bounded by unconformities or other correlatable surfaces. It is commonly assumed that the bounding surfaces are essentially time lines, and that they are related to sea-level fall. However, evidence for such interpretation is commonly lacking.

Relative age determination

Rock structure

The basis of relative time scales prior to the 19th century was lateral continuity and superimposition of strata, cross-cutting structures (discordances), and inclusions of “foreign” rock (xenoliths). This essentially lithostratigraphic approach (Figure A-29), involves certain assumptions: (1) sedimentary strata were originally laterally continuous such that they can be correlated lithostratigraphically over specified lateral distances; (2) younger strata are laid down on top of older strata; (3) sedimentary strata were originally approximately horizontal; (4) with cross-cutting structures (discordances) such as faults, igneous intrusions, and unconformities, the rock that is cut is older than the cutting structure, and; (5) inclusions of “foreign” rock are older than the encasing rock. In reality, many sedimentary strata are not deposited as horizontal strata, and thrust faults and igneous intrusion can superimpose older rocks on or adjacent to younger ones. Furthermore, overturned and recumbent folds can superimpose older strata over younger strata, and cause some strata to be upside down. Sedimentary structures discussed in Part 3 of this book are typically used to determine whether or not deformed strata are upside down. The

CROSS SECTION



- PRINCIPLES:**
- (1) Youngest, undeformed sedimentary rocks lie above older ones
 - (2) Sedimentary strata originally deposited on low slope
 - (3) Sedimentary strata originally laterally extensive
 - (4) Discordant surfaces (unconformities, faults, margins of intrusion) post date rocks that they cut

- GEOLOGICAL HISTORY:**
- (1) Deposition, burial, folding of lower sedimentary series
 - (2) Igneous intrusion
 - (3) Faulting
 - (4) Uplift and erosion of unconformity
 - (5) Deposition and burial of upper sedimentary series
 - (6) Uplift and erosion of topography

Figure A-29. Relative age dating using rock structure

terms Primary, Secondary and Tertiary arose from this method of relative age dating. The oldest Primary rocks are very hard and deformed igneous and metamorphic rocks, Secondary rocks are hard sedimentary rocks that are commonly deformed, and Tertiary rocks are flat-lying, soft sedimentary rocks. The term Tertiary is still used today. However, Tertiary rocks are commonly deformed and comprise the full gamut of sedimentary, igneous and metamorphic rocks.

Fossils

The basis of the modern relative time scale (Figure A-31), for rocks less than 600 million years old, is fossils. Fossils can only be used for relative age dating because organisms have evolved through time, and they have left a record of their existence in sedimentary strata. Those who do not believe in the scientific basis of evolution not only fail to appreciate a large body of paleontological information: they are also at a great disadvantage when it comes to establishing the relative age of rocks. One of the important characteristics of the fossil record is that it is common to find morphologically distinct fossils of a particular taxonomic group in immediately superimposed formations. It has long been argued whether this is due to an incomplete stratigraphic record, or episodic evolution of organisms, or both. An incomplete stratigraphic record can be due to lack of preservation of organisms and/or due to preservation and subsequent erosion of the stratigraphic record. Study of the nature of preservation of fossils is called *taphonomy*. Apparently, morphological evolution of a species can be gradual or punctuated. With punctuated evolution, relatively long periods of little change (stasis) are punctuated by relatively short periods of rapid speciation.

The most useful fossils for biostratigraphic dating are those that: (1) are abundant; (2) are the same age as the rocks in which they are found (i.e. not reworked); (3) have a wide geographic distribution, not restricted to specific lithofacies; (4) occur in strata that are uninterrupted by long breaks due to erosion or non-deposition, and; (5) evolved rapidly. Examples include: graptolites in the Cambrian and Ordovician; ammonites in the Jurassic and Cretaceous; plant spores in the Devonian and Carboniferous; mammals in the Tertiary. When a biostratigraphic time scale is calibrated with an absolute time scale, the best resolution possible is generally on the order of 1 million years. Thus, if deposition rates vary between 0.1 and 1 mm/year, the age of less than 0.1 km to 1 km of strata, respectively, cannot be distinguished with any accuracy.

Definition of biostratigraphic units

Definition of biostratigraphic units normally involves examination of a long, continuous sequence of sedimentary rocks (with no obvious major breaks in deposition) and collection of key fossil types at closely spaced intervals. This hopefully results in a variety of fossil species at

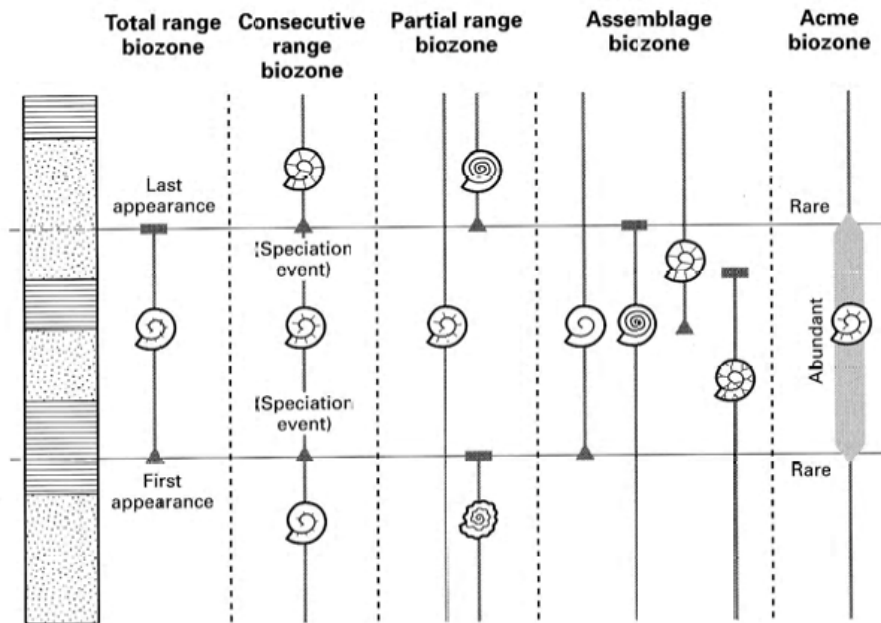


Figure A-30. Explanation of biozone types (from Nichols, 1999).

| Phanerozoic | | Eonothem | | Eon | | Eratthem | | System | | Period | | Series | | Epoch | | Age | | | | |
|-------------|-----------|-----------|----------|--------|-----------|------------|-------------|---------------|-------------------------|-------------------------|-------------------------|-------------------------|-----------|-----------------|-------------------------|-------------------------|-------------------------|-----------|-----------|------|
| Phanerozoic | Cenozoic | Neogene | Holocene | 0.0115 | Upper | Cretaceous | Pleistocene | 1.806 | Lower | 88.6±0.9 | Permian | Lopingian | 280.4±0.7 | Neo-proterozoic | Ediacaran | 630 | 1000 | 1800 | | |
| | | | | | | | | | | | | Guadalupian | | | | | | | 270.6±0.7 | |
| | | | Pliocene | 5.332 | Lower | | 145.5±4.0 | Carboniferous | Pennsylvanian | 318.1±1.3 | Mesoproterozoic | Paleoproterozoic | 289.0±0.8 | Devonian | Upper | 385.3±2.6 | 2500 | 2800 | 3200 | 3800 |
| | | | | | | | | | | | | | | | Middle | | | | | |
| | | | Miocene | 23.03 | Upper | | 181.2±4.0 | Middle | 416.0±2.8 | 418.7±2.7 | Paleo-proterozoic | Neo-archean | 422.9±2.5 | Silurian | Wenlock | 428.2±2.3 | 2500 | 2800 | 3200 | 3800 |
| | | | | | | | | | | | | | | | Lower | | | | | |
| | Paleogene | Oligocene | 33.9±0.1 | Lower | 199.6±0.6 | Upper | 471.8±1.6 | Archean | Paleo-archean | 443.7±1.5 | Ordovician | Upper | 480.8±1.8 | 3200 | 3800 | 3800 | 3800 | | | |
| | | | | | | | | | | | | Middle | | | | | | 471.8±1.6 | | |
| | | Eocene | 58.8±0.2 | Upper | 228.0±2.0 | Middle | 488.3±1.7 | Furongian | 501.0±2.0 | Eoarchean | 513.0±2.0 | Cambrian | Middle | 542.0±1.0 | Lower limit not defined | Lower limit not defined | Lower limit not defined | | | |
| | | | | | | | | | | | | | Lower | | | | | 245.0±1.5 | | |
| | | Paleocene | 65.0±0.3 | Lower | 251.0±0.4 | Lower | 513.0±2.0 | 542.0±1.0 | Lower limit not defined | | | | | | | | |

Figure A-31. Geological Time Scale.

Table A-4. *Definition of terminology for rock and time units.*

| Time unit | Rock unit |
|--|---|
| Eon (e.g. Phanerozoic) | |
| Era (e.g. Paleozoic) | Erathem |
| Period (e.g. Devonian) | System |
| Epoch (e.g. Middle Devonian) | Series |
| Age (e.g. Frasnian) | Stage |
| Also divisions into Early, Middle, Late | Also divisions into Lower, Middle, Upper |

Table A-5. *Typical minerals used for radiometric dating, with parents, daughters, half lives, and practical dating ranges.*

| Parent | Daughter | Half life (10⁹ yr) | Dating range (Ma) | Minerals |
|-------------------|-------------------|--------------------------------------|--------------------------|-------------------------|
| ⁴⁰ K | ⁴⁰ Ar | 1250 | 1 to > 4500 | Many silicates |
| ⁸⁷ Rb | ⁸⁷ Sr | 48.8 | 10 to >4500 | Many silicates |
| ¹⁴⁷ Sm | ¹⁴³ Nd | 1.06 | >200 | |
| ¹⁷⁶ Lu | ¹⁷⁶ Hf | 3.5 | >200 | |
| ²³² Th | ²⁰⁸ Pb | 14.01 | 10 to >4500 | |
| ²³⁵ U | ²⁰⁷ Pb | 0.704 | 10 to >4500 | Zircon, sphene, apatite |
| ²³⁸ U | ²⁰⁶ Pb | 4468 | 10 to >4500 | Zircon, sphene, apatite |
| ¹⁴ C | ¹⁴ N | 5730 yr | < 80,000 yr | Wood, charcoal, bone |

any particular stratigraphic level, and changes in these fossil assemblages through the sequence. The fossil assemblages are then subdivided into biostratigraphic units or biozones (Figure A-30). A total range zone is the strata encompassing the entire range of a particular species. A concurrent range zone is the strata encompassing the overlapping ranges of two or more selected species. An assemblage zone is the stratigraphic interval with a specific assemblage of fossil species that may or may not be related. Not all components of the assemblage must be present everywhere, and no attention is paid to ranges. Statistical analysis (e.g. cluster analysis, principal component analysis) can be used to identify significant assemblages of species.

The geological time scale in use today (Figure A-31) has subdivisions based largely on rock types and characteristic fossils. Table A-4 shows the hierarchy of terms used to define biostratigraphic units, and their lithostratigraphic equivalents. Biostratigraphic units can be considered to be chronostratigraphic units if it is assumed that evolution and dispersal of species are rapid relative to sediment accumulation. If it takes a relatively long time for evolution, dispersal and preservation of a species, a biostratigraphic zone may be diachronous.

Paleomagnetism

Paleomagnetic age dating, based on magnetic polarity reversals, potentially has a resolution at least an order of magnitude better than biostratigraphic dating. This method depends upon: (1) magnetic sediment particles (generally iron oxides) that attained a magnetic orientation at or soon after deposition, aligned with the prevailing field; (2) recognition and isolation of subsequently superimposed magnetic fields; (3) reasonably continuous deposition to obtain a faithful record of reversals. These criteria are not always met. Different phases of acquisition of remanent magnetism are recognized by thermal demagnetization, the earliest field generally being stable at the highest temperature. The sequence of polarity zones (chrons) is only useful if it is distinctive enough to be matched with parts of a global magnetic polarity time scale, that has been established based on oceanic sediments and basalts, and calibrated with radiometric dating (i.e., Cretaceous to Recent). Such matching of polarity zones requires making the very important assumption that deposition rate is approximately constant, such that a long period of normal or reversed polarity appears as a relatively thick polarity zone. The best time resolution of this

method is on the order of 100,000 years (10 to 100 m of strata at deposition rates of 0.1 to 1 mm/year), although this resolution may be increased by detailed study of the changes in the paleomagnetic field over polarity transitions (e.g., Tauxe & Badgley, 1988). For rocks older than Cretaceous, magnetic polarity dating can still be useful, even though an absolute time scale may not be available.

Cyclostratigraphic dating

There has been a suggestion that if cyclicity in sediments can be related to Milankovitch climatic cycles, then relative age dating with a resolution of better than 100,000 years is possible. This suggestion is flawed for several reasons: (1) with the exception of some well-dated Quaternary examples, the effects of the spectrum of Milankovitch climatic cycles on the nature of deposition are poorly understood, and cannot be separated easily from the effects of other processes that give rise to cyclicity at similar time scales; (2) as the resolution of radiometric age dating decreases with rocks of increasing age, it is never generally possible to establish independently that any sedimentary cycle was deposited in the order of 10^4 to 10^5 years, and; (3) the periods and magnitudes of Milankovitch cycles may have varied in the past.

Absolute age determination

Radiometric

Radiometric dating is based on the knowledge that certain radioactive isotopes of elements (parents) become transformed into a different element (daughter) at a fixed rate (Figure A-32).

The rate of isotopic disintegration is negative exponential, given by

$$N/N_0 = e^{-\lambda t}$$

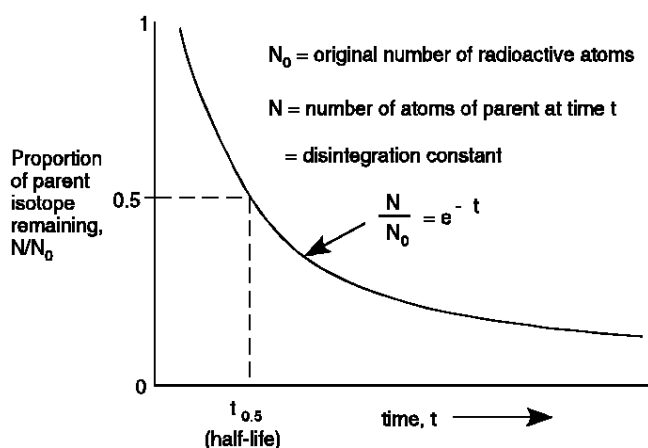


Figure A-32. Radiometric dating. Radiometric decay versus

in which N is the number of radioactive atoms of the parent at time t after the rock formed, N_0 is the original number of radioactive atoms, and λ is the disintegration constant. The half life is the time required to reduce the original number of parent atoms by half, and equals $0.693/\lambda$. The resolution of radiometric dating decreases as the half-life of the parent radioisotope increases. Thus, as radioisotopes with the shortest half-lives are used for dating the youngest rocks, the resolution of radiometric dating is generally best for the youngest rocks (Table A-5). For material on the order of 10^3 years old, the resolution is on the order of 10^1 to 10^2 years (C^{14} method), whereas the resolution is on the order of 10^6 years for rocks that are 10^7 to 10^8 years old.

Radiometric dating involves measurement of the relative amounts of a parent and daughter elements in a sample using a mass spectrometer. This will give the date when the mineral crystallized (or recrystallized), as long as no atoms of the daughter element were lost or added from elsewhere. Errors in radiometric dating are related to loss of daughter atoms and measurement of very small amounts of certain elements. Nichols (1999) gives a brief review of various methods of radiometric dating.

Luminescence

Luminescence dating is being used increasingly for dating Quaternary sediments (Duller, 1996; Aitken, 1998; Murray & Wintle, 2000). This technique is based on the ionizing effects of natural radioactivity from minerals containing potassium, thorium and uranium. Electrons released by ionizing radiation become trapped in defects in crystal lattices and accumulate through time. The age of the mineral can be calculated by measuring the “dose” of electrons received, given knowledge of the radioactivity of the surrounding sediment. When the grain is subjected to light, the charged particles are liberated and the grain exhibits luminescence. Optically stimulated luminescence (OSL) relies on the fact that sunlight bleaches the luminescence signal, so that the time since the grain was last exposed to sunlight (i.e. was buried in the sediment) can be calculated. OSL can be used to date sand grains (quartz and feldspar) that are tens to hundreds of thousands of years old. However, if the sediment was transported in a

very turbid fluid, sunlight might not have fully bleached the sediment. In this case, the burial age would be over-estimated.

Fission track

Fission track dating is based on radioactive isotopes such as ^{238}U (occurring in zircon, sphene and apatite) that emit alpha particles and cause damage to the crystals called fission tracks. The density of the fission tracks increases with increasing age. In order for a fission track to be formed, the temperature of the mineral must be below a so-called blocking temperature (about 300°C for zircon and 90°C for apatite). Therefore, the age determined is when a cooling mineral passed through the blocking temperature. The main use of fission track analysis is to determine the uplift and exhumation history of a rock. If the geothermal gradient is known, it is possible to determine the time when the rock was raised above the depth of the blocking temperature.

Cosmogenic nuclides

Highly energetic cosmic rays bombard rocks and sediments and produce very small amounts of rare radioactive nuclides such as ^{10}Be , ^{14}C , ^{26}Al , and ^{36}Cl , and stable noble gases ^3He and ^{21}Ne , within the upper few meters of the land surface. The resulting terrestrial *in situ* cosmogenic nuclide concentrations (TNC) vary with depth, latitude, altitude, time off exposure, and mineralogy of the surface material. Therefore, nuclide concentration profiles can be used to determine age since a surface was exposed to the atmosphere for time ranges on the order of 10^2 to 10^7 years. Complications arise if the surface is being eroded or undergoing deposition, moving vertically or tilting, sporadically covered by ice or rubble, or if cosmogenic nuclides formed during a previous episode of exposure of the material. Reviews of TNC dating can be found in Cerling and Craig, (1994), Gosse and Phillips (2001), and the references in Knight, (2006).

Annual cycles

It is well known that seasonal variation in the growth rate of trees gives rise to tree rings. The thickness of a tree ring is the product of the length of the growing season and the rate of growth. Tree-ring analysis can therefore be used to date trees and climatic fluctuations (if they affect the thickness of tree rings). Laminae in lake sediments (varves) have also been used to indicate annual fluctuations in sediment supply. However, varves are not necessarily annual, as discussed in Chapter 17.

Correlation of sedimentary strata

Lithostratigraphic correlation

Lithostratigraphic correlation is interpretation of the physical continuity of particular sediment types from place to place. Physical continuity must be interpreted because observation is very difficult even with well-exposed strata. The practice of lithostratigraphic correlation involves making important assumptions regarding the distinctiveness, geometry, orientation and lateral extent of the rock types correlated, and the presence or absence of structural discordances such as faults. It is essential to state clearly what assumptions are being made when attempting lithostratigraphic correlation. For most sedimentary rocks, there appears to be a relationship between the thickness of strata or stratasesets (th) and their lateral extent (le) in a given direction relative to paleocurrent direction. Values of le/th are commonly on the order of 10^1 to 10^3 . Thus, it is dangerous to make long-distance correlations of small thicknesses of strata (e.g., strata less than 1 m thick over distances of more than 1 km). It is common for well spacing associated with hydrocarbon reservoirs to be on the order of hundreds of meters. Some meters-thick fluvial strata may not be able to be traced between adjacent wells. However, some types of strata (e.g. coal seams, paleosols, volcanic-ash layers) are considered to be distinctive and widespread enough to be correlated over distances many orders of magnitude greater than their thickness. Such "marker beds" are commonly used to provide a framework of stratigraphic datums within which correlation of less distinctive strata is attempted (e.g., Miall, 1996). However, great caution should be exercised in assuming that "marker beds" are distinctive and laterally continuous.

Correlation of sandstone bodies using wireline-logs is the most common method for estimating their widths and orientations. Contour maps of sandstone body thickness are commonly constructed following the correlation procedure. The spatial resolution of this mapping technique can be no better than the average well spacing. Therefore, if well spacing is 300 m, sandstone bodies less than 300 m wide cannot be resolved. The validity of this technique is very much dependent on the correlation rules utilized. Once a suitable horizontal datum has been chosen for the wells to be correlated, it is necessary to establish whether sandstone bodies at similar stratigraphic levels in different wells can be correlated. Well-to-well correlation is commonly compromised by simplistic or erroneous assumptions, such as: (1) bases and tops of sandstone bodies are flat; (2) sandstone bodies positioned at the same stratigraphic level must be connected between adjacent wells; (3) sandstone body width/thickness ratios are closely related to depositional environment, and; (4) vertical sequences through sandstone bodies indicate depositional environment and hence the geometry of the sandstone bodies.

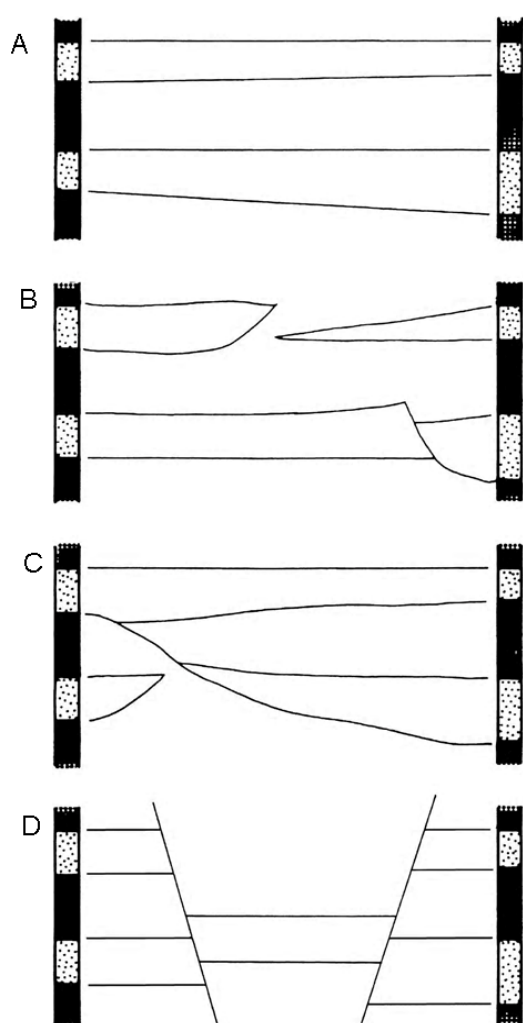


Figure A-33 illustrates some of the possibilities for correlation of sedimentary rock units between two wells. Some of the possibilities could be eliminated with additional data such as seismic profiles or tests of connectivity of permeable strata using changes in fluid pressure or fluid composition during production. Mathematical methods are available for correlating sections (e.g. cross correlation and cross association: see below), but many assumptions need to be made that cannot generally be justified. In order to reduce the uncertainty in lithostratigraphic correlation, attempts have been made to define the geometries of the various kinds of sediment bodies in different depositional environments, and to model their distribution in space. These attempts are fraught with difficulty.

Figure A-33. Different ways of correlating rock units between two wells. (A) simple-minded approach. (B) imaginative sedimentologist approach. (C) sequence stratigrapher approach. (D) structural geologist approach.

Chronostratigraphic and Biostratigraphic correlation

Chronostratigraphic correlation is establishment of the time equivalence of rocks in different areas. Biostratigraphic correlation can be considered equivalent to chronostratigraphic correlation if it can be assumed that organisms evolved in different areas simultaneously (no gradual migration of species) and that this evolution was faithfully recorded in the sediments (no preferential preservation). In view of the resolution of age dating discussed above, chronostratigraphic correlation throughout most of the rock record (except the Quaternary) is only possible for sequences that accumulated over time spans in excess of 100,000 years and normally in excess of a million years. However, correlation of rocks that accumulated over shorter time spans may be possible if a particular stratum or bedding plane can be traced laterally and there is strong evidence that it is coeval everywhere. For example, certain reflectors in seismic profiles are commonly assumed to be time lines and are used for chronostratigraphic correlation.

The relationship between lithostratigraphic correlation and chronostratigraphic correlation is illustrated in Figure A-34, which indicates that lithostratigraphic boundaries and time lines may be coincident in some sections but not in

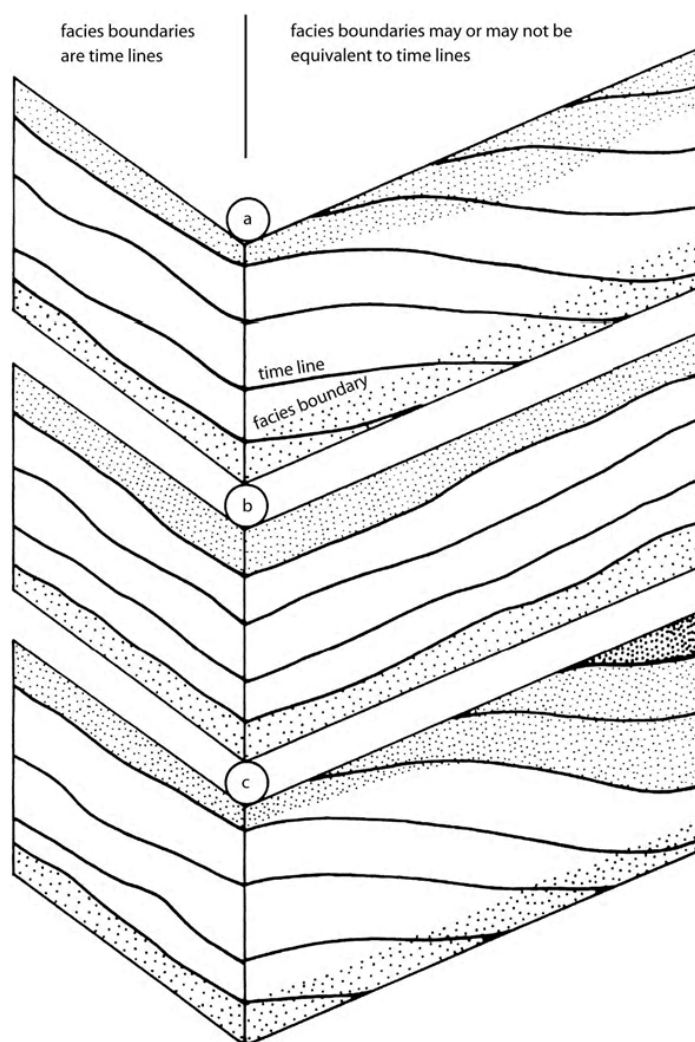


Figure A-34. Distinction between lithostratigraphic and chronostratigraphic units, where depositional conditions and facies change in (a) space, (b) time, and (c) time and space.

others (i.e., diachronous). A particular vertical sequence of lithofacies can be produced by lateral translation of an inclined surface across which the lithofacies vary (Walther's law of facies), but also by changing the conditions of deposition in time across the whole depositional area. It is extremely difficult to separate these two effects in rocks, and they commonly occur simultaneously.

Interpretation of origin of sedimentary deposits

Methods

The only rational way to start interpreting the origin of ancient sedimentary deposits is from knowledge of modern sedimentary processes and environments. The application of this principle, *the present is the key to the past*, presents a number of dilemmas related to differences in the nature of data available from ancient deposits and modern sedimentary environments, and to whether modern environments are representative of those in the past.

Sedimentary rocks are normally observed in one- or two-dimensional vertical sections, and it is rarely possible to obtain a view of a paleo-land-surface. Sedimentary rocks yield a record of sediment accumulation over millions of years, and the age of rocks can generally only be established with a resolution of 100,000 years at best. In contrast, modern sedimentary environments yield essentially a two-dimensional view of deposits parallel to the land surface, and it is difficult to study the deposits in extensive two-dimensional vertical planes, even with cores and geophysical profiling. The observable sedimentary processes are those going on now, or those that have been recorded over the past few centuries, i.e., essentially a snapshot in time. Even though it is possible to date Recent sediments (less than about 10^4 years old) quite accurately, historic records are not normally sufficient to directly link the nature of the deposits to the processes responsible. This uncertainty has led to the question of whether ancient deposition was related mainly to “catastrophic” events such as 1000-year floods, or was due to more “normal” seasonal events. Attempts to solve these dilemmas have involved scale-model experiments and quantitative theoretical modeling. The smaller-scale sedimentary stratatasets that formed over relatively short time spans (say, less than 10^3 years) can be interpreted by direct comparison with modern processes and deposits studied in the laboratory and in the field.

However, interpretation of the larger-scale strataset that accumulated over longer time spans requires increasing reliance on theoretical models.

How can we be sure that modern sedimentary processes and environments are representative of the past, when we have evidence of quite different environmental conditions during the Pleistocene glacial maxima, and that the biosphere, oceans and atmosphere have all evolved throughout Earth history? The consensus of opinion appears to be that basic scientific principles have not changed, even though certain processes and forms have. In other words “the rules are the same, but the players may be different”.

Different scales of strata

Different scales of strataset or facies have different genetic connotations. Facies, as commonly defined, can be interpreted in terms of depositional processes and sediment supply. Formative depositional processes can be observed in modern environments and in laboratories because of the relatively small time and space scales involved. For example, trough cross-stratified sand (facies) is deposited on a sand bed from bedload moving as curved-crested ripples or dunes. The combination of mean grain size and the interpreted bed-form geometry can give quantitative information on ancient flow depth and flow velocity. The thickness of the cross sets may yield information on the sequence of bed forms of different height that passed through the area, plus the deposition rate relative to the bed form migration rate (see Chapter 5). Paleocurrent data give the local flow direction of unidirectional currents of a given velocity (Allen, 1966). Sandstone petrology can yield information on the provenance of the grains, their weathering and transport history, and diagenetic changes.

Facies associations (and synonyms given previously) give information about depositional environments that are associations of distinctive processes and landforms. The facies association shown in Figure A-6 is interpreted as a channel bar and channel fill, based on the spatial association of facies and their geometry and orientation. The association of facies is due to depositional conditions that changed in time and space. In addition to the information obtainable from the individual facies, the association of facies can yield information about the geometry,

flow, sediment transport, erosion and deposition in the channel and how it changed with time. This facies association could have formed entirely as a result of “normal” sedimentary processes. However, it is important to consider whether a change of facies in a particular environment (e.g. the change from channel-bar deposition to channel filling represented in Figure A-6) is due to “normal” processes or a cyclic or progressive change in controlling factors such as climate, tectonism and base level.

Groups of facies associations give information on how associated depositional environments (e.g., river channels, floodplains, tidal flats) changed in time and space. Once again, such changes may be due to “normal” sedimentary processes, or associated with changes in climate, tectonism and base level either within or external to the depositional basin. In order to interpret such groups of facies associations, it is necessary to have correlated stratigraphic data throughout the sedimentary basin (including accurate age dating) and to make use of a range of theoretical models.

Depositional facies models

A facies-association model for a given depositional environment is supposed to represent the main physiographic and depositional features of the environment accurately and unambiguously, such that the model can be compared with sedimentary features observed in rocks, thus leading to interpretation of ancient depositional environments. Most facies-association models in the literature are inadequate for anything more than a very general qualitative environmental interpretation because: (1) the deposits are normally represented in only one or two vertical sections, normal and parallel to the flow direction; (2) the information shown in these two-dimensional sections lacks critical detail of the spatial variation of strata thickness and orientation, grain size, internal structures, paleocurrents and biological features; (3) the nature of preservation of the strata is not indicated, because the models are not dynamic, and; (4) the models are purely qualitative and many do not even contain scales. The reasons for this state of affairs are: (1) incomplete knowledge of modern depositional environments (difficulties in sampling below the water table, and in observing high-energy sedimentary processes); (2) incomplete knowledge of the evolution of depositional environments and their deposits over time

periods in excess of a few hundred years (lack of a long-term dynamic context), and; (3) uncertainties in translating essentially two-dimensional (parallel to land surface) information representing a single snapshot in time into a fully three-dimensional dynamic model. The solutions to these problems require much more serious, comprehensive studies of modern processes and deposits, supplemented by scale-model experimentation and quantitative theoretical modeling. Our ability to use models for predictive purposes will remain severely limited until this situation is improved.

Larger-scale models for groups of facies associations (e.g., basin-filling models, sequence stratigraphy models) suffer from all of the same drawbacks as the facies association models mentioned above, and more, because modern depositional processes cannot be observed for millions of years and over the large spatial scales involved. Thus, such models must be largely hypothetical or theoretical, and are commonly based on interpretation of the rocks themselves (circular reasoning). Also, there is a tendency among the authors of such models to stress the influence of only a limited number of the various possible controls on depositional architecture (e.g. glacio-eustatic sea level change as a control on accommodation space).

Interpretation of subsurface data

Many of the sedimentary features that allow interpretation of the origin of deposits are not readily observable in cores, wireline logs and seismic profiles. Therefore, interpretation of deposits from subsurface data will be limited. Interpretation of depositional environments from cores relies on relatively small-scale features (such as small-scale cross strata, ripple marks, fossils, trace fossils, desiccation cracks, and concretions), and vertical variations of composition, texture, and sedimentary structure. Wireline logs calibrated with cores can be used to describe vertical trends in stratal thickness, grain size and composition where core data are absent (Asquith, 1982; Doveton, 1994). Paleocurrent data can be obtained from a dipmeter or FMS. In some cases, the thickness and grain size trends of various scales of stratigraphic set can be used to define the heights of topographic features such as dunes, bars, channels, deltas, etc. Also, it may be possible to estimate the width of sediment bodies from their thickness, thus aiding lithostratigraphic correlation. Correctly correlated logs give an indication of lateral extent,

proportion and connectedness of facies. 3-D seismic can indicate the thickness and plan form of thick sandstone bodies, perhaps leading to interpretation of depth, width and pattern of subaerial or submarine channels.

Appendix 3: Modeling of Earth surface processes, landforms, and sedimentary strata

Introduction

Understanding of Earth surface processes, landforms, and sedimentary processes has come from: (1) field studies of modern environments; (2) laboratory flume studies using physical models, and; (3) construction of idealized models based on these studies. Understanding and prediction of ancient sedimentary deposits is based on direct modern analogs or idealized models.

Field studies of modern environments are essential for understanding Earth surface processes, landforms, and deposits. However, such studies are difficult to undertake during extreme Earth-forming events (such as floods, hurricanes, volcanic eruptions), over large areas, and for a long time, and it is difficult to describe deposits below the water table. Some of these problems are beginning to be overcome by: using remote-sensing images and digital elevation models (DEMs) for studying changes in Earth surface geometry; using a new generation of submersibles for studying the deep sea bed; measurement of fluid flow and sediment transport during extreme flow events using new types of equipment (e.g., acoustic Doppler current profilers; multibeam sonar; positioning using GPS); description of deposits using high frequency geophysical profiling (e.g., ground-penetrating radar) in combination with coring; using new sediment dating methods such as optically stimulated luminescence (OSL) dating.

Laboratory flumes have been used to study Earth surface processes, landforms, and deposits over a wide range of physical scales. These physical models may be full-scale, reduced scale, or un-scaled (analog). However, scaling problems can limit the applicability of these studies to the real world, and these problems increase as the scale of the physical model decreases relative to the real-world prototype. In particular, all superimposed scales of bed-form and associated strata cannot be produced in flumes, and rates of sedimentary processes are unrealistically high. Laboratory models are discussed below.

Idealized models are widely used to understand and predict the nature of Earth surface processes, landforms, and deposits, and many examples have been described in this book. Idealized models may be qualitative (graphic), quantitative (numerical); static, dynamic (forward); stochastic, deterministic. As these models are ultimately based on studies of modern Earth surface processes, landforms and sediment deposits, models that describe relatively short time spans (less than a thousand years) and small spatial scales (less than a few tens of square kilometers) are well developed and most easy to test. As the spatial and temporal scale increase, it becomes impossible to undertake field and laboratory studies, and increasing reliance is put on models for our understanding. Unfortunately, useful models for large scales and long time periods are difficult to construct and test, and it is difficult to link models of different scales. Numerical models are briefly discussed below, including process-based models, stochastic models, and fuzzy logic models.

Physical laboratory models

Laboratory rivers and floodplains

Water flow, sediment transport, bed topography, erosion and deposition in rivers and floodplains have been studied extensively in laboratories using scale models. There are also laboratory models of drainage systems and of rivers entering standing bodies of water. Laboratory experiments are undertaken because of the relative ease of controlling important variables (such as water and sediment discharge, and channel slope) and in making measurements in a manageable environment. However, the advantages of laboratory experiments are commonly compromised by certain disadvantages, such as unrealistic experimental conditions, and problems of scaling. Useful discussions of the procedures and limitations in using scale models are by Schumm et al. (1987), Parker & Wilcock (1991), Peakall et al. (1996), and Paola (2000).

Some experimental channels are constructed with solid fixed boundaries and carry only water. Such channels cannot be used for studying the interaction between water flow, sediment transport and bed topography. Other channels have boundaries made of sediment that can be

moved by the flow, although the sidewalls are commonly solid. In some cases, the water in such channels is recirculated, but the sediment is not. In this case, sediment must be continuously fed from upstream. In other cases, both water and sediment are recirculated, although extra sediment can still be fed in. The behavior of a laboratory channel is influenced by whether or not sediment is recirculated (Parker & Wilcock, 1991). The entrance and exit conditions in laboratory channels are commonly very unrealistic, which limits the useable part of the channel. Many channel sidewalls are fixed and straight (unrealistic), and many channels have width/depth ratios that are much too small compared with real rivers.

In some cases, laboratory channels are full-scale models of small rivers, although it is rare for such a channel to be exactly the same as the real one. In the world of laboratory flow channels, a channel that is more than about 10 m long, 1 m wide and 0.5 m deep would be considered large. In most cases, laboratory channels are reduced-scale models. In order to be able to apply the results of a reduced-scale model to a real-world prototype, the model and the prototype should ideally be dynamically, kinematically and geometrically similar. This means that the model and the prototype should have the same (or similar) values of a set of dimensionless numbers that describe the physical system. These dimensionless numbers are derived from combining the important variables of the system, using the Buckingham (1915) Pi theorem. In the case of a wide, water-carrying channel with a fixed rough bed, the important variables are fluid viscosity μ , fluid density ρ , flow velocity U , flow depth d , bed slope S , bed roughness height D , and gravitational acceleration g . Typically, these parameters would be combined into the following dimensionless numbers (see chapter 5):

| | |
|---------------|----------------------|
| $Ud\rho/\mu$ | (Reynolds number) |
| U/\sqrt{gd} | (Froude number) |
| d/D | (relative roughness) |
| S | (slope) |

If the bed is made of mobile sediment of density σ and grain size D , additional dimensionless numbers would be:

| | |
|------------------------------------|----------------------------------|
| $U_* D \rho / \mu$ | (grain Reynolds number) |
| $\rho U_*^2 / (\sigma - \rho) g D$ | (dimensionless bed shear stress) |
| σ / ρ | (density ratio) |

in which U_* is shear velocity defined as $\sqrt{\tau_o / \rho}$. In this case, S is not necessary.

In many models, the water viscosity and density are the same as the prototype. Typically the depth in a model is less than the prototype. Therefore, in order to maintain similarity in Reynolds and Froude numbers, the flow velocity in the model must be reduced. If the velocity is reduced too much, the Reynolds number may be so small that the flow is barely turbulent. If the velocity is not reduced enough, the Froude number may exceed 1 and the flow becomes supercritical. Therefore, in order to model a fully turbulent, subcritical flow, it may not be possible to have both Reynolds and Froude similarity. In this case, Froude similarity would probably be maintained, and the requirement for Reynolds similarity would be relaxed as long as the flow was turbulent. One way round this dilemma might be to reduce viscosity in the model by increasing water temperature.

If the depth in the prototype river is 1 meter and the sediment size is 10 mm (relative roughness of 100), then a laboratory channel with a depth of 0.1 m should have a sediment size of 1 mm. In this case, the grain Reynolds number of a mobile bed would be large enough to ensure hydraulically rough flow, even though it is not as large as the prototype. Thus the model would be a reasonable scale model of a shallow gravel-bed river. It is not so easy to make a scale model of a deep, sand-bed river, because the sediment size in the scale model would need to be so small that it would probably be cohesive. For example, if the prototype river depth was 10 m and the bed sediment size was 1 mm (relative roughness 10,000), a model channel with a depth of 0.1 m would require bed sediment size to be 0.01 mm.

Complete similarity is very difficult to attain, and some of the scaling requirements must be relaxed. When trying to model long-term, large-scale processes, such as the development of drainage networks, deltas, alluvial fans, and shallow-marine sedimentary basins, it is difficult to maintain any scaling relationships. Such models are essentially unscaled, and are referred to as

analog models. Great care must be exercised in applying the results of analog models to the real world. Two modern examples of such experimental facilities are the so-called *Jurassic Tank* at the University of Minnesota, USA and the *Eurotank* at the University of Utrecht, Netherlands. Both of these “experimental stratigraphy” tanks are 13 m by 6.5 m in area and 1.3 to 1.4 m deep. Novel features of these tanks are computer-controlled adjustable floors (to simulate basin subsidence and uplift), and sophisticated scanning of surface topography to produce digital elevation models. These facilities have been used to model the effects of sea-level and climate change and tectonism on the processes and stratigraphy of river systems, coasts and shallow sedimentary basins.

Wind tunnels

Wind tunnels are the air-flow equivalents of flumes, and are used for studying air flow velocity, sediment transport, and bedforms (see White, 1996). The design, mode of operation, and scaling issues are similar to those for water flows in flumes. Wind tunnels can be open circuit or closed circuit. It is common for air to be moved by a fan at the downstream end of the working section. Wind tunnels must be long enough such that fully developed turbulence is attained. This development length is 10 to 25 boundary layer heights (10 to 15 m). Scaling of wind-tunnel flows carrying sediment involves the flow Reynolds number, grain Reynolds number, Froude number, and Richardson number. As in the case of water flows, it is not possible to scale all of these parameters simultaneously. However, it is normally possible to obtain a turbulent, hydraulically rough flow. Wind tunnels can be scaled to model bed-load and suspended-load transport and small dunes in the lowest 100 m of the atmospheric boundary layer. Coriolis force effects obviously cannot be simulated.

Turbidity current tanks

Flumes and tanks have been used widely for experimental studies of turbidity currents. (reviews by Simpson, 1997; Kneller and Buckee, 2000; Peakall et al., 2001). Scaling parameters that must be considered include flow Reynolds number, densimetric Froude number, Richardson number, density ratio of the turbidity current and the ambient fluid, grain size/flow

thickness ratio, and bed slope (see chapter 8). It is very difficult to scale the grain size properly because of cohesive forces in the fine-grained sediment that must be used. Realistically creating a sediment suspension that becomes turbulent in a flume is challenging. Many experiments have been conducted using release of a dense sediment suspension (or a dense fluid such as milk) from a reservoir at the upstream end of a flume (so-called lock release). These experiments suffer from excess flow disturbance at the lock gate, reflection of the density flow from both ends of the flume, and overemphasis on the head of the turbidity current (Peakall et al., 2001). More recent experiments with a steady supply of a dense sediment suspension upstream from the flume entrance are more realistic. There are also difficulties in measuring turbulent flow velocities in high-concentration, transient flows. New flow measuring techniques are also being developed for measuring turbulence in dense suspensions (Peakall et al., 2001).

Wave tanks

Wave tanks are widely used for measuring patterns of water flow, sediment transport and bedforms under progressive water-surface waves, particularly in the case of shoaling waves approaching a beach. Important scaling parameters are wave length/depth, wave height/depth, bed slope, near-bed orbital diameter/grain size, grain-size Reynolds number, dimensionless bed shear stress, and grain density/fluid density (see chapter 7). The flow velocities used in the grain Reynolds number and the dimensionless bed shear stress are normally the maximum near-bed orbital velocity. In many wave tanks, waves of a specified period, length and height are generated mechanically at one end of the tank. There are obvious limits to wave size and period in these tanks. Bedforms such as wave ripples and plane beds can be formed in these wave tanks. However, bedforms such as hummocks (large 3D wave ripples) would require very large orbital diameters, hence wave sizes. Southard et al (1990) attempted to get round this problem by periodically reversing flow direction and velocity in a flume tank using plungers at either end of the flume.

Numerical, process-based models

Understanding and prediction of Earth surface processes, landforms and sediment deposits is aided by numerical modeling. The most desirable approach to such numerical modeling, irrespective of scale, is through solution of the fundamental equations of motion for the fluid and the sediment (e.g., conservation of mass, momentum and energy), so-called computational fluid dynamics. Construction of the equations of motion requires an understanding of the interactions among the fluid flow (which may be unsteady, non-uniform, and turbulent), the transported sediment, and the topography of the sediment bed. This understanding is very incomplete, and requires much more study of modern environments in the field and laboratory. Books and reviews concerning construction of numerical, process-based models in the Earth Sciences include Harbaugh and Bonham-Carter (1970), Cross (1990), Franseen et al. (1991), Kirkby (1994), Slingerland et al. (1994), North (1996), Harbaugh et al. (1999), Harff et al. (1999), Paola (2000), Merriam and Davis (2001), and Bridge (2006).

Simplified numerical forward models have been applied to relatively short term, small-scale processes such as: flow and sediment transport over bed forms, and resulting bedform geometry, growth, and migration; bed degradation and armoring downstream of dams; reservoir sedimentation; and sorting of sediment (e.g., downstream fining) during deposition in spatially decelerating flows, to name just a few. Many examples of these types of models are discussed throughout this book. However, such models are rarely applied over long time periods, over large spatial scales, and where there are complicated temporal and spatial variations in the Earth surface geometry, fluid and sediment supply. This is because of limitations to computing facilities, and because of lack of understanding of the workings of the Earth surface system. As a result, long-term, large-scale surface processes are commonly treated using “process-imitating” models. Process-imitating models do not necessarily represent processes accurately or completely. Process-based models are generally undeveloped, and linkages between models for different scales are lacking. Process-based modeling is in its infancy. As a result, stochastic models are widely used in their place. However, although stochastic models can be used for describing Earth surface processes, landforms and deposits, they cannot aid understanding, nor can they make predictions beyond the data region used to define them.

Numerical, stochastic models

The word stochastic means random, involving chance or probability (therefore not deterministic). Books and reviews concerning stochastic models in the Earth Sciences include Krumbein and Graybill (1965), Harbaugh and Bonham-Carter (1970), Davis (1973), Schwarzacher (1975, 1985), Haldorsen & Damsleth (1990), Srivastava (1994), Yarus and Chambers (1994), North (1996), Koltermann & Gorelick (1996), Anderson (1997), Dubrule (1998), Deutsch (2002).

Regression models

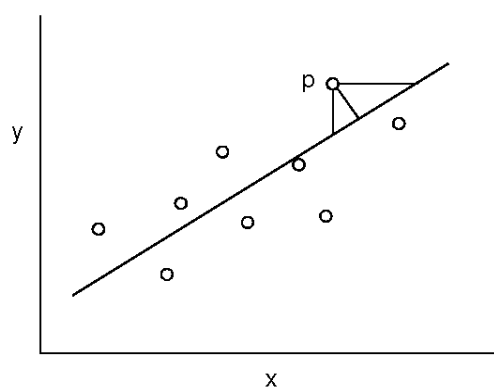


Figure A-35. Example of a regression model on an x - y plot.

One of the simplest examples of a numerical stochastic model is a linear regression equation, which is a straight line fitted to data points in a bivariate (x,y) plot (Figure A-35). The best-fit line is obtained by minimizing the sums of squares of deviations of the data points from the line. There are several ways of doing this (Figure A-35). The equation describes the statistical relationship between the two variables, and can be used to determine the most likely value of one variable

given a value of the other variable. The standard error of a linear regression equation is a measure of the confidence of the estimate of the variable value. This type of regression analysis can also be done with more than two variables (multivariate regression), and by fitting various curve shapes to bivariate data (polynomial regression).

Time (space) series models

Time series of data are very common in the Earth Sciences. Examples of time series include: turbulence fluctuations in flow velocity; discharge variations in rivers; water surface

elevations in wavy seas; seismic reflection data. Spatial series include: sinuosity of rivers; perimeters of sediment grains; elevations of bedforms; plan views of coastlines. Analysis of time series can be very simple, involving calculation of means and standard deviations of data values, or more complicated, involving calculation of the temporal (and spatial) scale of the fluctuations in data values. In some cases, time (space) series are smoothed in order to remove high frequency variation (possibly noise), and in other cases low frequency variations or trends are removed in order to analyse the high frequency fluctuations. Removal of high-frequency variations is called low-pass filtering. The simplest method of doing this is a moving average, in which successive groups of adjacent data points (e.g. 3 in a 3-point moving average) are averaged in a stepwise fashion. Many other types of filter are available.

One example of time (space) series analysis involves correlation of sequences of data pairs that are separated by specific time or space intervals (lag times or distances). Such analysis is called autocorrelation. The autocorrelation coefficient is normally plotted against the lag time or distance, and this plot is called the autocorrelation function (Figure A-36). If a data value at a given point is strongly correlated with the value(s) at an adjacent point(s), the time series is said to have a Markov property, as discussed further below.

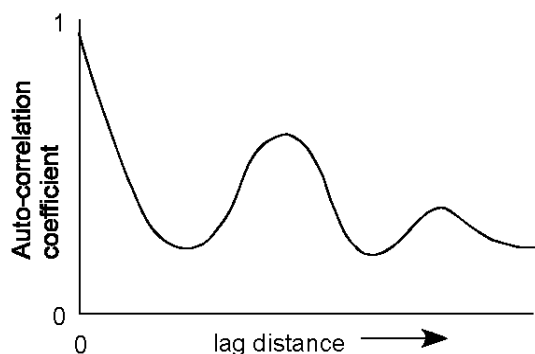


Figure A-36. Example of an autocorrelation analysis.

In the absence of well-defined cyclicality in the data, the correlation coefficients for short lag times or distances are the largest, and can approach 1 (Figure A-36). If the data have a well-defined cyclicality, as in the case of a series of similar water waves on the sea, there will be peaks in this plot corresponding to the mean wave period or length.

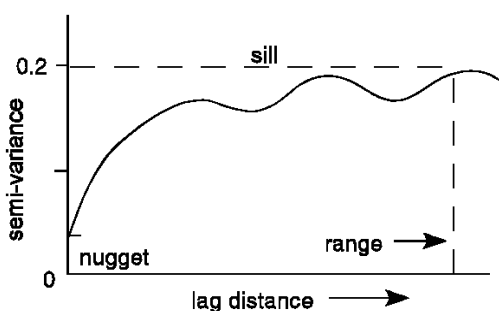


Figure A-37. Example of a semivariogram with definition of terms.

A variant of the autocorrelation method is to calculate the co-variance or semi-variance of pairs of points at varying lag distances, and then plot variance against lag distance or time

(producing a semivariogram: Figure A-37). Semivariograms are widely used for simulation of the spatial distributions of values of continuous variables such as permeability. Various empirical functions are fitted to data in semivariograms.

Another type of analysis, particularly suited to cyclic or periodic data is called Fourier series analysis. This involves fitting a series of sine and cosine waves of varying wavelength (or period) and amplitude to time (space) series. The longest wavelength λ (lowest frequency $1/\lambda$) is called the first harmonic. The second harmonic has a wavelength of $\lambda/2$, the third harmonic has a wavelength of $\lambda/3$, and so on. The different harmonics may well have different amplitudes. The amplitudes of the different harmonics are used to calculate the variance (or *power*) in the series that is accounted for by a particular harmonic. A power spectrum (Figure A-38) is a plot of the variance due to a particular harmonic plotted against the harmonic number (expressed as either a wavelength, period or frequency). Fitting of Fourier series to time series is computationally intensive, and special computer algorithms (Fast Fourier Transforms) have been developed for the task. In some cases, the Fourier and autocorrelation analyses are combined, for example with meteorological or hydrological time series. The Fourier terms account for cyclicity in the data, the autocorrelation function accounts for short lag “memory” (Markov property), and there is normally a stochastic component that follows a specified probability distribution. Time series can be simulated simply by Monte Carlo sampling from the probability distribution provided that the coefficients in the Fourier and autocorrelation models are known.

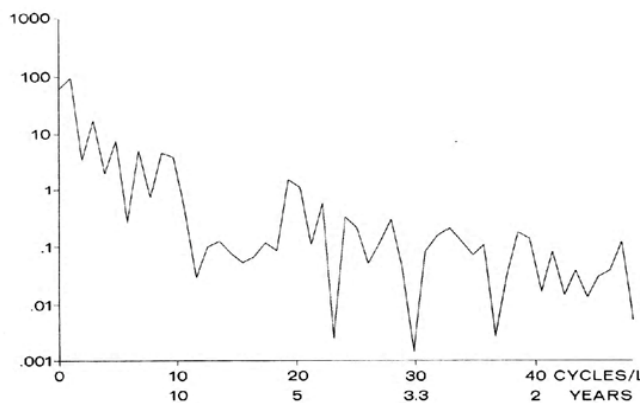


Figure A-38. Example of a power spectrum (from Davis, 1973)

Two different time (space) series can be compared, and their similarity assessed, by calculating correlation coefficients for all pairs of data points from the two series that are adjacent to each other. Then the series are shifted relative to each other and the cross-correlation

coefficients are recalculated. The maximum cross-correlation coefficient will be that when the two series are in a position such that they are most similar. A variant on cross-correlation is cross-association, in which two series of discrete quantities (e.g. lithologies) are compared with each other. The series are moved relative to each other and the number of quantities in the two series that match each other are counted for each position. The matching ratio is calculated as the number of matches/number of positions compared. The maximum matching ratio occurs where the two series are most similar. The significance of cross-correlation coefficients or matching ratios can be assessed using Chi-square tests. These methods are used for lithostratigraphic correlation. Unfortunately, in cyclic sequences, there can be many relative positions with large cross-correlation coefficients or matching ratios.

Applications of time (space) series models to analysis of sedimentary strata

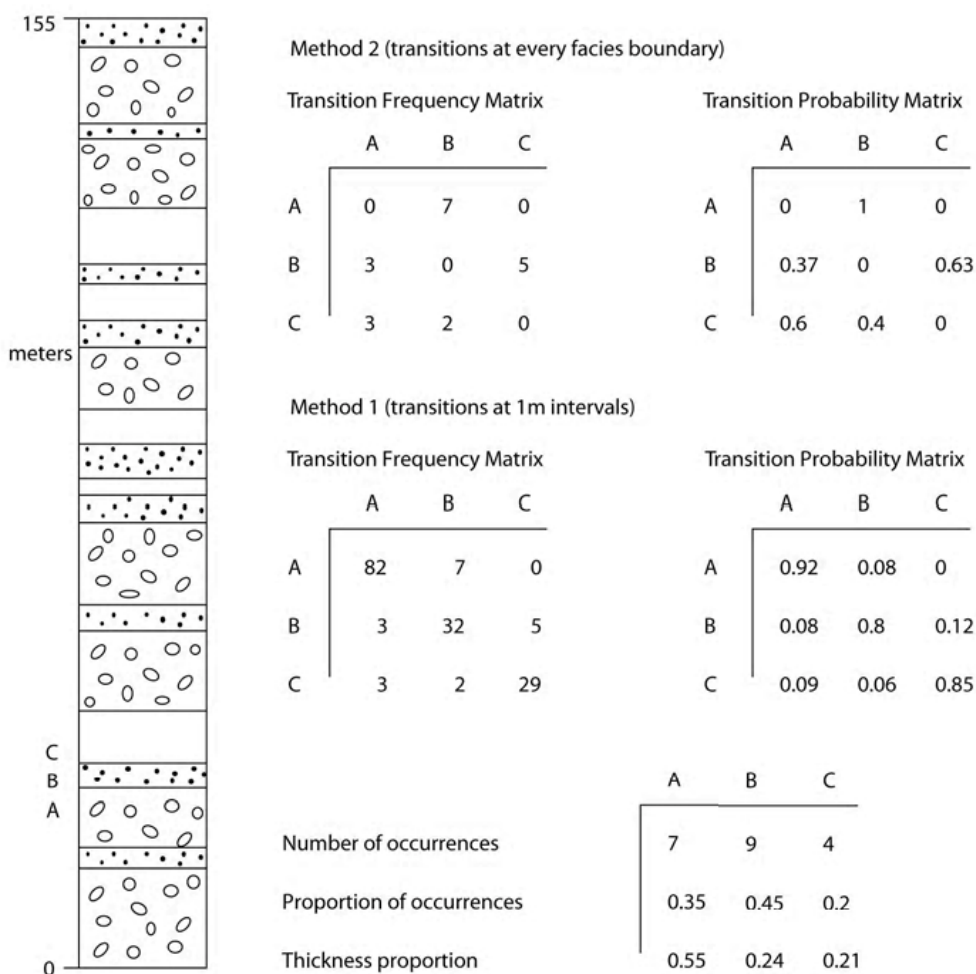


Figure A-39. Example of one-dimensional, first-order Markov models using two methods (from Bridge, 2003).

Transition probability (Markov) models can predict the spatial change from one discrete state (e.g. sand) to another (e.g., mud) based on the probability of the state transition (reviews in Harbaugh & Bonham-Carter, 1970; Davis, 1973; Schwarzacher, 1975, 1985). The probability of spatial transition to a given state depends on the existing state or states, and this dependence is called a Markov property. A Markov chain is a spatial series of states that have a Markov property. A first-order Markov chain is one in which the occurrence of a particular state in the chain is dependent only on the previous state. In a second-order Markov chain, the occurrence of a state depends on the two previous states. Markov chains used in stratigraphic models are normally first-order because of their simplicity.

A simple example of the development of a one-dimensional, first-order Markov model is illustrated in Figure A-39. A vertical stratigraphic section is divided into three discrete lithofacies (A, B, C). The sequence of lithofacies can be analyzed in either of two ways. With the first method, the section is divided into equal intervals, and the number of upward transitions (e.g., A to A, A to B, A to C, B to A, etc.) over the total number of intervals is tallied to produce a tally matrix (Figure A-39). The tally matrix is transformed into a transition probability matrix by dividing each tally number by the row total. In this type of analysis, the transition probabilities reflect the thickness of the lithofacies as well as the probability of a transition to a different lithofacies. With the second method, only the numbers of upward transitions from one lithofacies to another are tallied, such that the step length is not constant. In this case, the transition probability matrix has zeros along one diagonal, because transitions from one lithofacies to the same one are not recognized (Figure A-39). The transition probabilities in this case depend on the number of occurrences of a particular lithofacies as well as the probability of transition between lithofacies. By considering the thicknesses of the different lithofacies (first method) or the number of occurrences of the different lithofacies (second method), it is possible to define a transitional probability matrix for the case where the spatial occurrence of a given lithofacies is completely random, and not dependent on previous lithofacies. A Chi-square test is then performed using the observed and "random" matrices to determine if the succession of lithofacies is random or has a Markov property.

Markov analyses have been conducted on many sedimentary successions, in order to give a quantitative assessment of preferred spatial distribution or cyclicity of facies, and to allow stochastic simulation. There are actually many other statistical ways of accomplishing this objective, as discussed below. Markov analysis must be treated with caution for several reasons. The analysis normally requires reduction in the number of lithofacies in a sedimentary succession to a manageable number, and gradations between lithofacies cannot be treated using this approach. It is very difficult to define transition probabilities in three dimensions.

Simulation of sedimentary successions can be done by Monte-Carlo sampling of a transition probability matrix (Harbaugh & Bonham-Carter, 1970). If the first method of analysis is used, there is no need for data on the thickness of the lithofacies. However, if the second method of analysis is used, it is necessary to specify and sample a distribution of thickness for each lithofacies. The simple one-dimensional approach that was taken initially has now been extended for use in two- and three-dimensional models. Determination of transition probabilities in the vertical direction using well logs and cores is relatively easy. However, this is very difficult in the horizontal plane. It has been done by analysis of two-dimensional sections produced by correlation of well logs. Analog outcrop data are not sufficient for this purpose: however, Markov analysis of sections output from process-based models is a viable alternative (North, 1996).

Structure-imitating models of subsurface sedimentary architecture

A major concern of geologists dealing with subsurface hydrocarbon reservoirs and aquifers is determination of the character and 3-D spatial distribution (architecture) of the subsurface rocks. These cannot be determined directly from the data available: well logs, cores, geophysical data. It is necessary to make quantitative models of the sedimentary architecture from the data available and using basic geological knowledge. The most common approach to modeling the architecture of subsurface reservoirs and aquifers (discussed in Bridge & Tye, 2000) is to: (1) interpret the geometry, proportion and location of different types of sediment bodies (e.g., sandstones, shales) from well logs, cores, seismic or GPR; (2) interpret the origin of the sediment bodies; (3) use outcrop analogs to predict more sediment-body characteristics, and;

(4) use stochastic (structure-imitating) models to simulate the alluvial architecture between wells, and the rock properties with sediment bodies such as channel-belt sandstones. Stochastic (structure-imitating) models are either object-based (also known as discrete or Boolean) or continuous, or both (reviewed by Haldorsen & Damsleth, 1990; Srivastava, 1994; North, 1996; Koltermann & Gorelick, 1996; Dubrule, 1998; Deutsch, 2002). A common combined approach is to use object-based models to simulate the distribution of the various types of sediment bodies (objects), and then use continuous stochastic models for simulating “continuous” variables such as porosity and permeability within the objects.

With object-based models, the geometry and orientation of specified objects (e.g., channel-belt sandstone bodies or discrete shales) are determined by Monte-Carlo sampling from empirical distribution functions derived mainly from outcrop analogs. “Conditioned simulations” begin by placing objects such that their thickness and position correspond with the available well data. Then, objects are placed in the space between wells until the required volumetric proportion is reached. Objects are placed more-or-less randomly, although arbitrary overlap/repulsion rules may be employed to produce “realistic” spatial distributions of objects (see Chapter 13).

Continuous stochastic models have been used mainly to simulate the spatial distribution of continuous data series such as permeability, porosity, or grain size. With these models, a parameter value predicted to occur at any point in space depends on its value at a neighboring site. The conditional probabilities of occurrence are commonly based on an empirical semivariogram or autocorrelation function. These approaches have been modified to predict the distribution of discrete facies by using indicator semivariograms and simulated annealing. A variant of the indicator semivariogram approach is transition probability (Markov) models in which the spatial change from a particular sediment type (e.g. channel sandstone) to another (e.g., floodplain mudstone) is based on the probability of the transition. The probability of spatial transition to a particular sediment type depends on the existing sediment type, and this dependence is called a Markov property. The matrix of probabilities of transition from one sediment type to another can be used to simulate sedimentary sequences in one, two or three dimensions.

It is commonly difficult to define the input parameters for stochastic models, especially the semivariograms and transition probability matrices in lateral directions. The shapes, dimensions and locations of objects in object-based models are difficult to define realistically. If definition of the dimensions of objects relies upon use of outcrop analogs, there may be serious problems (Bridge & Tye, 2000). Process-based models and sequence-stratigraphy models demonstrate that the spatial distribution of “objects” is not random. Unrealistic shapes, dimensions and spatial distributions of sediment types means that it is difficult to get the model to fit observed data and predict reservoir/aquifer behavior. Furthermore, as stochastic models do not simulate processes of deposition, they cannot give any insight into the origin of the stratigraphic architecture, and they have no predictive value outside the data region.

If there are so many problems with stochastic models, why are they used? Commercial software is available. Simulations can easily be conditioned using well data, cores, seismic, GPR, and other types of geological information. Detailed understanding of the origin of the subsurface strata is not necessary in order to use stochastic models, even though it is desirable. Numerical forward (process-imitating) models are considered difficult to fit to subsurface data, and the models and software not well developed. Therefore, process-imitating models have had limited application in quantitative simulation of the architecture of hydrocarbon reservoirs or aquifers. However, process-imitating models provide genetic interpretations of deposits, and can predict more realistic sedimentary architecture than structure-imitating stochastic models. Actually, fitting of process-based models to well data using an essentially trial-and-error approach is possible in principle. Such an approach involves multiple runs of a process-based model under different input conditions, and optimization of the fitting of output data to observed data. Process-based models are being developed, including development of software so that models can be fitted to subsurface data (inversion approach). Another approach is to use output from process-imitating forward models to provide input for stochastic models that can be more easily conditioned with subsurface data.

Fuzzy logic models

Much of the information on sedimentary systems is a blend of measurements and anecdotal observations. Fuzzy logic was developed in the 1960s by Lotfi Zadeh (Zadeh, 1965; Klir and Yuan, 1995) to handle such data types in robot control programming. In general, fuzzy logic allows any conditional 'if-then' statement to be treated in a rigorous mathematical way. For example, the statement 'if wave energy is high and the water is shallow, then sand will be transported' carries information that is not easily quantifiable. The key here is that the terms 'high' and 'shallow' and 'sand' are context-dependent, continuous variables that have ranges that we know generally, but may not know in detail in a given situation. Fuzzy sets allow such variables to be described using natural language concepts. For example, wave energy is naturally described as 'low', 'intermediate', or 'high' just as the skies are naturally described as partly sunny or mostly cloudy. Various portions of such continuous variables are divided into fuzzy sets that take on values between 0 and 1 and can overlap. Thus, wave energy may be both intermediate to a degree of 0.3 and high to a degree 0.7 at the same time. This is in distinct contrast to so-called 'crisp sets' where an individual is either a member of the set (value 1) or not (value 0).

Nordlund (1996) was the first to apply fuzzy logic to sedimentary basin-fill models using 'if then' fuzzy-set based rules to model a delta. Such a model comprises a number of rules for deposition culled from general statements about deltaic deposition such as what grain size and how much sediment is deposited in proximal versus distal settings. Demicco and Klir (2004) describe a number of basin-fill models based on Nordlund's approach, as well as other applications of fuzzy logic to geological problems.

Appendix References

- Adams, A.E. and MacKenzie, W.S. (1998) A colour atlas of carbonate sediments and rocks under the microscope. Manson Publishing, London, 180 p.
- Adams, A.E., MacKenzie, W.S., and Guilford, C. (1984) Atlas of sedimentary rocks under the microscope. Longman, Harlow, 104 p.
- Aitken, M.J. (1998) *An introduction to optical dating*. Oxford University Press, Oxford, 267 p.
- Allen, J.R.L. (1966) On bedforms and paleocurrents. *Sedimentology*, **6**, 153-190.
- Allen, J.R.L. (1983) Studies in fluvial sedimentation: bars, bar-complexes and sandstone sheets (low-sinuosity braided streams) in the Brownstones (Lower Devonian), Welsh Borders. *Sediment Geol.*, **33**, 237-293.
- Anderson, M.P. (1997) Characterization of geological heterogeneity. In Dagan, G. & Neuman, S.P. (eds.), *Subsurface Flow and Transport: A Stochastic Approach*. Cambridge University Press, 23-43.
- Ashmore, P.E. & Church, M. (1998) Sediment transport and river morphology: a paradigm for study. In: Klingeman, P.C., Beschta, R.L., Komar, P.D. & Bradley, J.B. (eds.) *Gravel-Bed Rivers in the Environment*, 115-148, Water Resources Publications, Highlands Ranch, Colorado.
- Ashworth, P.J., Best, J.L., Roden, J.E., Bristow, C.S. & Klaassen, G.J. (2000) Morphological evolution and dynamics of a large, sand braid-bar, Jamuna River, Bangladesh. *Sedimentology*, **47**, 533-555.
- Asquith, G. (1982) *Basic well log analysis for geologists*. Am. Assoc. Petrol. Geol., Tulsa, Oklahoma, 216 pp.
- Bachalo, W.D. (1994) Experimental methods in multiphase flows, *Int. J. Multiphase Flow*, **20**, 261-295.
- Baines, D., Smith, D.G., Froese, D.G., Bauman, P., and Nimeck, G. (2002) Electrical resistivity ground imaging (ERGI): a new tool for mapping the lithology and geometry of channel-belts and valley-fills: *Sedimentology*, **49**, 441-449.
- Bennett, R.H., Bryant, W.R., and Hulbert, M.H. (1991) *Microstructure of Fine-Grained Sediments: From Mud to Shale*. New York, Springer-Verlag, 582 p.

- Bennett, S.J., Bridge, J.S. & Best, J.L. (1998) The fluid and sediment dynamics of upper-stage plane beds. *J. Geophys. Res.*, **103**, 1239-1274.
- Best, J.L. & Ashworth, P.J. (1994) A high-resolution ultrasonic bed profiler for use in laboratory flumes, *J. Sed. Res.*, **A64**, 674-675.
- Best, J.L., S.J. Bennett, J.B. Bridge, & M.R. Leeder (1997) Turbulence modulation and particle velocities over flat sand beds at low transport rates, *J. Hydraul. Eng., ASCE*, **123**, 1118-1129.
- Blatt, H., Middleton, G.V. and Murray, R. (1980) *Origin of Sedimentary Rocks*, 2nd Ed., Prentice- Hall.
- Bouma, A.H. (1969) *Methods for the study of sedimentary structures*. Wiley, New York, 458p.
- Bridge, J.S. (1981) Hydraulic interpretation of grain-size distributions using a physical model for bed-load transport. *J. Sed. Pet.*, **51**, 1109-1124.
- Bridge, J.S. (1993) Description and interpretation of fluvial deposits: a critical perspective. *Sedimentology*, **40**, 801-810.
- Bridge, J.S. (1995a) Description and interpretation of fluvial deposits: a critical perspective: Reply. *Sedimentology*, **42**, 384-389.
- Bridge, J.S. & Gabel, S.L. (1992) Flow and sediment dynamics in a low sinuosity, braided river: Calamus River, Nebraska Sandhills. *Sedimentology*, **39**, 125-142.
- Bridge, J.S. & Jarvis, J. (1982) The dynamics of a river bend: a study in flow and sedimentary processes. *Sedimentology*, **29**, 499-541.
- Bridge, J.S. & Tye, R.S. (2000) Interpreting the dimensions of ancient fluvial channel bars, channels, and channel belts from wireline-logs and cores. *Am. Assoc. Petrol. Geol. Bull.*, **84**, 1205-1228.
- Bristow, C.S. and Jol, H.M. (eds.) (2003) *Ground Penetrating Radar in Sediments*. *Geol. Soc. London Spec. Publ.* **211**, 330 p.
- Brookfield, M.E. (1977) The origin of bounding surfaces in ancient eolian sandstones. *Sedimentology*, **24**, 303-332.
- Brown, A.R. (1996) Interpretation of three-dimensional seismic data, 4th ed. *AAPG Mem*, **42**, Tulsa, OK.
- Buchave, P. (1987) A new instrument for the simultaneous measurement of size and velocity of spherical particles based on the laser Doppler method. In: Ariman, T. & Veziroglu, T.N.

- (eds.), *Particulate and Multiphase Processes, vol. 2: Contamination Analysis and Control*, 55-67, Hemisphere Publ. Corp., New York.
- Buchhave, P., George, W.K. Jr. & Lumley, J.L (1979) The measurement of turbulence with the laser-Doppler anemometer, *Ann. Rev. Fluid Mech.*, **11**, 443-503.
- Buckingham, E. (1915) Model experiments and the forms of empirical equations. *Trans. Am. Soc. Mech. Engrs.*, **37**, 263-292.
- Campbell, C.V. (1967) Laminae, lamina set, bed and bedset. *Sedimentology*, **8**, 7-26.
- Carling, P.A. (1981) Freeze-sampling coarse river gravels. *British Geomorphological Research Group Technical Bulletin* **27**, 19-29.
- Carling P.A. & Reader N.A. (1981) A freeze-sampling technique for coarse river bed-material. *Sed. Geol.*, **29**, 233-239.
- Carver, R.E. (ed.) (1971) *Procedures in sedimentary petrology*. Wiley-Interscience, New York, 653 p.
- Cerling, T. E., & Craig, H. 1994. Geomorphology and in-situ cosmogenic isotopes. *Annual Reviews of Earth & Planetary Sciences* **22**, 273-317.
- Church M.A., McLean D.G. & Wolcott J.F. (1987) River bed gravels: Sampling and analysis. In: Thorne, C.R., Bathurst, J.C. & Hey, R.D. (Eds.) *Sediment transport in gravel bed rivers*, Wiley, New York, 43-79.
- Choquette, P.W. and Pray, L.C. (1970) Geologic nomenclature and classification of porosity in sedimentary carbonates. *AAPG Bull.*, **54**, 207-250.
- Clark, J.D. and Pickering, K.T. (1996) *Submarine channels: processes and architecture*. Vallis Press, London, 231 p.
- Cross, T.A. (ed.) (1990) *Quantitative Dynamic Stratigraphy*. Prentice-Hall, Englewood Cliffs, NJ.
- Crowder, D.W. & Diplas, P. (1997) Sampling heterogeneous deposits in gravel-bed streams. *J. Hydraul. Engrg., ASCE*, **123**, 1106-1117.
- Curray, J.R. (1956) The analysis of two dimensional orientation data. *J.Geol.*, **64**, 117-131.
- Davis, J.C. (1973) *Statistics and data analysis in geology*, Wiley, New York.
- Davis, J. L. & Annan, A.P. (1989) Ground penetrating radar for high-resolution mapping of soil and rock stratigraphy. *Geophysical Prospecting*, **37**, 531 - 551.

- Demicco, R.V., and Klir, G.J. (eds.) (2004) *Fuzzy Logic in Geology*. Amsterdam, Elsevier, 347 p.
- Deutsch, C.V. (2002) *Geostatistical reservoir modeling*. Oxford University Press, New York.
- De Vries M. (1971) On the accuracy of bed-material sampling. *J. Hydraul. Res.*, **8**, 523-533.
- Dietrich, W.E. & Smith, J.D. (1984) Bedload transport in a river meander. *Wat. Resour. Res.*, **20**, 1355-1380.
- Dingler, J.R., Boylls, J.C. & Lowe, R.L. (1977) A high frequency sonar for profiling small-scale subaqueous bedforms. *Mar. Geol.*, **24**, 279-288.
- Diplas P. & Fripp J.B. (1992) Properties of various sediment sampling procedures. *J. Hydraul. Engrg., ASCE*, **118**, 955-970.
- Diplas P. & Sutherland A.J. (1988) Sampling techniques for gravel sized sediments. *J. Hydraul. Engrg., ASCE*, **114**, 484-501.
- Doveton, J.H. (1994) *Geologic log interpretation*. SEPM Short Course Notes 29, Tulsa, Oklahoma, 169 pp.
- Doveton, J.H. (1994) Theory and applications of vertical variability measures from Markov Chain analysis. In: Yarus, J.M. & Chambers, R.L. (eds.), *Stochastic Modeling and Geostatistics, Am. Assoc. Petrol. Geol. Computer Applications in Geology*, **3**, 55-64.
- Drake, T.G., Shreve, R.L., Dietrich, W.E., Whiting, P.J. & Leopold, L.B. (1988) Bedload transport of fine gravel observed by motion-picture photography. *J. Fluid Mech.*, **192**, 193-217.
- Dubrulle, O. (1998) *Geostatistics in Petroleum Geology*. AAPG Continuing education Course Notes Series # 38.
- Duller, G.A.T. (1996) Recent developments in luminescence dating of Quaternary sediments. *Prog. Phys. Geog.*, **20**, 127-145.
- Dunham, R.J. (1962) Classification of carbonate rocks according to depositional texture. In: Ham, W.E. (ed.) *Classification of Carbonate Rocks, AAPG Mem.* **1**, 108-121.
- Embry, A.F. and Klovan, J.E. (1971) A Late Devonian reef tract on north-eastern Banks island, N.W.T. *Bull. Can. Petrol. Geol.*, **19**, 730-781.
- Emmett, W.W. (1980) A field calibration of the sediment trapping characteristics of the Helley-Smith bedload sampler. *U.S. Geol. Surv. Prof. Pap.* **1139**, 44p.
- Ettema P. (1984) Sampling armour-layer sediments. *J. Hydraul. Engrg, ASCE*, **110**, 992-996.

- Folk, R.L. (1962) Spectral subdivision of limestone types. In: Ham, W.E. (ed.) *Classification of Carbonate Rocks*, AAPG Mem. **1**, 62-84.
- Folk, R.L. (1984) *Petrology of Sedimentary Rocks*. Hemphill, Austin, TX.
- Fraccarollo L. & Marion A. (1995) Statistical approach to bed-material surface sampling. *J. Hydraul. Engrg.*, ASCE, **121**, 540-545.
- Franseen, E. K., Watney, W.L., Kendall, C. St. C., and Ross, W. (1991) Sedimentary modeling: Computer simulations and methods for improved parameter definition. *Kansas Geol. Surv. Bull.* **233**.
- Fripp F.B. & Diplas P. (1993) Surface sampling in gravel streams. *J. Hydraul. Engrg.*, ASCE, **119**, 473-490.
- Fujita, I., Muste, M. & Kruger, A. (1998) Large-scale particle image velocimetry for flow analysis in hydraulic engineering applications. *J. Hydraul. Res.*, **36**, 397-414.
- Gabel, S.L. (1993) Geometry and kinematics of dunes during steady and unsteady flows in the Calamus River, Nebraska, USA. *Sedimentology*, **40**, 237-269.
- Gale S.J. & Hoare P.G. (1992) Bulk sampling of coarse clastic sediments for particle size analysis. *Earth Surf. Proc. Land.*, **17**, 729-733.
- Gastaldo, R.A., Savrda, C.E., & Lewis, R.D. (2004). [*Deciphering Earth History: A Laboratory Manual with Internet Exercises*](#). 3rd ed. Contemporary Publishing Company of Raleigh, Inc
- Gaudet, J.M., Roy, A.G. & Best, J.L. (1994) Effect of orientation and size of Helley-Smith sampler on its efficiency. *J. Hydraul Engrg.*, ASCE, **120**, 758-766.
- Gaweesh, M.T.K & Van Rijn, L.C. (1994) Bed-load sampling in sand-bed rivers. *J. Hydraul. Engrg.*, ASCE, **120**, 1364-1384.
- Hammond, F.D.C., Heathershaw, A.D. & Langhorne, D.N. (1984) A comparison between Shields' threshold criterion and the movement of loosely packed gravel in a tidal channel. *Sedimentology*, **31**, 51-62.
- Ginsburg, R.N., Bernard, H.A., and Moody, R.A. (1966) The Shell method of impregnating cores of unconsolidated sediment. *J. Sed. Pet.*, **36**, 1118-1125.
- Gomez, B. (1983) Representative sampling of sandy fluvial gravels. *Sed. Geol.*, **34**, 301-306.
- Gomez, B. & Troutman, B.M. (1997) Evaluation of process errors in bed-load sampling using a dune model. *Wat. Resour. Res.*, **33**, 2387-2398.
- Gosse, J. C., & Phillips, F. M. 2001. Terrestrial in situ cosmogenic nuclides: theory and applications. *Quaternary Sciences Reviews* **20**, 1475-1560.

- Haldorsen, H.H. & Damsleth, E. (1990). Stochastic modeling. *J. Petrol. Technol.*, **42**, 404-412.
- Harbaugh, J.W. & Bonham-Carter, G. (1970) *Computer simulation in geology*. Wiley.
- Harbaugh et al. (eds.) (1999) *Numerical Experiments in Stratigraphy: Recent Advances in Stratigraphic and sedimentologic Computer Simulations, SEPM Spec. Pub. 62*.
- Harff, J., Lemke, W. and Stattegger, K (eds.) (1999) *Computerized modeling of sedimentary systems*. Springer, Berlin.
- Hartkamp-Bakker, C.A. and Donselaar, M.E. (1993) Permeability patterns in point bar deposits: Tertiary Loranca basin, central Spain. *IAS Spec. Publ.* **15**, 157-168.
- Hey, R.D. & Rainbird, P.C.B. (1996) Three-dimensional flow in straight and curved reaches. In: Carling, P.A. & Dawson, M.R. (eds.) *Advances in fluvial dynamics and stratigraphy*. Wiley, Chichester, 33-66.
- Hey R.D. & Thorne C.R. (1983) Accuracy of surface samples from gravel bed material. *J. Hydraul. Engrg, ASCE*, **109**, 842-851.
- Hubbell, D.W., Stevens, H.H., Skinner, J.V. & Beverage, J.P. (1985) New approach to calibrating bed load samplers. *J. Hydraul. Engrg., ASCE*, **111**, 677-694.
- Hubbell, D.W., Stevens, H.H., Skinner, J.V. & Beverage, J.P. (1987) Laboratory data on coarse sediment transport for bedload-sampler calibrations. *U.S. Geol. Surv. Wat. Supply Pap.* **2299**, 31 p.
- Hurst, A., Lovell, M.A., and Morton, A.C. (1993) *Geological applications of wireline logs*. Geol. Soc. Lond. Spec. Publ. Classics.
- Kellerhals, R. & Bray D.I., 1971, Sampling procedures for coarse fluvial sediments. *J. Hydraul. Div., ASCE*, **97**, 1165-1180.
- Kahn, J.S. (1956) The analysis and distribution of packing in sand-size sediments. *J.Geol.*, **64**, 385-395.
- Kearey, P., Brooks, M. and Hill, I. (2002) *An introduction to geophysical exploration*. 3rd edition. Blackwells, 262 p.
- Kirkby, M.J. (ed.) (1994) *Process models and Theoretical Geomorphology*. Wiley, Chichester.
- Kleinhans, M.G. & Ten Brinke, W.B.M. (2001) Accuracy of cross-channel sampled sediment transport in large sand-gravel-bed rivers. *J. Hydraul. Engrg., ASCE*, **127**, 258-269.
- Klir, G.J., and Yuan, B. (1995) *Fuzzy Sets and Fuzzy Logic – Theory and Applications*. New Jersey, Prentice-Hall, 574 p.

- Kneller, B. and Buckee, C. (2000) The structure and fluid mechanics of turbidity currents: a review of some recent studies and their geological implications. *Sedimentology*, **47** (Suppl. 1), 62-94.
- Knight, P.G. (ed.) (2006) *Glacier Science and Environmental Change*. Blackwells, Oxford, 527 p.
- Kraus, N.C., Lohrmann, A. & Cabrera, R. (1994) New acoustic meter for measuring 3D laboratory flows. *J. Hydraul. Engrg., ASCE*, **120**, 406-412.
- Krumbein, W.C. and Graybill, F.A. (1965) *An introduction to statistical models in geology*. McGraw-Hill.
- Koltermann, C.E. & Gorelick, S.M. (1996) Heterogeneity in sedimentary deposits: a review of structure-imitating, process-imitating and descriptive approaches. *Wat. Resour. Res.*, **32**, 2617-2658.
- Kostaschuk, R.A. & Villard, P. (1999) Turbulent sand suspension over dunes. In: Smith, N.D. and Rogers, J. (eds), *Fluvial Sedimentology VI, Spec. Publs. Int. Assoc. Sediment.*, **28**, 3-13.
- Lane, S.N., P.M. Biron, K.F. Bradbrook, J.B. Butler, J.H. Chandler, M.D. Crowell, S.J. McLelland, K.S. Richards, & A.G. Roy (1998) Three-dimensional measurement of river channel flow processes using acoustic Doppler velocimetry, *Earth Surf. Proc. Land.*, **23**, 1247-1267.
- Lane, S.N., Bradbrook, K.F., Richards, K.S., Biron, P.M. & Roy, A.G. (2000) Secondary circulation cells in river channel confluences: measurement artifacts or coherent flow structures? *Hydrol. Proc.*, **14**, 2047-2071.
- Lane, S.N., Chandler, J.H. & Porfiri, K. (2001) Monitoring river channel and flume surfaces with digital photogrammetry. *J. Hydraul. Engrg., ASCE*, **127**, 871-877.
- Lane, S.N., Richards, K.S. & Chandler, J.H. (1995) Morphological estimation of the time-integrated bedload transport rate. *Wat. Resour. Res.*, **31**, 761-772.
- Lane, S.N., Richards, K.S. & Chandler, J.H. (eds.) (1998) *Landform monitoring, modeling and analysis*. Wiley, Chichester.
- Lanesky, D.E., Logan, B.W., Brown, R.G. & Hine, A.C. (1979) A new approach to portable vibracoring underwater and on land. *J. Sed. Pet.*, **49**, 654-657.
- Lemmin, U. & Rolland, T. (1997) Acoustic velocity profiler for laboratory and field studies. *J. Hydraul. Engrg., ASCE*, **123**, 1089-1098.

- Lewis, D.W. (1984) *Practical sedimentology*. Hutchinson Ross Publishing Company, Stroudsburg, Pennsylvania.
- Marion, A. & Fraccarollo, L. (1997) new conversion model for aerial sampling of fluvial sediments. *J. Hydraul. Engrg., ASCE*, **123**, 1148-1151.
- McKee, E.D. and Weir, G. W. (1953) Terminology for stratification and cross-stratification in sedimentary rocks. *Bull. Geol. Soc. Am.*, **64**, 381-390.
- McLelland, S.J., Ashworth, P.J., Best, J.L., Roden, J. & Klaasen, G.J. (1999) Flow structure and transport of sand-grade suspended sediment around an evolving braid bar, Jamuna River, Bangladesh. In: Smith, N.D. & Rogers, J. (eds.) *Fluvial Sedimentology VI. Int. Assoc. Sediment. Spec. Pub.* **28**, 43-57.
- Mendes, G., Perez-Arlucea, M., Stouthamer, E. And Berendsen, H. (2003) The TESS-1 suction corer: a new device to extract wet, uncompacted sediments. *J. Sed. Res.*, **73**, 1078-1081.
- Merriam, D.F. & Davis, J.C. (eds.) (2001) *Geologic Modeling and Simulation: Sedimentary Systems*. Kluwer Academic/Plenum Publishers.
- Miall, A.D. (1996) *The geology of fluvial deposits*. Springer-Verlag, New York, 582 p.
- Middleton, G.V. (1976) Hydraulic interpretation of sand size distribution. *J. Geol.*, **84**, 405-426.
- Middleton, R., Brasington, J., Murphy, B.J. & Frostick, L.E. (2000) Monitoring gravel framework dilation using new digital particle tracking method. *Comp. Geosci.*, **26**, 329-340.
- Mosley, M.P. & Tindale D.S. (1985) Sediment variability and bed material sampling in gravel-bed rivers. *Earth Surf. Proc. Land.*, **10**, 465-482.
- Murray, A.S. & Wintle, A.G. (2000) Luminescence dating of quartz using an improved single-aliquot regenerative-dose protocol. *Radiat. Meas.*, **32**, 57-73.
- Neal, A. (2004) Ground-penetrating radar and its use in sedimentology: principles, problems and progress. *Earth-Science Reviews*, **66**, 261-330
- Nezu, I. & Nakagawa, H. (1993) *Turbulence in Open-Channel Flows*, Int. Ass. Hydraul. Res. Monograph Series, A.A. Balkema, Rotterdam, 281pp.
- Nezu, I., & Onitsuka, K. (2001) Turbulent structures in partly vegetated open-channel flows with LDA and PIV measurements. *J. Hydraul. Res.*, **39**, 629-642.
- Nichols, G. (1999) *Sedimentology & Stratigraphy*. Blackwells, Oxford.
- Nikora, V.I. & Goring, D.G. (1998) ADV measurements of turbulence: can we improve their interpretation. *J. Hydraul. Engrg., ASCE*, **124**, 630-634.

- Nordlund, U. (1996) Formalizing geological knowledge – with an example of modeling stratigraphy using fuzzy logic. *J. Sed. Res.*, **66**, 689-712.
- North, C.P. (1996). The prediction and modelling of subsurface fluvial stratigraphy. In: Carling, P.A. & Dawson, M.R. (eds.), *Advances in Fluvial Dynamics and Stratigraphy*. Wiley, Chichester, 395-508.
- North American Commission on Stratigraphic Nomenclature (1983) North American Stratigraphic Code. *AAPG Bull.*, **67**, 841-875.
- Paola, C. (2000) Quantitative models of sedimentary basin filling. *Sedimentology*, **47** (Suppl.1), 121-178.
- Parker, G. & Wilcock, P.R. (1993) Sediment feed and recirculating flumes: a fundamental difference. *J. Hydraul. Engrg., ASCE*, **119**, 1192-1204.
- Parsons, D.R., Best, J.L., Orfeo, O., Hardy, R.J., Kostaschuk, R. and Lane, S.N. (2005) Morphology and flow fields of three-dimensional dunes, Rio Parana, Argentina: Results from simultaneous multibeam echo sounding and acoustic Doppler current profiling. *J. Geophys. Res.*, **110**, F04S03, doi:10.1029/2004JF000231.
- Peakall, J., Ashworth, P. & Best, J. (1996) Physical modeling in fluvial geomorphology: principles, applications and unresolved issues. In: Rhoads, B.L. & Thorn, C.E. (eds.) *The Scientific Nature of Geomorphology*. Wiley, Chichester, 221-253.
- Peakall, J., Felix, M., McCaffrey, B. and Kneller, B. (2001) Particulate gravity currents: perspectives. In: McCaffrey, W.D., Kneller, B.C. and Peakall, J. (eds.), *Particulate Gravity Currents. IAS Spec. Publ.* **31**, 1-8, Blackwells, Oxford.
- Pettijohn, F.J. (1975) *Sedimentary Rocks*, 3rd ed. Harper and Row, London.
- Pettijohn, F.J. & Potter, P.E. (1964) *Atlas and glossary of primary sedimentary structures*. Springer-Verlag, Berlin, 370 p.
- Pettijohn, F.J., Potter, P.E. and Seiver, R. (1972) *Sand and Sandstone*. Springer-Verlag, NY.
- POSAMENTIER, H.W., AND KOLLA, V. (2003) Seismic geomorphology and stratigraphy of depositional elements in deep-water settings: *Journal of Sedimentary Research*, **73**, 367-388.
- Potter, P.E. and Pettijohn, F.J. (1977). *Palaeocurrents and basin analysis*. Springer-Verlag, Berlin.
- Prothero, D.R. (2004) *Bringing Fossils to Life: Second Edition*. Boston, McGraw Hill, 503 p.

- Raup, D.M., and Stanley, S.M. (1978) *Principles of Paleontology: Second Edition*. San Francisco, W.H. Freeman and Co., 481 p.
- Reineck, H.E. and Singh, I.B. (1973) *Depositional sedimentary environments*. Springer, Berlin, 439p.
- Reynolds, J.M. (1997) *An Introduction to Applied and Environmental Geophysics*. Wiley, Chichester.
- Rider, M.H. (1990) Gamma-ray log shape used as a facies indicator: critical analysis of an oversimplified methodology. In: Hurst, A., Lovell, M.A. & Morton, A.C. (eds.), *Geological applications of wireline logs*. *Geol. Soc. London. Spec. Publ.* **48**, 27-37.
- Rolland, T. & Lemmin, U. (1997) A two-component velocity profiler for use in turbulent open-channel flow. *J. Hydraul. Res.*, **35**, 545-561.
- Scholle, P.A. (1978) A color guide to carbonates. AAPG Mem 27, Tulsa, OK
- Scholle, P.A. (1979) A color guide to sandstones. AAPG Mem 28, Tulsa, OK
- Schumm, S.A., Mosley, M.P. & Weaver, W.E. (1987) *Experimental fluvial geomorphology*. Wiley, New York.
- Schwarzacher, W. (1975) *Sedimentation models and quantitative stratigraphy*. Developments in Sedimentology **19**, Elsevier, Amsterdam.
- Schwarzacher, W. (1985) Principles of quantitative lithostratigraphy - the treatment of single sections. In: Gradstein, F.M., Agterberg, F.P., Brower, J.C. & Schwarzacher, W.(eds.) *Quantitative Stratigraphy*. UNESCO, Paris and Reidel Publ. Co., Dordrecht, 361-386.
- Seelos, K. and Sirocko, F. (2005) RADIUS - rapid particle analysis of digital images by ultra high resolution scanning of thin section. *Sedimentology*, **52**, 669-681.
- Shen, C. & Lemmin, U. (1999) Application of an acoustic flux profiler in turbulent open-channel flow. *J. Hydraul. Res.*, **37**, 407-419.
- Sheriff, R.E. (1984) *Encyclopedic Dictionary of Exploration Geophysics*. Society of Exploration Geophysics, Tulsa, OK. 2nd ed. 266p.
- Simola H., Huttenen P. & Merilainen J. (1986) Techniques for sediment freezing and treatment of frozen sediment samples. *Univ. Joensuu, Publications of Karelian Inst.*, **79**, 99-107.
- Simpson, J.E. (1997) *Gravity Currents in the Environment and the Laboratory*, 2nd Ed. Cambridge University Press, New York.

- Slingerland, R., Harbaugh, J.W. & Furlong, K.P. (1994) *Simulating clastic sedimentary basins*. Prentice hall, Englewood Cliffs, New Jersey.
- Smith, D.G. (1984) Vibracoring fluvial and deltaic sediments: tips on improving penetration and recovery. *J. Sed. Pet.*, **54**, 660-663.
- Smith, D.G. (1998) Vibracoring: a new method for coring deep lakes. *Paleogeography, Paleoclimatology, Paleocology*, **140**, 433-440.
- Southard, J.B., Lambie, J.M., Federico, D.C., Pile, H.T., and Weidman, C.R. (1990) Experiments on bed configurations in fine sands under bidirectional purely oscillatory flow, and the origin of hummocky cross-stratification. *J. Sed. Petrol.*, **60**, 1-17.
- Spicer, K.R., Costa, J.E. & Placzek, G. (1997) Measuring flood discharge in unstable stream channels using ground-penetrating radar. *Geology*, **25**, 423-426.
- Srivastava, R.M. (1994) An overview of stochastic methods for reservoir characterization. . In: Yarus J.M. & Chambers, R.L. (eds.) *Stochastic modeling and Geostatistics, Am. Assoc. Petrol. Geol. Computer Applications in Geology* **3**, 3-16.
- Stocker Z.S.J. & Williams D.D. (1972) A freezing core method for describing the vertical distribution of sediments in a streambed. *Limnography and Oceanography*, **17**, 136-138.
- Stojic, M., Chandler, J.H., Ashmore, P. & Luce, J. (1998) The assessment of sediment transport rates by automated digital photogrammetry. *Photogram. Engrg. & Remote Sensing*, **64**, 387-395.
- Stow, D.A.V. (2005) *Sedimentary Rocks in the Field: A Color Guide*. Elsevier Academic Press, Burlington. 320 p.
- Stow, D.A.V., Reading, H.G., and Collinson, J.D. (1996) Deep seas. In Reading, H.G. (ed.) *Sedimentary Environments: Processes, Facies and Stratigraphy*, 395-453, Blackwells, Oxford.
- Sukhodolov, A.N. & Rhoads, B.L. (2001) Field investigation of three-dimensional flow structure at stream confluences: 2. Turbulence. *Wat. Resour Res.*, **37**, 2411-2424.
- Syvitski, J.P.M. (ed.) (1991) *Principles, methods and applications of particle size analysis*. Cambridge University Press, New York.
- Tait, S.J., Willetts, B.B. & Gallagher, M.W. (1996) The application of particle image velocimetry to the study of coherent flow structures over a stabilizing sediment bed. In:

- Ashworth, P.J., Bennett, S.J., Best, J.L. & McLelland, S.J. (eds.) *Coherent flow structures in open channels*. Wiley, Chichester, 185-201.
- Tauxe, L. & Badgley, C. (1988) Stratigraphy and remanence acquisition of a paleomagnetic reversal in alluvial Siwalik rocks of Pakistan. *Sedimentology*, **35**, 697-715.
- Ten Brinke, W.B.M., Wilbers, A.W.E. & Wesseling, C. (1999) Dune growth, decay and migration rates during a large magnitude flood at a sand and mixed sand-gravel bed in the Dutch Rhine river system. In: Smith, N.D. & Rogers, J. (eds.) *Fluvial Sedimentology VI. Int. Assoc. Sediment. Spec. Pub.* **28**, 15-32.
- Thoms, M.C. (1992) A comparison of grab- and freeze-sampling techniques in the collection of gravel-bed river sediment. *Sed. Geol.*, **78**, 191-200.
- Thoms M.C. (1994) A freeze-sampling technique for the collection of active stream sediments used in mineral exploration and environmental studies. *J. Geochem.Exploration*, **51**, 131-141.
- Thorne, P.D., Hardcastle, P.J. & Hogg, A. (1996) Observations of near-bed suspended sediment turbulence structures using multifrequency acoustic backscattering. In: Ashworth, P.J., Bennett, S.J., Best, J.L. & McLelland, S.J. (eds.) *Coherent flow structures in open channels*. John Wiley, Chichester, 343-358.
- Thorne, P.D., Hardcastle, P.J. & Soulsby, R.L. (1993) Analysis of acoustic measurements of suspended sediments. *J. Geophys. Res.*, **98**, 899-910.
- Thorne, P.D., Williams, J.J. & Heathershaw, A.D. (1989) In situ acoustic measurements of marine gravel threshold and entrainment. *Sedimentology*, **36**, 61-74.
- Tucker, M. E. (ed.) (1988) *Techniques in Sedimentology*, Blackwell, Oxford.
- Tucker, M. E. (2001) *Sedimentary Petrology*, 3rd ed. Blackwells, Oxford
- Tucker, M (2001) *Sedimentary petrology*, 3rd. ed. Blackwells, Oxford.
- Van De Meene, E.A., Van Der Staay, J. and Hock, T.L. (1979) The Van Der Staay suction corer – a simple apparatus for drilling in sand below groundwater table. Riks Geologisch Dienst.
- Weber, K. J. (1993) The use of 3-D seismic in reservoir geological modelling. In: S.S. Flint & I.D. Bryant (eds.) *The Geological Modelling of Hydrocarbon Reservoirs and Outcrop Analogues*, IAS Spec. Publ. **15**, 181-188.
- Weimer, P. & Davis, T.L. (eds.) (1996) *Applications of 3-D Seismic Data to Exploration and Production*. AAPG Studies in Geology **42** and SEG Geophysical Developments Series **5**, AAPG/SEG, Tulsa.

- Westaway, R. M., Lane, S.N. & Hicks, D.M. (2000) The development of an automated correction procedure for digital photogrammetry for the study of wide, shallow, gravel-bed rivers. *Earth Surf. Proc. Land.*, **25**, 209-226.
- White, B.R. (1996) Laboratory simulation of Aeolian sand transport and physical modelling. *Annals of Arid Zone*, **35**, 187-213.
- Whittaker, A., Cope, J.C.W., Cowie, J.W., Gibbons, W., Hailwood, E.A., House, M.R., Jenkins, D.G., Rawson, P.F., Rushton, A.W.A., Smith, D.G., Thomas, A.T., and Wimbledon, W.A. (1991) A guide to stratigraphical procedure. *J. Geol. Soc. Lond.*, **148**, 813-824.
- Wohl E.E., Anthony D.J., Madsen S.W. & Thompson D.M. (1996) A comparison of surface sampling methods for coarse fluvial sediments. *Wat. Resour. Res.*, **32**, 3219-3226.
- Wolcott J.F. & Church M.A. (1991) Strategies for sampling spatially heterogeneous phenomena: The example of river gravels. *J. Sed. Pet.*, **61**, 534-543.
- Wolman M.G. (1954) A method of sampling coarse river-bed material. *Trans. Am. Geophys. Union*, **35**, 951-956.
- Wren, D.G., Barkdoll, B.D., Kuhnle, R.A. & Derrow, R.W. (2000) Field techniques for suspended sediment measurement. *J. Hydraul. Engrg., ASCE*, **126**, 97-104.
- Xu, X., Bhattacharya, J.P., Davies, R.K., and Aiken, C.L.V. (2002) Digital geologic mapping of the Ferron Sandstone, Muddy Creek, Utah with GPS and reflectorless laser rangefinders. *GPS Solutions*, **5**, 15-24.
- Yarus J.M. & Chambers, R.L. (eds.) (1994) *Stochastic modeling and Geostatistics*, Am. Assoc. *Petrol. Geol. Computer Applications in Geology* **3**.
- Zadeh, L.A. (1965) Fuzzy sets. *Inf. Control*, **8**, 94-102.